TÉCNICO LISBOA

Analysis of the Implementation of LTE-Advanced in a Low Exposure Perspective

Dinis Alves Rocha

Thesis to obtain the Master of Science Degree in

Electrical and Computer Engineering

Examination Committee

Chairperson: Prof. Fernando Duarte Nunes

Supervisor: Prof. Luís Manuel de Jesus Sousa Correia

Member of Committee: Prof. Custódio José de Oliveira Peixeiro

Member of Committee: Doctor Eng. Michal Lukasz Mackowiak

October 2013

To my parents and brother

Acknowledgements

First of all, I would like to express my gratitude to Professor Luís M. Correia, for giving me the possibility to develop this thesis, within the European Project LEXNET. I am also thankful for his guidance, constant knowledge and experience sharing, as well as for his availability, support, discipline and professionalism, which were vital during the development of this work, and important to my personal growth.

I would like to thank Carla Oliveira, for following my work, giving her support, suggestions, and for the availability to clarify my doubts. I also thank her and Daniel Sebastião for the assistance provided in the measurements, which was fundamental.

To all the GROW members, for the opinions and suggestions given during the meetings, and for the knowledge sharing in the GROWing meetings, in which I was able to learn more about telecommunications, and to improve my presentations skills. I am grateful for being part of GROW.

To my colleagues and friends who shared the GROW's MSc Students Room with me, where this work was done, Diogo X. Almeida, Joana Fernandes and Ricardo Santos, for all the moments we have shared together, in an environment of friendship and cooperation, including the sharing of opinions, useful ideas and also the amusing moments. A special thanks to Diogo X. Almeida, who, besides his great fellowship, was always ready to discuss about several subjects, and to help me in my doubts, during the development of the thesis.

I also thank to all the IST colleagues and friends who followed me during this five-year journey, giving their friendship, sharing knowledge, without forgetting the amusing moments. Without them, this journey would be harder.

At last, but not least, I owe to my parents and brother all my gratitude, to whom I dedicate this thesis, for their unconditional daily support, encouragement, and for everything that they have done for me, as without them none of this would have been possible.

Abstract

The main objective of this thesis was to analyse the implementation of LTE-A in a low exposure perspective, considering the presence of signals from other networks, such as GSM and UMTS. This objective was achieved through the development and implementation of a model that assesses the exposure from both down- and uplinks in a typical urban scenario. Measurements were performed, in order to compare the measured data with the simulated results. The simulated results show that, for all the studied scenarios, the ICNIRP reference levels for exposure are satisfied, with the highest value of power density being 2.584 W/m^2, 4 times below the reference levels, obtained for the case where the user varies his position over the street. The maximum value of total exposure is obtained for the scenario with 3 base stations, being 0.545, 2 times below the limit value. The total exposure increases 33.6% and 49.8% when the MIMO configuration is changed from 2×2 to 4×4 and to 8×8, respectively. Finally, it is observed that the introduction of the 3 LTE carrier frequency versions, with other mobile communication systems being present, and using LTE2600 in uplink, approximately doubles the total exposure, when the user is static in a street.

Keywords

Exposure to Radiation, LTE, GSM, UMTS, Outdoor, Measurements

Resumo

O objectivo principal desta tese foi analisar a implementação do LTE-A do ponto de vista de baixa exposição, considerando os sinais provenientes de outras redes, tais como GSM ou UMTS. Este objectivo foi alcançado através do desenvolvimento e implementação de um modelo que avalia a exposição nas ligações descendente e ascendente num cenário urbano típico. Foram realizadas medidas, de forma a comparar os dados medidos com os resultados das simulações. Os resultados das simulações mostram que, para todos os cenários estudados, os níveis de referência da ICNIRP para a exposição são cumpridos, em que o valor mais elevado de densidade de potência é de 2.584 W/m^2, 4 vezes abaixo dos níveis de referência, obtido para o caso em que o utilizador varia a sua posição ao longo da rua. O valor máximo da exposição total é obtido para o cenário com 3 estações base, sendo 0.545, 2 vezes abaixo do valor limite. A exposição total aumenta 33.6% e 49.8% quando a configuração de MIMO é alterada de 2×2 para 4×4 e 8×8, respectivamente. Por fim, verifica-se que a introdução das 3 versões de portadoras de LTE, estando outros sistemas de comunicações móveis presentes, e usando LTE2600 na ligação ascendente, duplica, aproximadamente, a exposição total quando o utilizador está estático na rua.

Palavras-chave

Exposição à Radiação, LTE, GSM, UMTS, Exterior, Medições

Table of Contents

List of Figures

List of Tables

List of Acronyms

2G	Second Generation
3G	Third Generation
3GPP	Third Generation Partnership Project
4G	Fourth Generation
AMBR	Aggregate Maximum Bit Rate
ANACOM	*Autoridade Nacional de Comunicações*
AP	Access Point
ARP	Allocation and Retention Priority
ARQ	Automatic Repeat Request
BS	Base Station
CA	Carrier Aggregation
CDMA	Code Division Multiple Access
CP	Control Plane
CS	Circuit-Switch
DECT	Digital Enhanced Cordless Telecommunications
DeNB	Donor eNodeB
DL	Downlink
DS-CDMA	Direct Sequence-Code Division Multiple Access
ECC	Electronic Communications Committee
EDGE	Enhanced Data Rates for GSM Evolution
EIRP	Equivalent Isotropic Radiated Power
eNodeB	evolved NodeB
EPC	Evolved Packet Core
EPS	Evolved Packet System
ER	Exposure Ratio
E-UTRA	Evolved-Universal Terrestrial Radio Access
E-UTRAN	Evolved-Universal Terrestrial Radio Access Network
FDD	Frequency Division Duplex
FDMA	Frequency Division Multiple Access
FM	Frequency Modulation
FP7	Seventh Framework Programme
FST1	Frame Structure Type 1
FST2	Frame Structure Type 2
FTP	File Transfer Protocol

GBR	Guaranteed Bit Rate
GMSK	Gaussian Minimum Shift Keying
GPRS	General Packet Radio Services
GPS	Global Positioning System
GSM	Global System for Mobile Communications
HSDPA	High Speed Downlink Packet Access
HSPA	High Speed Packet Access
HSPA+	High Speed Packet Access Evolution
HSS	Home Subscription Service
HSUPA	High Speed Uplink Packet Access
ICNIRP	International Commission on Non-Ionising Radiation Protection
IMS	IP Multimedia Subsystem
IMT	International Mobile Telecommunications
IP	Internet Protocol
ISM	Industrial Scientific and Medical
LEXNET	Low Electromagnetic Fields Exposure Networks
LTE	Long Term Evolution
LTE-A	LTE-Advanced
MBMS	Multimedia Broadcast and Multicast Services
MBR	Maximum Bit Rate
MBSFN	Multicast/Broadcast over Single Frequency Network
MIMO	Multiple Input Multiple Output
MM	Mobility Management
MME	Mobility Management Entity
MS	Mobile Station
MT	Mobile Terminal
OFDM	Orthogonal Frequency Division Multiplexing
OFDMA	Orthogonal Frequency Division Multiple Access
PAR	Peak to Average Ratio
PBCH	Physical Broadcast Channel
PC	Personal Computer
PCEF	Policy Control Enforcement Function
PCFICH	Physical Control Format Indicator Channel
PCRF	Policy and Charging Resource Function
PDCCH	Physical Downlink Control Channel
PDN	Packet Data Network
PDSCH	Physical Downlink Shared Channel
PFM	Portable Field Meter
P-GW	PDN-Gateway
PHICH	Physical Hybrid ARQ indicator Channel

PMCH	Physical Multicast Channel
PRACH	Physical Random Access Channel
PS	Packet-Switch
PSS	Primary Synchronisation Signal
PUCCH	Physical Uplink Control Channel
PUSCH	Physical Uplink Shared Channel
QAM	Quadrature Amplitude Modulation
QCI	QoS Class Identifier
QoS	Quality of Service
QPSK	Quadrature Phase Shift Keying
R99	Release 99
RB	Resource Block
RE	Resource Element
RF	Radiofrequency
RLC	Radio Link Controller
RMS	Root-Mean-Square
RN	Relay Node
RRM	Radio Resource Management
RS	Reference Signal
SAE	System Architecture Evolution
SAR	Specific Absorption Rate
SC-FDMA	Single Carrier-Frequency Division Multiple Access
S-GW	Serving-Gateway
SISO	Single Input Single Output
SMS	Short Message Service
SNR	Signal-to-Noise Ratio
SRM	Selective Radiation Metre
SSS	Secondary Synchronisation Signal
TCP	Transmission Control Protocol
TDD	Time Division Duplex
TDMA	Time Division Multiple Access
TMN	*Telecomunicações Móveis Nacionais*
UE	User Equipment
UL	Uplink
UMTS	Universal Mobile Telecommunications System
UP	User Plane
VoIP	Voice over IP
WCDMA	Wideband Code Division Multiple Access
WiFi	Wireless Fidelity

List of Symbols

γ	Total exposure parameter
Γ	Reflection coefficient
Γ_i	Reflection coefficient associated to surface of the reflected ray i
Δf	Signal bandwidth
Δf_{cs}	Radio channel separation
Δr_i	Path length difference between the direct ray and reflected ray i
ΔP	Power compensation
ε_S	Exposure ratio referred to power density
λ	Wavelength
ρ_N	Signal-to-Noise Ratio
χ_i	Contribution of the signal i to the total exposure
A_{abs}	Absorption surface area
A_e	Antenna effective area
d_{BS}	Spacing between the BSs in the same side of the street
D	Largest dimension of the antenna
E	Electric field strength
E_i	Electric field strength at frequency i
$E_{L,i}$	Electric field reference level for frequency i
f	Frequency
$f_{c\,min}$	Minimum of the spectrum band
$f_{c\,n}$	Radio channel centre frequency
F	Noise figure
g_i	Gain of the transmitting antenna in the direction of the reflected ray i, normalised to the gain in the direction of the direct ray
G_P	Processing gain
G_r	Receiving antenna gain
G_t	Transmitting antenna gain
h_b	Height of BS antenna
h_m	Height of MT antenna
h_{torso}	Human torso's height
H	Magnetic field strength
k	Propagation constant
k_B	Boltzmann constant

L_c	Cable losses between the transmitter and the antenna
L_p	Path loss
L_u	User losses
$L_{P,k}$	Path loss regarding the position of analysis k
$L_{P,k-1}$	Path loss regarding the previous position $k-1$
M_s	Safety margin
N	Total noise power
N_p	Number of points of investigation
N_{rr}	Number of reflected rays
N_{th}	Thermal noise power
P_{abs}	Power absorbed by the user
P_{EIRP}	Effective Isotropic Radiated Power
P_{EIRP}^{DL}	DL EIRP
P_{EIRP}^{UL}	UL EIRP
$P_{EIRP,k}^{UL}$	UL EIRP corresponding to the position k
$P_{EIRP,k-1}^{UL}$	UL EIRP corresponding to the previous position, $k-1$
P_r	Power available at the receiving antenna
$P_{r\ target}$	Target available power at the receiving antenna
$P_{Rx\ min}$	Receiver sensitivity
P_{Rx}^{DL}	Power at the input of the receiver, considering DL.
P_{Rx}^{UL}	Power at the input of the receiver, considering UL
P_t	Power fed to the transmitting antenna
P_{Tx}	Transmitter output power
r	Distance from the radiating element to the point of investigation
r_b	Length of the ray reflected on the building
r_g	Length of the ray reflected on the ground
r_i	Length of the reflected ray i
R_b	Throughput
R_c	Chip rate
S	Power density
S_{DL}	DL power density
S_i	Power density at frequency i
$S_{i,k}$	Power density at frequency i, for the location k
$S_{L,i}$	Power density reference level for frequency i
S_r	Received power density
S_{UL}	UL power density
T	Noise temperature
w_{head}	Human head's width

w_s	Street width
w_{torso}	Human torso's width
x_{BS}	Coordinates of the BS in the *x*-axis
x_u	Coordinates of the user in the *x*-axis
X_i	Contribution of the signal i to the total exposure
y_{BS}	Coordinates of the BS in the *y*-axis
y_u	Coordinates of the user in the *y*-axis
Z_0	Free space impedance

List of Software

MATLAB R2010a	Numerical computing software
Microsoft Excel 2010	Calculation and graphical chart tool
Microsoft Visio 2010	Scheme design software
Microsoft Word 2010	Text editor software

Chapter 1

Introduction

This chapter presents an overview of the main subject of this work, followed by its motivation and general description of its scope and main contributions. At the end of the chapter, the structure of the work is described.

1.1 Overview

The way we communicate has changed along the years, motivated by the evolution of mobile communication systems, which are providing new services and applications to end-users. Third Generation Partnership Project (3GPP) has played an important role, being involved in the development of the latest releases concerning mobile communication technologies.

The first digital cellular system corresponds to the Second Generation (2G), where Global System for Mobile Communications (GSM) is the system widely implemented, which started to be deployed in the early 1990s. These systems were essentially designed for voice transmission, with a throughput up to 22.8 kbps [Corr13], but had also some simple data services, such as Short Message Service (SMS), as well as Circuit-Switch (CS) data services enabling e-mail and other applications, initially with a throughput of 9.6 kbps, with later releases providing higher throughputs. Some of the evolved versions have appeared during the second half of the 1990s, such as the General Packet Radio Services (GPRS), which brought the possibility of Packed-Switch (PS) data, and Enhanced Data Rates for GSM Evolution (EDGE), with a more efficient modulation, [Moli11] and [DaPS11].

A range of new services came with the Third Generation (3G) of cellular systems, known as Universal Mobile Telecommunications System (UMTS), as it uses PS for data transmission and it was designed to have higher data rate services [Luo11], being given a higher relevance to data traffic. The first UMTS release, Release 99 (R99), also named as Wideband Code Division Multiple Access (WCDMA), started to be deployed during 2002, with theoretical data rates up to 2 Mbps. Then, during 2005 and 2007, High Speed Downlink Packet Access (HSDPA), Release 5, and High Speed Uplink Packet Access (HSUPA), Release 6, started to be deployed, being the Downlink (DL) and Uplink (UL) standards that comprise High Speed Packet Access (HSPA), offering throughputs up to 14 Mbps. The latest version, Release 7, which is the HSPA evolution (HSPA+), started its deployments during 2009, providing throughputs up to 48 Mbps [HoTo11].

The Fourth Generation (4G), corresponding to the Long Term Evolution (LTE), had its first release, Release 8, being deployed in commercial networks in 2010. This technology is only dedicated to data, having a flat and full-PS architecture, and high performance targets, such as low latency, high spectral efficiency and high peak user throughput, which can reach up to 300 Mbps in DL, and 75 Mbps in UL [HoTo11]. These targets will overcome the increase of data traffic demand, supporting a wider variety of services (multiservice) and applications, and reduce costs, as mobile operators' revenue does not follow traffic evolution. In 2010, LTE Release 10 was approved, which includes new capabilities, such as Carrier Aggregation (CA), reaching up to 1 Gbps, the target value of the International Mobile Telecommunications (IMT) – Advanced. The schedule of the 3GPP standards and their commercial deployment, as well as the maximum theoretical throughput values for each technology, previously described, are presented in Figure 1.1 and Figure 1.2, respectively.

The technologies evolution is related to the increasing demand in terms of traffic and capacity. The number of mobile subscriptions has impact on the traffic that is put in the network, and, according to [Eric13], it is predicted that, by the end of 2018, it will reach 9.1 billion subscriptions. Today, the

majority of mobile phone subscriptions are for basic phones. However, mobile broadband subscriptions are expected to be 7 billion in 2018, where smartphones (devices with a wide range of applications, most of them making use of data traffic, representing the majority of the mobile broadband devices) are expected to have a greater impact in the future; it is predicted that the number of smartphones subscriptions will be 4.5 billion in 2018, with 850 million corresponding to Personal Computers (PCs), tablets and mobile routers, as depicted in Figure 1.3.

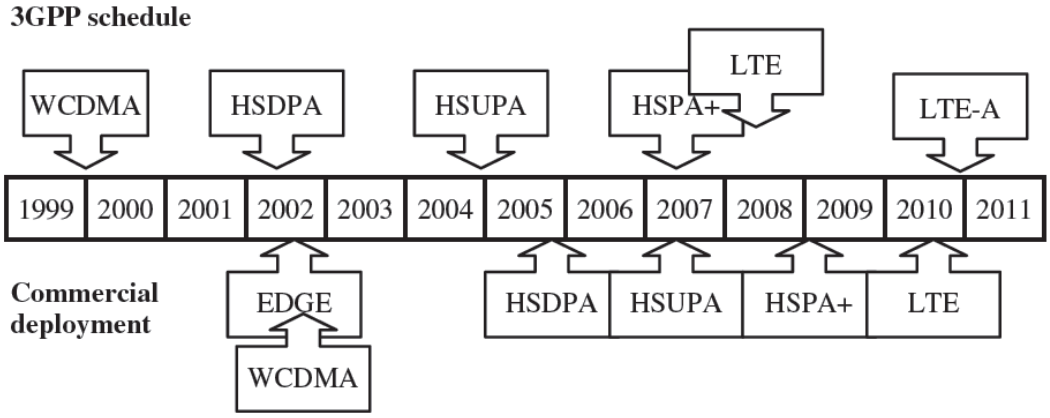

Figure 1.1. Schedule of the 3GPP standards and their commercial deployment (adapted from [HoTo11]).

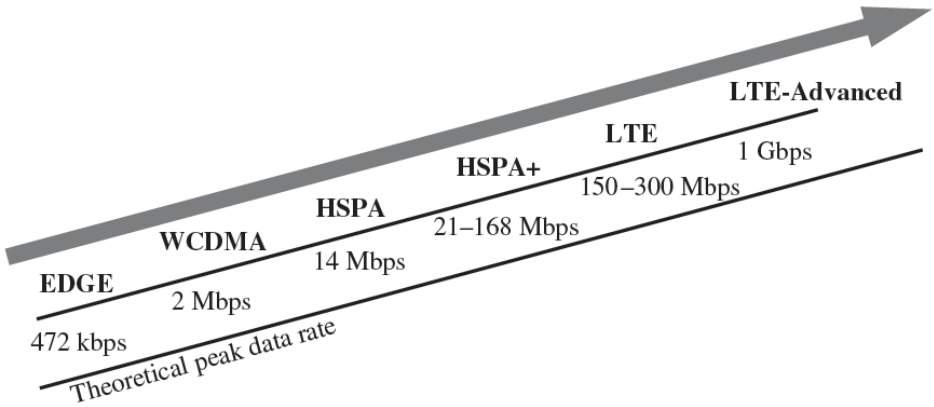

Figure 1.2. Peak data rate evolution of the 3GPP standards (extracted from [HoTo11]).

Traffic is influenced by the rapid increase of smartphone subscriptions, especially data traffic, as, over time, the trend is that more advanced services emerge leading to greater demands. The overall mobile data traffic is expected to continue the trend of doubling each year, presenting a growth of approximately 12 times between 2012 and 2018. Figure 1.4 shows this evolution, with a comparison between data traffic due to mobile phones and due to PCs, tablets and mobile routers, as well as the trend of voice traffic, which is constant compared to the increase of data traffic, which is much higher. In addition, the application that will have the fastest growing in mobile data traffic is video, driven by the growth in the amount of available content, as well as due to the higher throughputs provided by LTE and HSPA.

As the demands in terms of traffic and capacity increase, LTE needs to be widely deployed in order to satisfy them, being predicted that LTE will cover approximately 60% of the world's population. This will

include the deployment of heterogeneous networks, in order to provide users with a higher data throughput, as well as quality of service, which comprises several types of cells with various sizes, leading to the existence of heterogeneous networks.

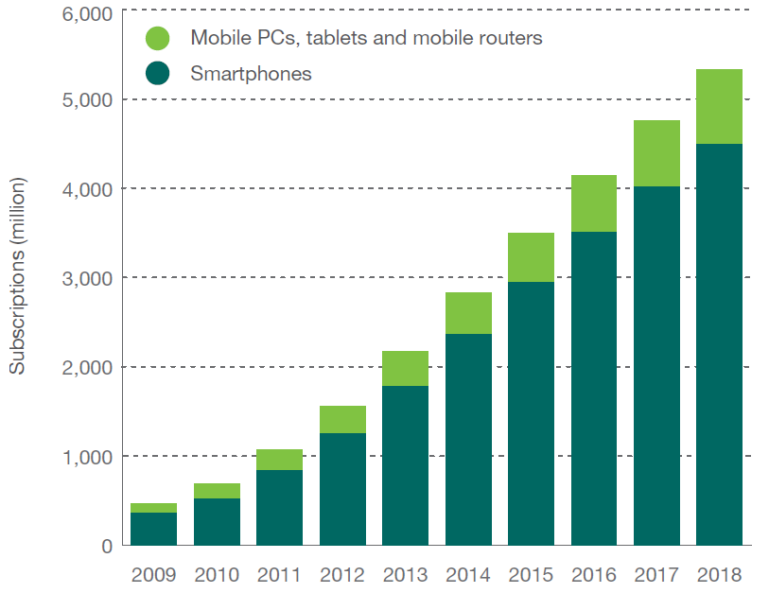

Figure 1.3. Mobile devices with cellular connection, from 2009 to 2018 (extracted from [Eric13]).

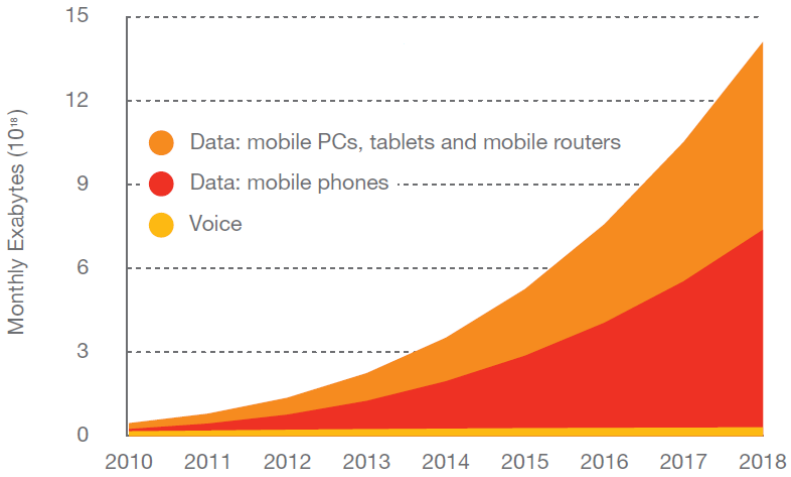

Figure 1.4. Global data and voice mobile traffic, from 2010 to 2018 (extracted from [Eric13]).

1.2 Motivation and Contents

The implementation of LTE, considering the data traffic demands previously described, has impact in many aspects, namely on the electromagnetic field existing in public areas, as LTE is working in conjunction with the other systems that were already implemented. This introduction of more systems in the network can have impact in the general public's risk perception on the exposure to electromagnetic fields. The increase of the number of BS installations, which are needed to provide

more capacity, especially the BSs corresponding to small cells, which are closer to the general public, might be related to this perception, causing some concerns in the general public. The increase of the subscriptions can also lead to the increase of the concerns about the exposure related to the use of the mobile equipment. Hence, multiple exposure needs to be evaluated, considering LTE coexisting with other systems, in order to assess its influence and to verify if the joint systems are compliant with the guidelines defined by the International Commission on Non-Ionising Radiation Protection (ICNIRP).

The main scope of this thesis is to analyse the implementation of LTE-A in a low exposure perspective, considering the presence of signals from other networks, such as GSM and UMTS, the legacy systems already operating when LTE was deployed. These objectives are achieved with the implementation of a model in a simulator, which enables this analysis. The global model accounts for the exposure in both links, comprising a model for DL, and another for UL. Results are obtained for a typical urban scenario, varying some parameters to make a proper analysis, and determining the total exposure parameter, being compared with ICNIRP's reference value. Moreover, measurements were made, in order to obtain exposure values in a real scenario.

The topic of this work is within the Low Electromagnetic Fields Exposure Networks (LEXNET) project [LEXN13], a research project supported by the European Commission under the Seventh Framework Programme (FP7), which aims to develop effective mechanisms to reduce, at least, 50% of the public exposure to electromagnetic fields, without compromising the quality of service.

This thesis provides results about the implementation of LTE, and the impact of its main features (including LTE-A) in the exposure, considering the coexistence with the mobile communication systems operating in the bands defined for LTE, and both DL and UL. In the end, the total exposure parameter is obtained, comprising the contributions of each of the systems, so that the impact of each analysed configuration can be assessed.

The thesis comprises 5 chapters, including the present one, followed by a set of annexes. Chapter 2 presents the fundamental concepts of LTE, describing its network architecture and radio interface, followed by a description regarding the type of services and applications. Then, basic aspects about the most relevant systems coexisting with LTE are presented, concluding with an overview of the exposure requirements and the most relevant works done in the scope of LTE exposure.

Chapter 3 describes the adopted models, being presented in the beginning of the chapter. Afterwards, an overview of the simulator is given, detailing its input and output parameters, followed by the specification of the algorithms, and finishing with its assessment, where some test cases are done, in order to validate the implemented model.

Chapter 4 begins with the description of the scenarios under analysis. Then, it presents the procedure of the measurements and the analysis of the obtained results. Afterwards, the results concerning the simulations are presented, as well as their analysis, beginning with the reference scenario and, then, analysing the influence of the variation of each chosen parameter. At the end of the chapter, a comparison between measurement and simulation results is done.

Chapter 5 finalises this thesis, presenting the main conclusions and addressing future work.

A set of annexes is presented in the end of the thesis, providing additional information. Annex A concerns LTE frequency bands; Annex B presents the list of the systems operating within the bands defined for LTE; Annex C gives a detailed description of the link budget, followed by measurement data, which are presented in Annex D. Some additional results obtained in simulations are shown in Annex E, with Annex F having additional results regarding measurements, where a complementary analysis is done.

Chapter 2

Fundamental Concepts

This chapter provides a general view of the fundamental concepts in LTE/LTE-A, focusing on the aspects directly related to the purpose of this thesis. Firstly, a description of the LTE/LTE-A network architecture is done. Secondly, radio interface aspects are introduced, followed by an approach on services and applications. Thirdly, the coexistence of LTE with the most relevant systems of this work is also referred and, finally, relevant studies that assess LTE exposure are mentioned.

2.1 Network Architecture

In this section, the LTE and LTE-A network architecture is presented, based on [HoTo11] and [SeTB11]. LTE and LTE-A have the same network architecture, as the improvements to the latter were not made in this domain. The network has an evolved architecture, in order to follow the evolution in the radio interface and taking some targets into account, such as system optimisation for PS services and performance improvement. So, as a result of the 3GPP System Architecture Evolution (SAE), one has a flat architecture, through the reduction of the network elements, being simpler than the existing ones for 3GPP and other cellular systems, and improving network scalability and end-to-end latency. User Equipment (UE), Evolved-Universal Terrestrial Radio Access Network (E-UTRAN), Evolved Packet Core (EPC) and Services are the four high level domains of the LTE network architecture, where the E-UTRAN and EPC correspond to the radio access and core networks, respectively. These domains are represented in Figure 2.1, where the network architecture is shown considering only E-UTRAN as the radio access network.

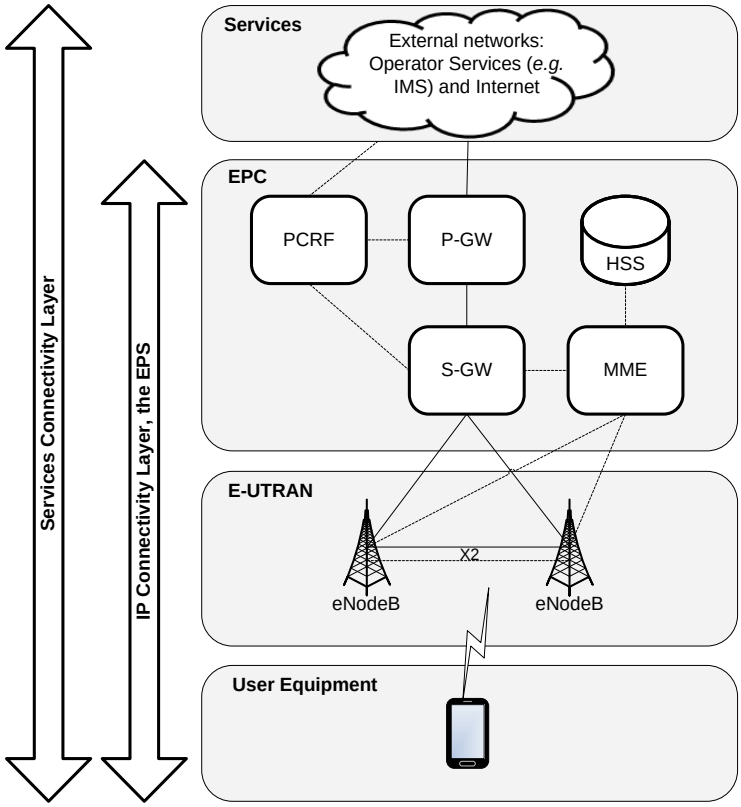

Figure 2.1. Network Architecture for an E-UTRAN only network (adapted from [HoTo11]).

As shown in Figure 2.1, the Evolved Packet System (EPS) comprises the UE, the E-UTRAN and the EPC, providing Internet Protocol (IP) connectivity between the UE and the Packet Data Network (PDN), whose architecture remains the same, since the new architectural developments are made in the E-UTRAN and in the EPC.

The UE provides the interface to the end-user, being a platform for communication applications. This equipment can be a handheld device, such as a mobile phone, a tablet, or a data card to connect to a

computer. It communicates with the network in order to establish, maintain and remove a link, including mobility management functions, as handover and terminal location report. UE is the logical designation of UMTS or LTE equipment, Mobile Terminal (MT) being the generic designation.

Concerning the LTE radio access network, E-UTRAN is composed of a mesh of evolved NodeBs (eNodeBs), connected through the X2 interface, and provides connectivity to the EPC. An eNodeB is a Base Station (BS), responsible for all radio functionalities:

- Ciphering/deciphering User Plane (UP) data, for security purposes when transmitting data through the radio interface;
- Header compression/decompression, which allows an efficient use of the radio interface, through the compression of IP packet headers, avoiding repeatedly sending the same data in IP headers;
- Radio Resource Management (RRM), which controls the radio interface usage, including resources allocation based on requests, prioritisation and schedule of traffic according to required Quality of Service (QoS), as well as constant monitoring of the resource usage situation;
- Mobility Management (MM), that controls and analyses the radio signal level measurements made by the UE, also doing similar measurements and taking decisions according to these to handover between cells, which includes exchanging handover signalling between other eNodeBs and the Mobility Management Entity (MME).

The EPC, the core network of the EPS, is responsible for the overall control of the UE and for the bearers' establishment, being a totally packed-based network with no direct connectivity to traditional CS networks. Unlike the E-UTRAN, where the eNodeB is the single node, the EPC has several kinds of nodes, Figure 2.1:

- Mobility Management Entity, the main control element in the EPC, which operates only in the Control Plane (CP), processing the signalling between the UE and the EPC. It supports functions related to bearer and connection management, and also to the inter-working with other networks, for example, legacy networks;
- Serving-Gateway (S-GW), having as high level function the UP tunnel management and switching, acting as a local mobility anchor during mobility between eNodeBs;
- PDN-Gateway (P-GW), which is the edge router between the EPS and other external PDNs making the IP allocation to the UE, so that it can communicate with other IP hosts in external networks, QoS enforcement and flow-based charging;
- Policy and Charging Resource Function (PCRF), the network element responsible for policy and charging control, making decisions in how to handle the services in terms of QoS and providing information to the Policy Control Enforcement Function (PCEF), which resides in the P-GW, in order to set up the appropriate bearers and policing;
- Home Subscription Service (HSS), which is a data base server containing all the user permanent data, such as the subscriber profile and whether roaming to a particular visited network is allowed or not.

2.2 Radio Interface

This section is mainly based on [HoTo11] and [Agil09], and approaches the fundamental aspects of LTE radio interface, including the assigned frequency bands, multiple access techniques, frame structure, Multiple Input Multiple Output (MIMO), and finishing with the main features of LTE-A.

According to 3GPP Release 11 [3GPP13b], Evolved-Universal Terrestrial Radio Access (E-UTRA) is defined to operate in 39 frequency bands, distributed by the two duplex schemes used in LTE: the Frequency Division Duplex (FDD), which separates DL from UL in the frequency domain, and the Time Division Duplex (TDD), that alternates the transmission direction in the time domain. Thus, 27 frequency bands are assigned to FDD (paired bands), and 12 to TDD (unpaired bands), wherein in Europe, the main frequency bands correspond to 800, 900, 1800, 2100 and 2600 MHz. In Portugal, the National Communications Authority (ANACOM) auctioned the bands of 450, 800, 900, 1800, 2100 and 2600 MHz, with the Portuguese operators adopting the 800, 1800 and 2600 MHz for LTE [ANAC13]. These frequency bands, as well as the frequency usage in different world's regions, and also the Portuguese auction results, are presented in more detail in Annex A.

Concerning the multiple access techniques, LTE uses Orthogonal Frequency Division Multiple Access (OFDMA) in DL and Single Carrier-Frequency Division Multiple Access (SC-FDMA) in UL, providing orthogonality between the users, reducing the interference, and improving the network capacity. With the basic principle of Frequency Division Multiple Access (FDMA), which is applied both in OFDMA and SC-FDMA, one has different users using different carriers or sub-carriers to access the same system, having their data modulated around a different centre frequency.

OFDMA is a variant of Orthogonal Frequency Division Multiplexing (OFDM), a digital multi-carrier modulation scheme, whose principle is to have orthogonality among sub-carriers, so that they do not interfere with each other, even if they overlap in the frequency domain. This is achieved by selecting the centre frequencies for the sub-carriers, in order to have a difference in frequency domain, such that the neighbouring sub-carriers have zero value at the sampling instant of the desired sub-carrier. The allocation of sub-carriers is done in groups of 12, spaced by 15 kHz, corresponding to a Resource Block (RB). These are modulated with Quadrature Phase Shift Keying (QPSK) or Quadrature Amplitude Modulation (QAM), and transmitted in parallel. Cyclic extension is used to avoid inter-symbol interference, which means that, in the time domain, instead of having a break in the transmission, a cyclic prefix is added by copying part of the symbol at the end, and attaching it to the beginning of the symbol, being designed so that it exceeds the delay spread in the radio channel. There are also reference symbols, used by the receiver, to facilitate the channel estimation when the sub-carriers experience frequency dependent phase and amplitude changes, due to the radio channel. OFDMA allows subsets of sub-carriers to be dynamically allocated among the different users, being considered a multi-carrier scheme, sending several symbols at a time.

In spite of having spectral efficiency as major advantage, the OFDMA scheme has a main challenge related to the high Peak to Average Ratio (PAR) of the transmitted signal, due to the existence of multiple sinusoidal waves with different frequencies in the time domain, which corresponds to parallel

sub-carriers in the frequency domain. As a consequence, the signal envelope varies strongly, an amplifier with additional back-off being required to operate in the linear area, leading to a reduced power amplifier efficiency or a smaller output power. This causes either range shortening, or higher power consumption when the mean output power is maintained, which is a problem for mobile devices. Hence, OFDMA is not the appropriate multiple access scheme for UL, where UE's power consumption is quite relevant, being used only in DL.

SC-FDMA, the multiple access scheme used in UL, combines many of the flexible aspects of OFDMA with the low PAR techniques of a single carrier system [Agil09], in order to optimise the range and the power consumption. Thus, unlike OFDMA, SC-FDMA is a single carrier scheme that only sends each symbol at a time, similarly to Time Division Multiple Access (TDMA), which leads to a faster symbol rate in the time domain, so cyclic prefix is used between a block of symbols, instead after each symbol. According to carrier allocation, SC-FDMA requires allocation across a contiguous block of spectrum, which decreases the scheduling flexibility verified in OFDMA, where the carrier allocation is non-contiguous. The maximum allocated bandwidth can be up to 20 MHz, but other bands are specified at 1.4, 3, 5, 10 and 15 MHz [Agil11]. The differences in carrier allocation between SC-FDMA and OFDMA are illustrated in Figure 2.2.

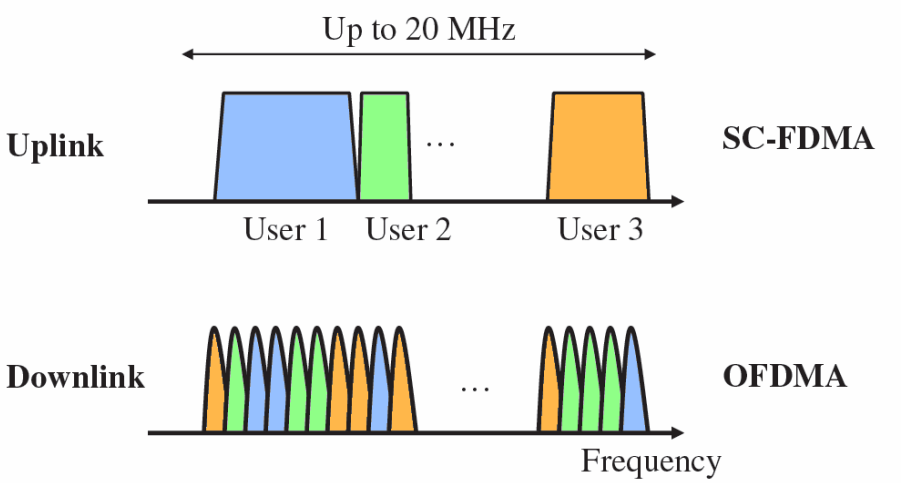

Figure 2.2. Carrier allocation in SC-FDMA and OFDMA (adapted from [HoTo11]).

In order to have a better comprehension of the main differences between the two schemes, Figure 2.3 presents an example comparing OFDMA and SC-FDMA. Although LTE signals are allocated in units of 12 sub-carriers, for simplicity only 4 sub-carriers are considered, as the principle is the same. Basically, as shown in the left side of Figure 2.3, in OFDMA, each symbol, represented by a colour, modulates a sub-carrier and the 4 sub-carriers are transmitter in parallel, in the frequency domain. In this case, the sub-carriers are contiguous, but could be non-contiguous, as it is OFDMA. After sending the first 4 symbols in parallel, which takes an OFDMA symbol period (66.7 µs), the cyclic prefix is added, and the transmission of the next 4 symbols is done in the same way, taking into account that each symbol can modulate different sub-carriers at different symbol periods.

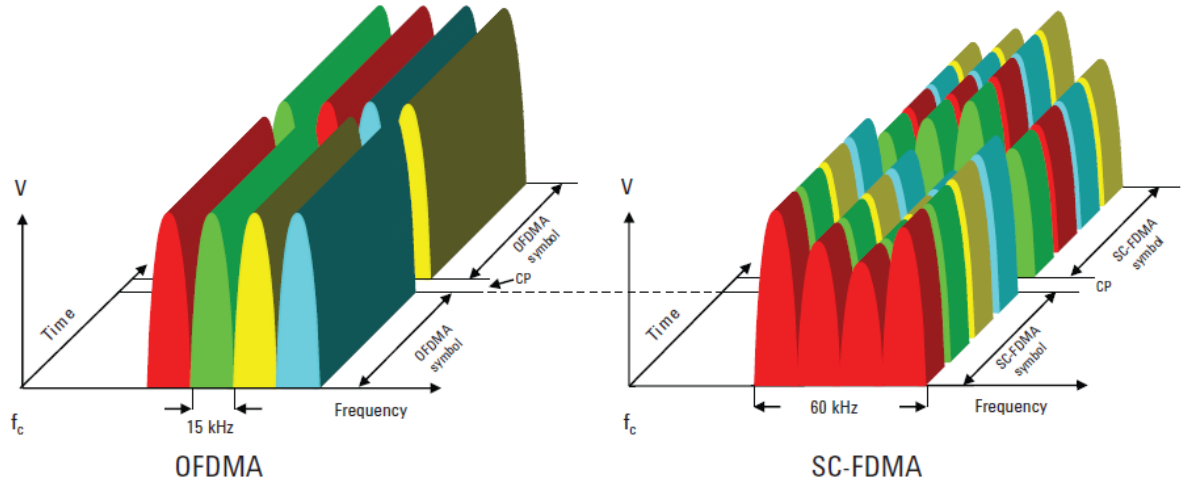

Figure 2.3. Comparison between the transmission in OFDMA and SC-FDMA (adapted from [Agil09]).

In SC-FDMA, shown in the right side of Figure 2.3, the main difference from OFDMA is the transmission of the 4 symbols in series at 4 times the rate, *i.e.*, each symbol is transmitted at a time (single carrier), represented by one wide signal with "sub-symbols" corresponding to the data that is modulated in a single carrier. This single carrier occupies the bandwidth corresponding to the number of assigned sub-carriers, which corresponds to 180 kHz in LTE if one has 12 sub-carriers.

Regarding the frame structure, two types of frames are defined for LTE: Frame Structure Type 1 (FST1), for FDD, and Frame Structure Type 2 (FST2), for TDD. As FDD is predominant, only the FST1 is described, shown in Figure 2.4, where each radio frame is 10 ms long, consisting of 10 sub-frames. Each sub-frame has two slots, each one corresponding to an RB, the smallest unit that can be scheduled for transmission, occupying 0.5 ms in the time domain and 180 kHz in the frequency domain. It corresponds to 12 sub-carriers spaced by 15 kHz and can contain six or seven symbols, whether the cyclic prefix is extended or short (normal), respectively. The sub-carrier spacing of 7.5 kHz is also supported in DL, used for Multicast/Broadcast over Single Frequency Network (MBSFN). Each RB comprises a smaller unit, the Resource Element (RE), which consists of one sub-carrier for a duration of one OFDM symbol. The allocation is made in frequency and time domain with 180 kHz and 1 ms resolution, although an RB corresponds to 0.5 ms.

User and system information are carried by physical channels. In LTE, one has six channels for DL and three for UL. In DL, the Physical Broadcast Channel (PBCH) carries system information needed to access the system, such as cell's bandwidth. All user data, broadcast system information which is not carried on the PBCH, and paging messages are carried on the Physical Downlink Shared Channel (PDSCH), while the Physical Multicast Channel (PMCH) carries the data for Multimedia Broadcast and Multicast Services (MBMS) [SeTB11]. Control information is carried by the Physical Control Format Indicator Channel (PCFICH), the Physical Hybrid Automatic Repeat Request (ARQ) Indicator Channel (PHICH), and by the Physical Downlink Control Channel (PDCCH). In UL, the Physical Random Access Channel (PRACH) is used for carrying random access information; the Physical Uplink Shared Channel (PUSCH) carries UL data, and the Physical Uplink Control Channel (PUCCH) carries control information, as the PDCCH does for DL.

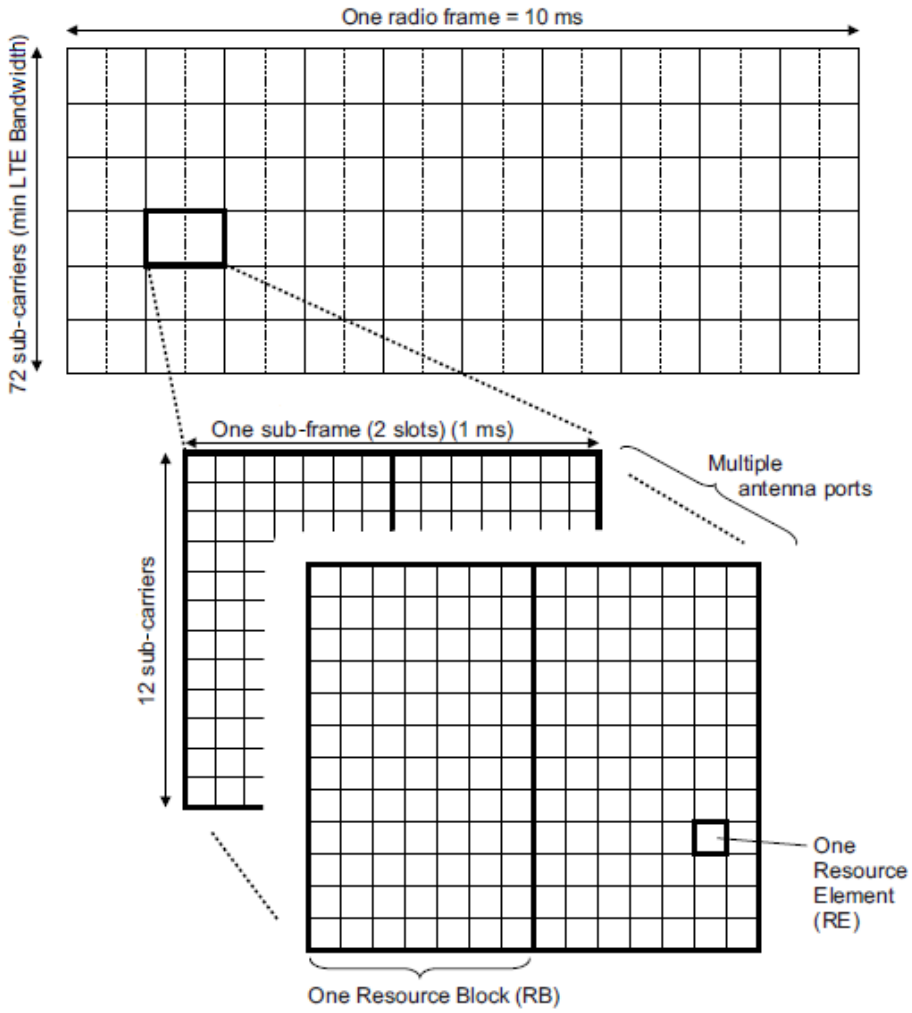

Figure 2.4. LTE FDD frame structure (adapted from [SeTB11]).

One of the main features introduced with LTE is MIMO operation, which requires two or more transmitters and two or more receivers, in order to reach performance improvements, such as high peak data rates. For a system to fully exploit as MIMO, it must have at least as many receivers as transmit streams. MIMO operation includes spatial multiplexing, pre-coding and transmit diversity. The principle of spatial multiplexing is to send signals from two or more different antennas with different data streams and process them in the receiver, separating the data streams, which increases the peak data rates by a factor of 2, with 2×2 antenna configuration, or 4, with a 4×4 configuration. Pre-coding weights the signals to be transmitted from different antennas to maximise the received Signal-to-Noise Ratio (SNR), and transmit diversity sends the same signal from multiple antennas. In MIMO operation, the transmissions from each antenna must be uniquely identifiable, so that each receiver can determine which combinations of transmissions it receives, which is done with reference symbols, each one used by a single transmit antenna.

Concerning power levels, in LTE, for both BS and UE there are maximum values defined. For the UE, a power class (power class 3) is defined for all operating bands, corresponding to a maximum output power of 23 dBm, the power that is fed to the transmitting antenna, with a tolerance of ±2 dB

[3GPP13b]. On the other hand, for the BS, a value for the maximum output power in a macro-cell is not defined, but typical values range in [43, 48] dBm [HoTo11]. Power control is only specified for UL, wherein the transmitted power is adjusted to the necessary level for maintaining a good quality of the received signal, increasing the UE's battery lifetime, and reducing the interference between adjacent cells [Moli11]. The values specified for the maximum output power, concerning extreme conditions, are presented in Table 2.1, which should remain within ±2.5 dB [3GPP13c].

Table 2.1. LTE BS maximum output power (adapted from [3GPP13c] and [Corr13]).

BS		**Maximum Output Power [dBm] (Extreme conditions)**
Macro-Cell		-
Micro-Cell		[35.5, 40.5]
Pico-Cell		[21.5, 26.5]
Femto-Cell	1 transmit antenna port	[17.5, 22.5]
	2 transmit antenna ports	[14.5, 19.5]
	4 transmit antenna ports	[11.5, 16.5]
	8 transmit antenna ports	[8.5, 13.5]

The power radiated by the antenna depends on the power fed to it and its gain. In DL, the radiated power also depends on the losses in the cable that connects the transmitter to the BS antenna; whereas in UL, it depends on whether voice or data is being used, as one needs to take into account the losses due to the user. Typically, for voice services, these losses are higher than for data [Corr13], which is related to mobile device's position when in use, *i.e.*, for voice, the MT is handled near the head, which highly contributes for the losses, whereas, for data services, the device is in a most favourable position in the signal propagation viewpoint, as it is not close to the head.

LTE-A emerges with some improvements with respect to LTE, in order to meet IMT-Advanced requirements, such as the support of 100 Mbps and 1 Gbps for high and low mobility cases, respectively, as well as the interworking with other technologies, and the provision of high-quality services. The main features introduced in Release 10 LTE-A include: Carrier Aggregation (CA) up to a total band of 40 MHz, with a potential to be up to 100 MHz; MIMO evolution to 8×8 in DL and 4×4 in UL, with the introduction of more antennas; relay nodes, to provide simple transmission solution; and heterogeneous networks, to optimise the interworking between cell layers, including macro-, micro-, pico- and femto-cells. These features, summarised in Figure 2.5, are designed taking into account the backwards compatibility, so that LTE-A can be considered as a "toolbox of features" that can be flexibly implemented on the top of LTE Release 8/9.

The extension of the maximum bandwidth is possible due to the use of CA, a key component of LTE-A, which aggregates multiple LTE Release 8/9 carriers, keeping backwards compatibility, can be used for both FDD and TDD modes. Each carrier that can be aggregated is named component carrier; five component carriers is the maximum that can be aggregated, leading to the maximum bandwidth of 100 MHz, considering the larger possible carrier bandwidth (20 MHz).

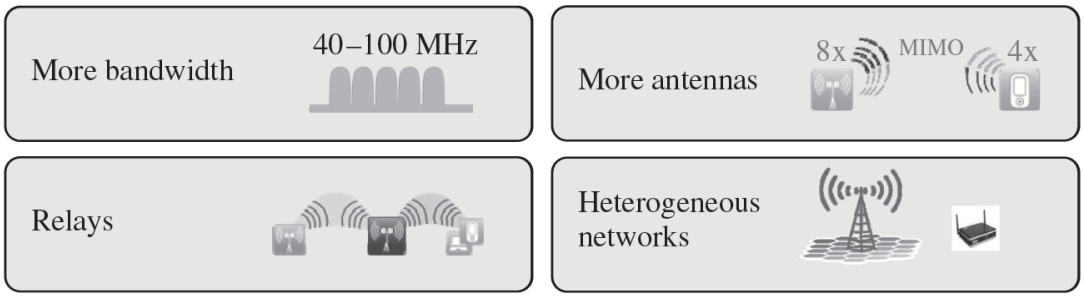

Figure 2.5. LTE-A main features (adapted from [HoTo11]).

There are two main types of CA, namely intra- and inter-bands, depicted in Figure 2.6. In intra-band CA, the component carriers' aggregation is done within a frequency band and can be contiguous or non-contiguous. On the other hand, in inter-band CA, the component carriers belong to different frequency bands (non-contiguous) [Wann12], being more easily used in DL, as in most cases each operator does not have more than 20 MHz in a given frequency band. In UL, carrier aggregation is not so attractive, as it requires the use of two transmitters simultaneously, being more challenging than having two receivers simultaneously.

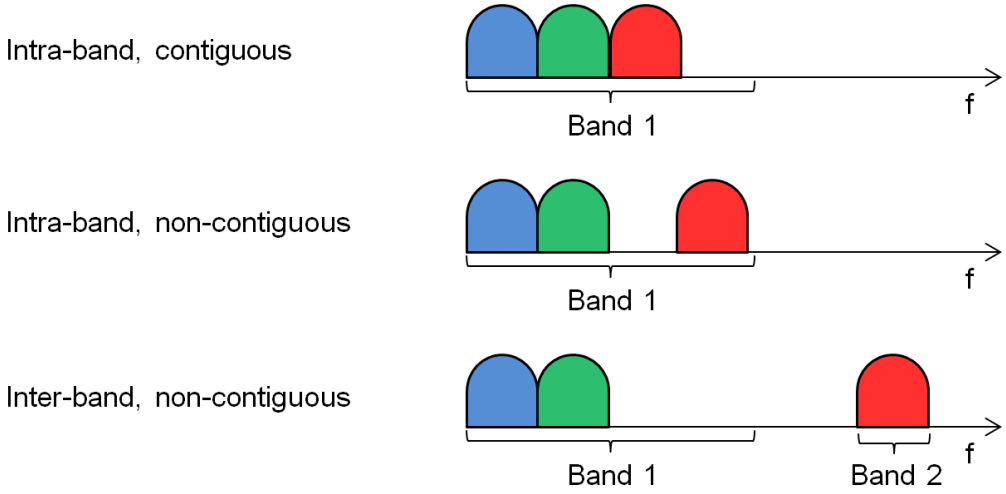

Figure 2.6. Types of CA (adapted from [Wann12]).

Concerning the improvements in MIMO configurations, LTE-A supports DL transmission with up to 8 transmit antennas, which, together with 8 receivers at the UE, corresponds to the 8×8 configuration. In UL, the UE is dimensioned to support up to four transmitters, the physical space required for the antennas being the main issue, leading to the 4×4 configuration in UL when combined with four eNodeB receivers [Agil11]. These enhancements allow the increase of peak data rates and spectral efficiency, but they also increase radiated power of the BS, due to the introduction of more antennas.

Another new component introduced in LTE-A is relaying, which is a method of improving coverage in difficult conditions. The main use cases for relays are to improve urban and indoor throughput, to add dead zone coverage, or to extend coverage in rural areas. This is made by a Relay Node (RN), which basically acts as a repeater: it receives, amplifies and retransmits DL and UL signals [Agil11]. It is connected to a Donor eNodeB (DeNB), which takes care of the data connection towards the core

network. Compared to the eNodeBs implemented in macro-cells (macro-eNodeBs), the RNs have lower transmit power, and the backhaul is done wirelessly, so that its deployment is easier, enabling the implementation of LTE in places where it is hard to get a wired line backhaul.

Finally, with the increase of the data traffic and the number of subscriptions, there is the need for capacity enhancement, which, in densely populated areas, can be achieved with smaller cells, from macro- to micro- and pico-cells, and, in some cases, even to femto-cells. Thus, as there are several types of cells being used in the same network, the network is considered a heterogeneous one, which, for the aforementioned reasons, has to be considered in the deployment of LTE-A. Figure 2.7 shows an example of a heterogeneous network.

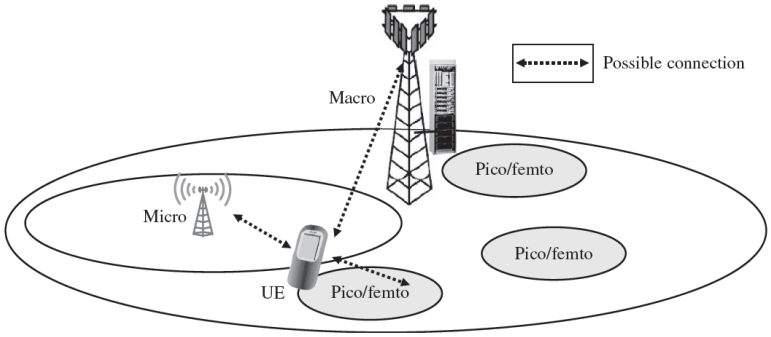

Figure 2.7. Heterogeneous network (extracted from [HoTo11]).

2.3 Services and Applications

The type of the MT usage depends on the services and applications, being useful for the assessment of the exposure, as the user can handle the MT near the head (*e.g.*, voice) or in different positions further from it (*e.g.*, data). Data services have, nowadays, the main role in mobile communications, due to the latest generations of mobile systems, with other services being supplied beyond the ones supplied by previous generations [Corr13], so that several data applications providing contents to the users exist, motivated by the wide diversity of multi-service MTs, such as tablets and smartphones.

According to these developments, an MT can run a variety of applications, each one having different QoS requirements, leading to the need of creating classes of services, *i.e.*, grouping services into classes according to their characteristics [Corr13]. In 3GPP specifications, four different UMTS QoS classes are defined: conversational, streaming, interactive, and background. The main distinguishing factor between them is the delay sensitiveness: the conversational class is the most sensitive to delay, in opposite to the background one, which is the less sensitive. Due to the high delay requirements, conversational and streaming classes are mainly meant to be used to carry real time data flows, while interactive and background classes are intended to be used by traditional internet applications, as these have lower delay requirements [3GPP12].

The conversational class is the only one where the required characteristics are strictly given by human perception, being characterised by low end-to-end delay and symmetric, or nearly symmetric, traffic between UL and DL in person-to-person communications, being applied to video and audio conversation. The streaming class is applied when the user is consuming real time video (or audio), requiring bandwidth like conversational class, but more flexibly concerning the delay, tolerating some delay variations. The interactive class has to do with services where the end-user interacts with the remote equipment, requesting data and expecting the response within a certain time, such as in web browsing. In the background class, the end-user sends and receives data in the background, where it is assumed that the destination is not expecting the data within a certain time, *e.g.*, the background delivery of e-mails and SMSs [3GPP12] and [HoTo04]. These QoS classes, as well as the main attributes associated to them, are summarised in Table 2.2, being available in more detail in [3GPP12].

Table 2.2. UMTS Class of Services (adapted from [Corr13] and [3GPP12]).

Service Class	**Conversational**	**Streaming**	**Interactive**	**Background**
Real Time	Yes	Yes	No	No
Symmetric	Yes	No	No	No
Switching	CS	CS	PS	PS
Guaranteed Rate	Yes	Yes	No	No
Delay	Minimum Fixed	Minimum Variable	Moderate Variable	High Variable
Buffer	No	Yes	Yes	Yes
Bursty	No	No	Yes	Yes
Example	Voice	Video Streaming	Web Browsing	E-mail, SMS

The need for support of these multiple QoS requirements by the EPS leads to the definition of different bearers, each one being associated with a QoS [SeTB11].

An EPS bearer, or simply bearer, identifies packet flows that receive common QoS treatment, *i.e.*, all the packet flows corresponding to the same bearer have the same treatment [Ekst09]. Bearers can be classified into two categories, based on the nature of the QoS they provide: Guaranteed Bit Rate (GBR) bearers, which have an associated GBR value with a permanent allocation of transmission resources when the bearer is established/modified; and non-GBR bearers, which do not guarantee any particular bit rate, so the services using this type of bearers, like web browsing or File Transfer Protocol (FTP), must be prepared to experience congestion-related packet loss, *i.e.*, packet losses caused by overflowing offers, which do not occur in GBR bearers if the associated GBR QoS parameter is satisfied, adequate for services like Voice over IP (VoIP) [SeTB11] and [Ekst09].

In the specifications, a limited set of QoS parameters are included [SeTB11] and [HoTo11]:

- QoS Class Identifier (QCI), an index that identifies a set of logically configured values for priority, delay and loss rate, which is signalled instead of the values of these parameters. For the two bearer categories (GBR and non-GBR), nine QCIs are specified for LTE, as shown in Table 2.3, wherein to each bearer is associated one of these QCIs;

- Allocation and Retention Priority (ARP), used for admission control, *i.e.*, to decide if the requested bearer should be established or not in case of radio congestion, and also to indicate the priority of a bearer related to the others;
- Maximum Bit Rate (MBR), identifying the maximum bit rate for the bearer;
- Guaranteed Bit Rate (GBR), which specifies the minimum bit rate for the bearer, *i.e.*, the bit rate that is guaranteed to the bearer;
- Aggregate Maximum Bit Rate (AMBR), which indicates the total maximum bit rate that a UE may have for all the bearers in the same PDN connection, as many IP flows may be mapped to the same bearer. This enables the operators to limit the total amount of bit rate consumed by a single subscriber [Ekst09].

The specified QCIs for LTE are present in Table 2.3, where, for each class, the parameters' values are specified: the resource type, which indicates the bearer class associated to them; the priority, used to specify the priority for the packet scheduling of the radio interface; and the loss rate, that helps to use appropriate Radio Link Controller (RLC) settings, such as the number of re-transmissions [HoTo11]. Furthermore, some services examples are also indicated for each QCI.

Table 2.3. Specified QCIs for LTE (extracted from [3GPP13a]).

QCI	Resource Type	Priority	Packet Delay Budget [ms]	Packet Error Loss Rate	Example Services
1	GBR	2	100	10^{-2}	Conversational Voice
2		4	150	10^{-3}	Conversational Video (Live Streaming)
3		3	50	10^{-3}	Real Time Gaming
4		5	300	10^{-6}	Non-Conversational Video (Buffered Streaming)
5	Non-GBR	1	100	10^{-6}	IP Multimedia Subsystem (IMS) Signalling
6		6	300	10^{-6}	Video (Buffered Streaming) Transmission Control Protocol (TCP)-based (e.g., www, e-mail, chat, FTP, peer-to-peer file sharing, progressive video, etc.)
7		7	100	10^{-3}	Voice, Video (Live Streaming) Interactive Gaming
8		8	300	10^{-6}	Video (Buffered Streaming) TCP-based (*e.g.*, www, e-mail, chat, peer-to-peer file sharing, progressive video, etc.)
9		9			

2.4 Coexistence of LTE with Other Systems

Other systems coexisting with LTE in the same frequency ranges have to be taken into account when analysing the exposure from the user viewpoint, as all systems contribute to the total power to which the user is exposed. The most relevant systems are GSM and UMTS, the other cellular systems, which have some frequency bands in common with LTE.

Concerning GSM, its first version operates in frequencies around 900 MHz (GSM900), in which the defined frequency ranges are [890, 915] MHz for UL and [935, 960] MHz for DL. For the 1800 MHz GSM version (GSM1800), the frequency ranges are [1710, 1785] MHz for UL, and [1805, 1880] MHz for DL. This system employs a combination of FDMA and TDMA, using FDD as duplex scheme. FDMA divides both DL and UL frequency bands into 200 kHz radio frequency channels, with TDMA being applied to each of these sub-bands, which are shared by 8 users, each user corresponding to a 576.92 μs time slot [Moli11].

In what refers to the GSM maximum output power, eight classes are defined for the transmitters, the maximum output power for macro-cell BS ranging in [34, 58] dBm, whereas for micro-cell it ranges in [9, 32] dBm; for the MT, or Mobile Station (MS), the logical designation of the MT for GSM, the values range in [29, 39] dBm [Corr13], with typical maximum values being 33 dBm (2 W). The detailed values corresponding to each class are present in Table 2.4. In GSM, power control is used for DL and UL, in the BS and in the MT, respectively [Corr13].

Table 2.4. GSM maximum output powers (adapted from [Corr13]).

Power Class	**Maximum Output Power [dBm]**					
	BS				**MT**	
	Macro-Cell		**Micro-Cell**			
	900 MHz	**1800 MHz**	**900 MHz**	**1800 MHz**	**900 MHz**	**1800 MHz**
1	[55, 58]	[43, 46]	]19, 24]	]27, 32]	39	30
2	[52, 55[	[40, 43[	]14, 19]	]22, 27]	37	24
3	[49, 52[	[37, 40[	]9, 14]	]17, 22]	33	36
4	[46, 49[	[34, 37[			29	
5	[43, 46[					
6	[40, 43[					
7	[37, 40[					
8	[34, 37[					

UMTS is based on WCDMA, a wideband Direct Sequence-Code Division Multiple Access (DS-CDMA) system, wherein the user information bits are spread over a wide bandwidth, by multiplying the user data with quasi-random bit sequences (chips) derived from Code Division Multiple Access (CDMA) spreading codes, each user having access to an orthogonal code. FDD and TDD are the supported modes of operation: in FDD, carrier frequencies separated by 5 MHz are used for DL and UL, while in

TDD only one 5 MHz carrier is shared by DL and UL [HoTo04]. This system works in the 2100 MHz band and, more specifically, in the case of Europe and most of Asia, FDD mode operates in [2110, 2170] MHz for DL, and in [1920, 1980] MHz for UL, whereas for TDD there are assigned frequencies in [1900, 1920] MHz and in [2010, 2025] MHz (which, however, is not operational), although GSM bands can also be used [HoTo04] and [Corr13].

There is no upper limit defined for the maximum output power for a macro-cell BS, but, typically, it varies in [40, 46] dBm [NaDA06]. For the UE, power is below the maximum level of 33 dBm (power class 1) [Corr13]. The values defined for the different UE power classes, as well as for the UMTS BS, relatively to cell types, are presented in Table 2.5, the values for UE having a tolerance of ±2 dB for power class 4 and +1/-3 dB for the others. It is also important to refer that, as in GSM, in UMTS there is power control in both BS and UE [Corr13].

Table 2.5. Maximum UMTS output power for BS and UE (adapted from [3GPP09] and [Corr13]).

Maximum Output Power [dBm]							
BS				**UE**			
Cell Type				**Power Class**			
Macro	**Micro**	**Pico**	**Femto**	**1**	**2**	**3**	**4**
-	38	24	20	33	27	24	21

BS antennas used for transmission can be classified, according to their radiation patterns on the horizontal plane, as [Corr13]: omnidirectional (omni), radiating in all directions azimuthally, and sector, which have directive characteristics, mainly radiating into a specific direction (service area). On the other hand, MT's antennas are generally non-directive, having low gains, usually ranging in [0, 2] dBi, but the best way to model the MT's antenna gain is to assume a uniform radiation pattern in all directions (isotropic antenna), with the antenna gain of 0 dBi, as mentioned in [NaDA06].

Typical gain values of BS transmitting antennas in GSM, UMTS and LTE are shown in Table 2.6, according to the antenna classification, and its operation environment (indoor and outdoor).

Table 2.6. Typical gain values for GSM, UMTS and LTE antennas (adapted from [Antu12], [Kath12], [Comm13] and [Telc13]).

		Gain [dBi]					
Antenna Type		**GSM**		**UMTS**	**LTE**		
		900 MHz	**1800 MHz**		**800 MHz**	**1800 MHz**	**2600 MHz**
Indoor	**Omni**	[2, 7]	[2, 7]	[2, 7]	[2, 7]	[2, 7]	[2, 7]
	Directional	[5, 7]	[5, 7]	[5, 7]	[5, 7]	[5, 8]	[5, 7]
Outdoor	**Omni**	[2, 11]	[2, 11.8]	[2, 11.8]	[2, 11]	[2, 11.8]	[2, 11]
	Directional	[5, 22]	[5, 24.2]	[2.9, 24.2]	[2.9, 19.3]	[5, 21.8]	[8, 19.5]

Besides GSM and UMTS, some other systems can operate within the frequency bands assigned for LTE in Europe, or in between them, *i.e.*, in the frequency range of [800, 2600] MHz, the most relevant

for the analysis done in this work being Wireless Fidelity (WiFi), which has several versions, most of them operating in the 2400 MHz band and having a maximum typical Equivalent Isotropic Radiated Power (EIRP) of 100 mW (20 dBm) [OlMC13].

The other systems operating in the LTE band, such as Bluetooth or Digital Enhanced Cordless Telecommunications (DECT), the dominant standard for cordless phone systems in Europe [Moli11], are listed in Annex B.

2.5 Exposure to Radiation

Several parameters can be used to quantify the exposure to electromagnetic radiation, the basic one being the Specific Absorption Rate (SAR), which is the power dissipated by mass unit, not possible to measure under normal operating conditions. Practical assessment parameters derived from SAR, also known as reference parameters, are the electric (E) and the magnetic (H) fields strength, or the power density (S) of radiated waves, which are easy to measure [Corr13].

The effects of radiation in human beings can be of three types: thermal, related to the increase of body temperature, which depends on the period of exposure; non-thermal, where research is still being conducted, still not existing definitive conclusions on this matter; and psycho-somatic, which are a consequence of the general public perception of danger of the exposure to radiation, also caused by the alarm raised by the media [Corr13].

Different worldwide bodies, like ICNIRP, have established guidelines to limit electromagnetic exposure, in order to provide protection against adverse health effects. These guidelines need to be taken into account when assessing the exposure to radiation in public accessible areas, *i.e.*, there are reference levels that have to be compared with the measured values of physical quantities. If the measured values comply with the reference levels, the compliance with basic restrictions (SAR) is ensured; otherwise, a more detailed analysis is necessary to assess compliance. In situations of simultaneous exposure, and taking into consideration the frequency band under study, the following requirement for the electric field level should be applied [ICNI98]:

$$\sum_{i>800\ MHz}^{2600\ MHz} \left(\frac{E_{i[\mathrm{V/m}]}}{E_{L,i[\mathrm{V/m}]}} \right)^2 \leq 1 \tag{2.1}$$

where:

- E_i: electric field strength at frequency i;
- $E_{L,i}$: electric field reference level for frequency i.

A whole-body average SAR of 0.08 W/kg is a restriction that provides adequate protection for general public exposure. The reference levels for the general public exposure provided by ICNIRP are presented in Table 2.7, referring to the frequency bands of interest to this work.

There are several works assessing the LTE exposure through *in situ* measurements, verifying if

ICNIRP's reference levels are verified, some of them comparing LTE exposure levels with other Radiofrequency (RF) sources and concluding about the contribution of each of the systems to the exposure. Besides the measurements and the experimental results, there are also some methods described to determine and extrapolate the LTE exposure values.

Table 2.7. ICNIRP reference levels for general public exposure (adapted from [ICNI98]).

f [MHz]	E [V/m]	H [A/m]	S [W/m^2]
[400, 2 000]	$1.375f^{1/2}$	$0.0037f^{1/2}$	$f/200$
[2 000, **300 000]**	61	0.16	10

In [JVGV10], *in situ* electromagnetic field exposure of the general public to fields from LTE BSs is assessed, where the authors compare the exposure contribution due to different RF sources with the LTE exposure at 30 randomly selected measurement locations, in the urban environment of Stockholm, Sweden. The electromagnetic field measurements were made in [80, 6000] MHz, being verified that the total exposure satisfies ICNIRP reference levels in all locations, with electric field values ranging in [0.2, 2.6] V/m. For LTE, the measured exposure levels go up to 0.8 V/m, with an average and maximum contributions of its signal to the total RF exposure of 4.1% and 23.2%, respectively. It is also concluded that, in general, the RF exposure in Stockholm is dominated by GSM and UMTS (HSPA).

A similar assessment is made in [JVGV12a], where *in situ* exposure of different RF sources is characterised, also comparing LTE electric field levels with other RF sources, and proposing an extrapolation method to estimate the worst case LTE exposure, based on the measurement of the Reference Signal (RS) and of the Secondary Synchronisation Signal (SSS). The measurements were made in the same frequency range, at 40 locations in an urban environment of Reading, United Kingdom, the results showing that ICNIRP reference levels are satisfied, wherein the maximum total electric field is 4.5 V/m, dominated by Frequency Modulation (FM) radio systems at 55% of the measurement locations. Concerning LTE, its signal has a contribution to the total exposure of 0.4% (average) and 4.9% (maximal), and average and maximal exposure values of 0.2 V/m and 0.5 V/m, respectively. Applying the extrapolation method, the maximal extrapolated field value equals 1.9 V/m, being 32 times below ICNIRP reference levels for electric fields.

The assessment of the RF exposure due to emerging mobile communications systems made in [JVGV12b] is analogous to the previous ones, with 311 measurement locations spread over Belgium, Netherlands and Sweden, selected to characterise different types of environments, with LTE measurements only being made in Sweden, corresponding to the 30 locations referred in [JVGV10]. The obtained results show that the maximum total electric field equals 3.9 V/m, measured in a residential environment, being mainly due to GSM900 signals. It is also observed that exposure is the highest in urban environments and the lowest in rural ones, with the technologies that dominate outdoor and indoor exposures being GSM900 and DECT, respectively. Concerning their contributions to the total electric field, GSM900 has the higher contribution, 60%, UMTS (HSPA) has an average contribution of more than 3%, except for rural environments, and WiMAX and LTE have a contribution

of less than 1%, on average, which is explained by the wider deployment of GSM900 comparing to emerging technologies.

Concerning the methods for the evaluation of exposure values through measurements, the authors in [PyMu12] propose two different methods for LTE BS field measurements: code and frequency selectivities. The code selective method is based on the determination of the radiated field produced by the RS of the DL signal, while the frequency one is based on the power of the Primary Synchronisation Signal (PSS) and of SSS. These values are used to determine the extrapolated electric field strength, so that one can obtain the appreciation value and assess the compliance or non-compliance of an installation with the reference levels. With the code selective method, it is possible to assess both compliance or non-compliance, being considered as the reference method, while the frequency selective is considered as an approximate method, as only the compliance of an installation can be shown, due to the overestimating of the extrapolated field strength.

A distinct approach is presented in [BoSc11], where a measurement campaign on LTE exposure was performed at 77 measurement points, in five German cities, using a method that consists of determining the highest signal amplitude produced by one of the synchronisation signals, or by the PBCH, and multiply the exposure value by an extrapolation factor. The values obtained for the extrapolated exposure range in [0.001, 7.5] V/m, the median being 0.2 V/m, very low values regarding ICNIRP reference levels. A similar approach is proposed in [VJGV12], as it focuses on the measurement of PBCH, enabling the use of a basic spectrum analyser instead of expensive dedicated LTE decoders. This is validated both *in lab* and *in situ*, for a Single Input Single Output (SISO) LTE system, as well as for a MIMO 2×2 one, showing low deviations from the signals measured using dedicated LTE decoders. The same approach is also presented in [FeGW11].

Finally, concerning the exposure due to LTE terminals, [ShGD12] presents a simulation model of an LTE UE terminal with MIMO antenna, used to evaluate the corresponding SAR, and to make a comparison with other systems. From the simulation and the measurement results, it can be seen that LTE terminals with MIMO antennas can produce more electromagnetic radiation, leading to the highest SAR value. It is also concluded that some effective methods for antenna design to reduce SAR should be proposed, something that is made in [Tang12] with the introduction of some SAR reduced solutions for LTE UE antennas. Another related study is [ZZYB12], where the SAR of different LTE MIMO antennas designs is investigated.

Chapter 3

Model Development and Implementation

In this chapter, the description of the model is firstly presented, detailing the theoretical aspects taken into account. Then, an overview of the simulator is done, where its main components are described, followed by the description of the algorithms implemented on the simulator. Finally, an assessment of the simulator is done, including some test cases, in order to validate it.

3.1 Model Description

This section describes the models used for the theoretical calculation of exposure values, given by power density, in order to assess the LTE contribution, and presents an overview of the implemented simulator, its algorithms and an assessment to evaluate it.

3.1.1 DL Model for Outdoor Exposure

The exposure regarding DL has to do with the power radiated by the BS (or BSs) that reaches the user. Depending on the distance that the user is from the BS, the electromagnetic fields have different behaviours, so that three regions are identified: the reactive near-field, the radiating near-field and the far-field [SeBC12]. As, in this case, it is only relevant to distinguish between the near- and far-field, the reactive and radiating near-field regions are simply considered as near-field, so that the distance from which far-field region is verified is given by [SeBC12]:

$$r \geq \frac{2D^2_{[\mathrm{m}^2]}}{\lambda_{[\mathrm{m}]}} \tag{3.1}$$

where:

- r: distance from the radiating element to the point of investigation;
- D: largest dimension of the antenna;
- λ: wavelength.

The typical values for the largest dimension of the antennas used in mobile communication systems are presented in Table 3.1, as well as the values for the minimum far-field distances, where a worst case perspective is taken into account, *i.e.*, considering the highest frequency in each band [SeBC12].

Table 3.1. Typical values for antennas' dimensions and far-field distances (adapted from [SeBC12]).

	GSM		**UMTS**	**LTE**			**WiFi**
	900 MHz	**1800 MHz**		**800 MHz**	**1800 MHz**	**2600 MHz**	**2400 MHz**
Largest dimension of the antenna [m]	2.6		2.6	2.6			0.26
Minimum far-field distance [m]	43.26	84.73	97.80	38.85	84.73	121.23	2.58

The influence of the environment is considered, taken as the reflections on the surrounding buildings, or on the ground. The assumptions in this model are depicted in Figure 3.1, where the user is in the centre of a typical urban street, with buildings on the two sides, and a BS antenna on the roof-top of a building. Due to multipath, several rays reach the user, contributing to DL exposure; hence, besides the direct ray, two first-order reflected rays are considered: the ray that reflects on the building and reaches the user, and the one that reflects on the ground before reaching the user.

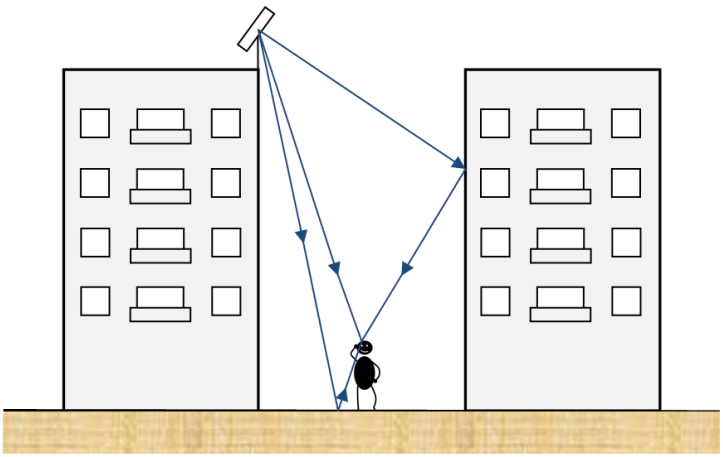

Figure 3.1. Typical scenario considered in the model.

In order to obtain the received power at the MT, one can use (3.2), taking the propagation as the interference between the direct ray and the several possible reflected rays. Therefore, according to [FiFe03], the general expression for the power available at the receiving antenna is written as:

$$P_{r[\mathrm{W}]} = \frac{P_{t[\mathrm{W}]} G_t G_r}{(4\pi)^2} \frac{\lambda^2_{[\mathrm{m}^2]}}{r^2_{[\mathrm{m}^2]}} \left| 1 + \sum_{i=1}^{N_{rr}} \frac{r_{[\mathrm{m}]}}{r_{i[\mathrm{m}]}} g_i \Gamma_i e^{jk_{[\mathrm{m}^{-1}]}\Delta r_{i[\mathrm{m}]}} \right|^2 \tag{3.2}$$

where:

- P_r: power available at the receiving antenna;
- P_t: power fed to the transmitting antenna;
- G_t: transmitting antenna gain;
- G_r: receiving antenna gain;
- N_{rr}: number of reflected rays ($N_{rr} = 2$ in the case of Figure 3.1);
- r_i: length of the reflected ray i;
- g_i: transmitting antenna gain in the direction of the reflected ray i, normalised to the gain in the direction of the direct ray;
- Γ_i: reflection coefficient associated to surface of the reflected ray i;
- k: propagation constant;
- Δr_i: path length difference between the direct ray and reflected ray i.

Each carrier corresponds to a radio channel, which is assigned according to the spectrum band that a mobile operator has for the system, as the BS is assumed to correspond to a mobile operator. The centre frequencies of each of the carriers can be assigned considering the radio channel separation of the system, as given by [Corr13]:

$$f_{c\,n[\mathrm{Hz}]} = f_{c\,min[\mathrm{Hz}]} + n\Delta f_{cs[\mathrm{Hz}]}\ , \qquad n = 1,2,3,\ldots \tag{3.3}$$

where:

- $f_{c\,n}$: radio channel centre frequency;
- $f_{c\,min}$: minimum of the spectrum band;
- Δf_{cs}: radio channel separation.

For each of the carriers, the maximum transmission power is considered, although DL power control exists in GSM and UMTS, because one is considering a worst case analysis, so that it is assumed that, although the user is not requiring the maximum power, there are other users in the cell edge, for instance, requiring the maximum transmission power, with the user being exposed to that power, as it is near the BS. More specifically, in GSM, power control controls the time-slot assigned to the user; the other 7 time-slots corresponding to other users, which are assumed to require the maximum transmission power. In the case of UMTS, the user has a code assigned, where the total transmission power is distributed by the codes, assigned to different users. Even if the user is not requiring the maximum power, the power is distributed for the other users, so that, in this context, the transmission power is the maximum.

According to (3.2), the received power exhibits a sequence of maximum and minimum values over a function decreasing with $1/r^2$, which corresponds to free space values, being due to the interference between the several rays. For the first values of r, due to the higher path length difference, the oscillations of the received power are higher, being much lower for high distances, as the path length difference decreases with the distance. As presented in [FiFe03], when only two rays are considered, there is a distance from which the sum of the direct and the reflected rays on the ground depends on the distance proportionally to $1/r^4$, but, when considering also the rays reflected on the building, as the power associated to each of them decrease with, approximately, $1/r^2$, this is the behaviour that predominates.

Also according to [FiFe03], there is a distance from which the power decreasing rate becomes higher than $1/r^2$, which is much larger than the one when considering only two rays, being due to the environment obstacles (*e.g.*, cars and trees), which is unavoidable when considering large distances between the BS and the MT. In the scenario under study, one does not consider any obstacles in the street, so that this effect is not verified, and the power should decrease according to $1/r^2$.

If the antenna pattern is considered, the MT received power could increase as the user moves away from the BS, due to the MT approximation to the maximum of the radiation pattern, where it would reach a maximum value. Then, it would decrease again. This behaviour is not observed, as one assumes the typical antenna maximum gain for all links, as the BSs can have different orientations, and it is not easy to specifically know the orientation of each one, being the worst case design, as this is an adequate approach when analysing exposure.

Regarding the reflection coefficient used in (3.2), Γ, it depends on the characteristics of the reflection surface, namely on the building and ground surfaces. A statistical approach is considered, taking a Uniform Distribution to describe this parameter, with its value being within [-10, -3] dB [FeAm03].

The difference in paths between the direct and reflected rays is determined through the expressions for the three rays taken into account, Figure 3.1, which are valid for the situation where the user is varying the position and moving away from the BS. To derivate these expressions, such that it is also applicable for the different user positions, and for the number of BS on the buildings' roof-tops, a reference is assumed in the BS of the building of the left, so that one can obtain the coordinates of the user, and of other possible BSs on the scenario, being useful to obtain the expressions for the lengths

of the rays. The expressions obtained by the geometry of the scenario are basically composed of a vertical component (height), and the distance from the MT to the BS in the horizontal plane.

For the length of the direct ray, which gives the distance between the radiating element to the point of investigation, and based on the geometry presented in Figure 3.2, the expression is the following:

$$r_{[\mathrm{m}]} = \sqrt{\left(h_{b[\mathrm{m}]} - h_{m[\mathrm{m}]}\right)^2 + \left(x_{u[\mathrm{m}]} - x_{BS[\mathrm{m}]}\right)^2 + \left(y_{u[\mathrm{m}]} - y_{BS[\mathrm{m}]}\right)^2} \tag{3.4}$$

where:

- h_b: height of BS antenna;
- h_m: height of MT antenna;
- x_u: coordinates of the user in the *x*-axis;
- x_{BS}: coordinates of the BS in the *x*-axis;
- y_u: coordinates of the user in the *y*-axis;
- y_{BS}: coordinates of the BS in the *y*-axis.

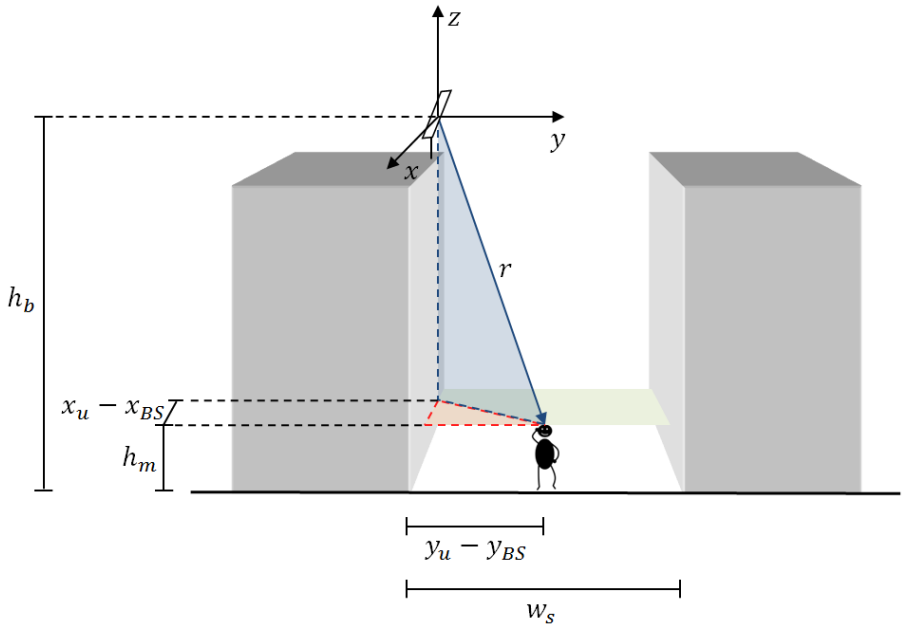

Figure 3.2. Scenario's geometry for the direct ray.

On the other hand, the length of the reflected ray on the building can be derived through the geometry of Figure 3.3, where one makes use of the user's image regarding the vertical plane to obtain the following expression:

$$r_{b[\mathrm{m}]} = \sqrt{\left(h_{b[\mathrm{m}]} - h_{m[\mathrm{m}]}\right)^2 + \left(x_{u[\mathrm{m}]} - x_{BS[\mathrm{m}]}\right)^2 + \left(2w_{s[\mathrm{m}]} - \left|y_{u[\mathrm{m}]} - y_{BS[\mathrm{m}]}\right|\right)^2} \tag{3.5}$$

where:

- r_b: length of the ray reflected on the building;
- w_s: street width.

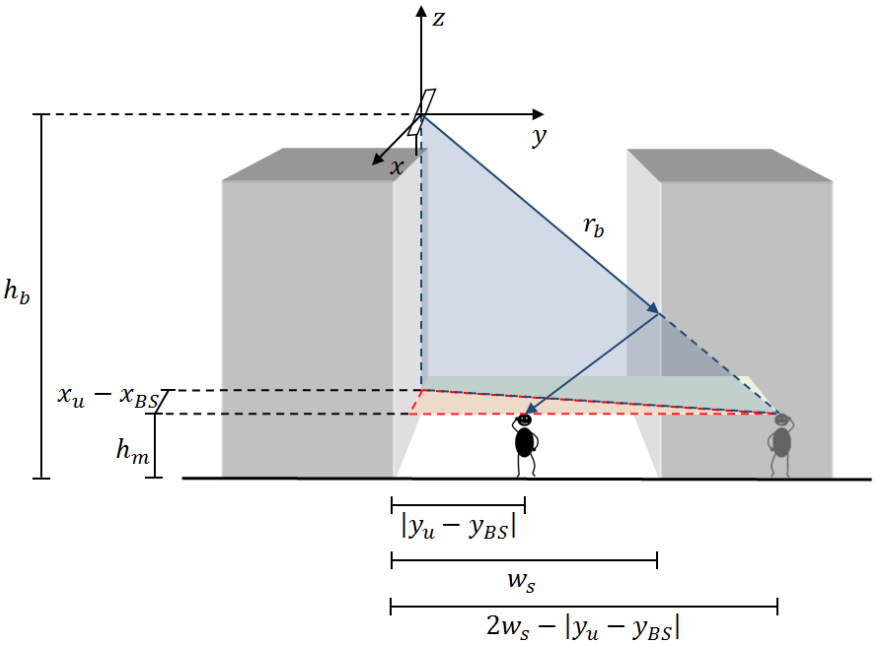

Figure 3.3. Scenario's geometry for the ray reflected on the building.

Finally, the third ray, the one reflecting on the ground and whose geometry is depicted in Figure 3.4, considering the user's image related to the horizontal plane, the expression is given by:

$$r_{g[\mathrm{m}]} = \sqrt{\left(h_{b[\mathrm{m}]} + h_{m[\mathrm{m}]}\right)^2 + \left(x_{u[\mathrm{m}]} - x_{BS[\mathrm{m}]}\right)^2 + \left(y_{u[\mathrm{m}]} - y_{BS[\mathrm{m}]}\right)^2} \tag{3.6}$$

where:

- r_g: length of the ray reflected on the ground.

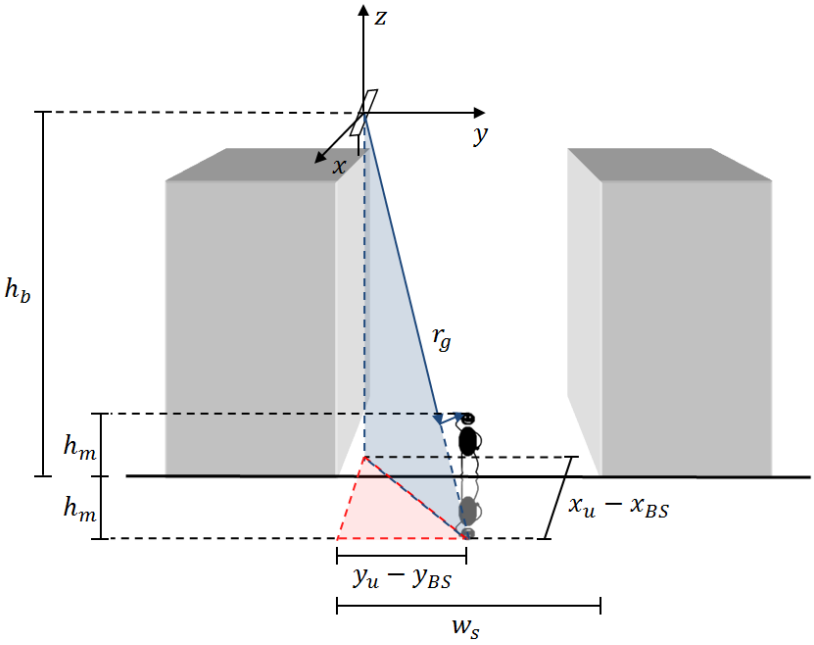

Figure 3.4. Scenario's geometry for the ray reflected on the ground.

Besides cellular systems, other systems such as WiFi can be taken into account when analysing exposure. To analyse the received power concerning these systems, the free space propagation

model is used, as it is the model where the path loss is minimum, and a more accurate model would be ray tracing, which, due to its complexity, is not considered. Thus, free space corresponds to the worst case design, with the received power being given by:

$$P_{r[\mathrm{W}]} = \left(\frac{\lambda_{[\mathrm{m}]}}{4\pi r_{[\mathrm{m}]}}\right)^2 P_{t[\mathrm{W}]} G_t G_r \tag{3.7}$$

To evaluate the exposure and to compare with the reference levels, one needs to convert the received power into the reference parameters. In order to assess if the obtained values comply with the reference ones, one can focus in one of these parameters, which, in this context, is power density, relating with the received power by the following expression:

$$P_{r[\mathrm{W}]} = S_{r[\mathrm{W/m^2}]} A_{e[\mathrm{m^2}]} \tag{3.8}$$

where:

$$A_{e[\mathrm{m^2}]} = \frac{\lambda^2_{[\mathrm{m^2}]}}{4\pi} G_r \tag{3.9}$$

- S_r: received power density;
- A_e: antenna effective area.

Once determined the received power, (3.2), one can get the exposure value in DL, assuming it as the power density that reaches the MT, with the DL power density being obtained by the following expression, which comes from (3.8):

$$S_{DL[\mathrm{W/m^2}]} = \frac{P_{r[\mathrm{W}]}}{A_{e[\mathrm{m^2}]}} \tag{3.10}$$

where:

- S_{DL}: DL power density.

3.1.2 UL Model for Outdoor Exposure

The UL component is relevant in the exposure assessment, as the user is not only exposed to the power that comes from the BS (DL), but also to the one radiated by the MT. Thus, in UL, one needs to evaluate the power radiated by the MT that reaches the user, which is in the near-field of the MT antenna, having power control into account, as all the cellular systems use power control in UL.

The power radiated by the MT is defined to be such that the target received power at the BS is satisfied, depending on path loss, whose expression is part of the Link Budget, Annex C, being useful to be rewritten:

$$L_{p[\mathrm{dB}]} = P_{EIRP[\mathrm{dBm}]} - P_{r[\mathrm{dBm}]} + G_{r[\mathrm{dBi}]} \tag{3.11}$$

where:

- L_p: path loss;
- P_{EIRP}: Effective Isotropic Radiated Power.

As the path is the same in both DL and UL, DL values are considered in the calculation of the path loss. Also from (3.11), and taking sensitivity calculation into account, which is also included in Annex

C, the MT's EIRP is determined such that the target received power is achieved, which is a value that guarantees that the receiver sensitivity is satisfied. Thus, the expression is the following:

$$P_{EIRP[\text{dBm}]}^{UL} = L_{p[\text{dB}]} + P_{r\ target[\text{dBm}]} - G_{r[\text{dBi}]} + L_{u[\text{dB}]} \quad (3.12)$$

where:

$$P_{r\ target[\text{dBm}]} = P_{Rx\ min[\text{dBm}]} + L_{c[\text{dB}]} + M_{s[\text{dB}]} \quad (3.13)$$

- P_{EIRP}^{UL}: UL EIRP;
- $P_{r\ target}$: target value for the available power at the receiving antenna;
- L_u: user losses;
- $P_{Rx\ min}$: receiver sensitivity;
- L_c: cable losses between the transmitter and the antenna;
- M_s: safety margin.

The sensitivity values depend on the SNR, which is obtained by its relation with throughput. One considers the SNR from which the throughput saturates and becomes constant, corresponding to the maximal throughout and, thus, to the higher SNR (worst case analysis), leading to the values presented in Annex C. Regarding the safety margin, it is typically used to guarantee that the target value satisfy the minimum required by the receiver (sensitivity), typically being around 30 dB, in order to prevent the effects that are not taken into account by reducing the value at the receiver to a value below the minimum required.

For the situation where the user is moving away from the BS, varying the position along the street, the value obtained for the MT EIRP also varies, depending on the position of the user related to the BS. Hence, power control aims to maintain the received signal at the MT constant. Considering power control such that it adds the necessary power to achieve the target power value, when the user is moving away from the BS, it implies that the MT EIRP needs to be re-determined at each position, through (3.12). At each point, the model is applied to obtain the values, but, in practice, the target received power at the BS remains constant, and only the path loss changes from one position to another, so that the changes into the radiated power in the UL can be interpreted as follows, which gives the EIRP corresponding to the position of analysis:

$$P_{EIRP,k[\text{dBm}]}^{UL} = P_{EIRP,k-1[\text{dBm}]}^{UL} + \Delta P_{[\text{dB}]} \quad (3.14)$$

where:

$$\Delta P_{[\text{dB}]} = (L_{P,k[\text{dB}]} - L_{P,k-1[\text{dB}]}) \quad (3.15)$$

- $P_{EIRP,k}^{UL}$: UL EIRP corresponding to the position k;
- $P_{EIRP,k-1}^{UL}$: EIRP corresponding to the previous position, $k-1$;
- ΔP: power compensation;
- $L_{P,k}$: path loss regarding the position of analysis k;
- $L_{P,k-1}$: path loss regarding the previous position, $k-1$.

From the exposure viewpoint, the power that is relevant to consider in UL is the power that is absorbed by the user, meaning that the power to which the user is exposed is equivalent to the power

that the user absorbs, which can be obtained through the user losses. This value is obtained through the difference between the MT radiated power and the power that is not lost in the user, being given by the following expression:

$$P_{abs[\mathrm{W}]} = P_{EIRP[\mathrm{W}]}^{UL} - \frac{P_{EIRP[\mathrm{W}]}^{UL}}{L_u} = P_{EIRP[\mathrm{W}]}^{UL}\left(1 - \frac{1}{L_u}\right) \tag{3.16}$$

where:

- P_{abs}: power absorbed by the user.

Similarly to DL, one needs to obtain the exposure in UL in terms of the reference parameter. As the process to accurately obtain this quantity involves the use of numerical tools, which goes beyond of the scope of this thesis, one assumes that the exposure is the UL power density that is obtained by dividing the absorbed power by the area of the absorption surface, as given by:

$$S_{UL[\mathrm{W/m^2}]} = \frac{P_{abs[\mathrm{W}]}}{A_{abs\ [m^2]}} \tag{3.17}$$

where:

- S_{UL}: UL power density;
- A_{abs}: absorption surface area.

Regarding the determination of the power absorbed by the user, one assumes that the losses due to the user are according to values available in [PFKP10], where the absorption loss for different antennas and configurations for both voice and data modes is investigated. It presents the values obtained by simulation for each mode and for two frequency bands: 900 and 1800 MHz. As one also needs to account for other frequency bands, the values of user losses can be obtained through the ones presented in this study, making an extrapolation assuming a linear behaviour of this parameter over $20\log(f_{[\mathrm{Hz}]})$. For voice, the maximum value verified in 900 MHz is 11.9 dB, and around 10.1 dB for 1800 MHz; for data, and assuming the same tendency of the user losses for voice, *i.e*, higher values for lower frequencies, one can get values around 4.4 dB for 900 MHz, and around 3.9 dB for 1800 MHz. Having these values, one can obtain the tendency for user losses for voice and data, which are shown in Figure 3.5.

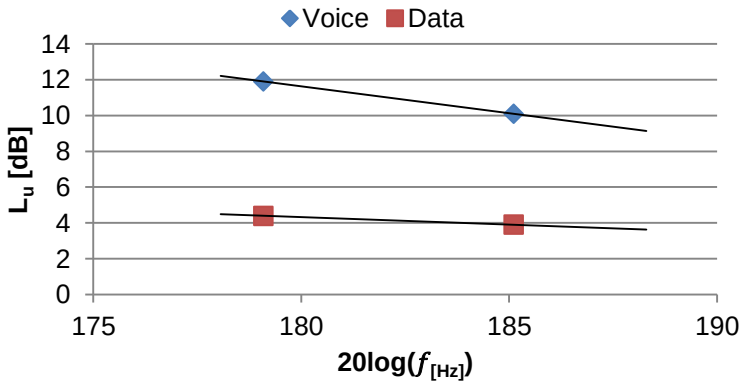

Figure 3.5. Linear behaviour of user losses for voice and data modes.

The linear equations corresponding to the user losses for both voice and data, which depend on the

frequency, and which is represented in Figure 3.5, allow to make the extrapolation for other frequencies. The expressions are given by:

$$L_{u[\mathrm{dB}]} = \begin{cases} -0.29897353 \times 20\log\left(f_{[\mathrm{Hz}]}\right) + 65.44162957, & \text{voice} \\ -0.08304820 \times 20\log\left(f_{[\mathrm{Hz}]}\right) + 19.27267488, & \text{data} \end{cases} \tag{3.18}$$

Using (3.18), one obtains the values of user losses for each band, being presented in Table 3.2. One could apply (3.18) to each systems carriers, but it would give no relevant differences in the values, so that one gets a value per band, which can be associated to the systems operating in that band.

Table 3.2. User losses values, extrapolated for the frequencies of interest.

Frequency Band [MHz]	$\mathbf{20log}(\boldsymbol{f})$	**User Loss [dB]**	
		Voice	**Data**
800	178.06	12.21	4.48
900	179.08	11.90	4.40
1800	185.11	10.10	3.90
2100	186.44	9.70	3.79
2600	188.30	9.15	3.63

For WiFi, one can use (3.18) to obtain the user losses, considering the frequency of 2400 MHz, leading to a value of 3.69 dB, being between the values for 2100 and 2600 MHz. One should note that this is an approximation, as the expressions are obtained taking into account results for cellular MTs.

Depending on the service being used, the losses due to the user are assumed to be in the head, for voice, or in the torso, for data, as depicted in Figure 3.6, being characterised by the head's width, w_{head}, and the torso's width, w_{torso}, and height, h_{torso}.

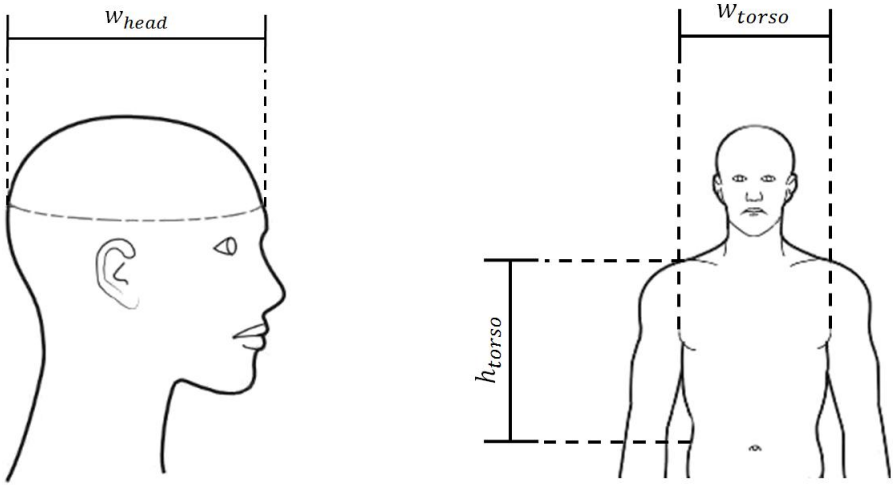

(a) Human head (b) Human torso

Figure 3.6. Body parts taken into account in the UL exposure (adapted from [NASA10]).

For the surfaces of absorption, one takes the lateral area of the head and the torso's front area, as depicted in Figure 3.7, depending on the service. Although these are not the only parts of the body that absorb the power and contribute to the user losses given in Table 3.2, this assumption is a way to simplify the assessment, being assumed that these parts also absorb the power corresponding to

other parts of the body, such as the hand, being an approximation. For the considered areas, having their dimensions, one can approximate the lateral area to a circumference with the head's width as diameter, Figure 3.7 (a), and assume a square with the sides being the torso's width and height for the torso's absorption area, Figure 3.7 (b).

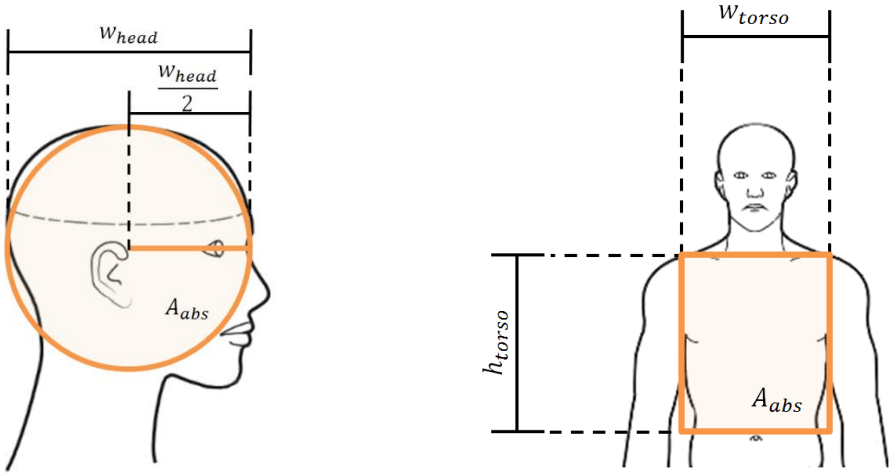

(a) Head (b) Torso

Figure 3.7. Surfaces of absorption and the corresponding areas (adapted from [NASA10]).

The values for the width of the head and torso, as well as the torso's height, are based on anthropometric dimensional data presented in [NASA10], where minimum and maximum values are presented for several body parts. The minimum values are taken into account, as they give a lower area of absorption, leading to a higher power density, being a worst case analysis. For the head's width, one uses 17.3 cm, considered as the diameter of the area of the absorption surface. For the torso, one takes 32.3 cm for its width and 34.1 cm for its height. Hence, one obtains the area of the absorption surfaces, which are 0.0235 m^2 and 0.1101 m^2 for the head and torso, respectively.

3.1.3 Global Exposure Model

This model takes into account all the relevant systems that operate in [800, 2600] MHz, through the use of the aforementioned models for DL and UL, which calculate the power density values for the frequencies of the carriers, corresponding to the systems taken into account. The power density value for each frequency is useful to assess the compliance with ICNIRP's requirements, as the exposure of fields of different frequencies are summed in their effects, as given by (2.1).

As power density is the reference parameter used in the analysis, the requirement given by (2.1) can be written in its terms, through the relation between power density and electric field strength, which is given by [Corr13]:

$$S_{[\mathrm{W/m^2}]} = \frac{E^2_{[\mathrm{V^2/m^2}]}}{Z_{0[\Omega]}} \tag{3.19}$$

where:

- Z_0: free space impedance.

The relation given by (3.19) is only valid for far-field region, where the electric and magnetic fields relate directly through the free space impedance [SeBC12]. As the use of a far-field model in a near-field region leads to an overestimation of the fields compared to real values [SeBC12], it means that the use of (3.19) in near-field regions is an approximation, which is the case of the UL values, where the user is always in the near-field of the MT, and of the DL ones where the user is within the near-field region of the antenna.

Hence, from (2.1) and (3.19), one gets the requirement that it should be applied for power density, giving the total exposure, comprising the sum of the signals contribution, being also used to assess the compliance of the requirements:

$$\gamma = \sum_{i>800\ MHz}^{2600\ MHz} \frac{S_{i[\mathrm{W/m^2}]}}{S_{L,i[\mathrm{W/m^2}]}} \leq 1 \tag{3.20}$$

where:

- γ: total exposure parameter;
- S_i: power density at frequency i;
- $S_{L,i}$: power density reference level at frequency i.

Using the results of (3.20), it is possible to obtain the contribution of each of the signals (carriers) with respect to the total exposure. For a given signal, the relative contribution to the total exposure is given by:

$$\chi_{i[\%]} = 100 \frac{\frac{S_{i[\mathrm{W/m^2}]}}{S_{L,i[\mathrm{W/m^2}]}}}{\gamma} \tag{3.21}$$

where:

- χ_i: relative contribution of the signal i to the total exposure.

To obtain the contribution of a given system, one should sum the contributions of the signals corresponding to that system.

There is other parameter that is useful to introduce, the Exposure Ratio (ER), which is useful to compare the electric field strength and power density levels with the reference ones provided by ICNIRP. The ER can be referred to the electric field and power density values, being the ratio between the maximum measured value over N_p locations (points of investigation) and ICNIRP's reference value. As one is considering power density to evaluate the exposure, only its expression is presented, being given by [JVGV12a]:

$$\varepsilon_{S[\%]} = 100 \frac{\max\limits_{k=1,\ldots,N_p} (S_{i,k\ [\mathrm{W/m^2}]})}{S_{L,i[\mathrm{W/m^2}]}} \tag{3.22}$$

where:

- ε_S: exposure ratio referred to power density;
- N_p: number of points of investigation;
- $S_{i,k}$: power density at frequency i, for the location k.

3.2 Simulator Overview

The simulator aims to evaluate the global exposure and to perform the calculations already described, being implemented in MATLAB [Math10]. It calculates the values to which the user is exposed, considering several systems, calculates their contributions to the total exposure, and verifies if the levels comply with the requirements specified by ICNIRP.

In a general view, the structure of the simulator is comprised of the models that determine DL and UL exposure values, which are used in the global exposure model. To make the calculations, the scenario configuration should be done, taking into account the parameters to be varied. Hence, before running the simulator, the input parameters should be configured, regarding the scenario under analysis. The configuration of the parameters is done in a MATLAB script, which initialises the variables and runs the simulator the specified number of times, in order to obtain the mean and standard deviation values of the statistical parameters. The following parameters can be configured on the simulator, although some of them can remain the same by default:

- the systems considered in DL and UL;
- the type of service being used (voice or data);
- number of BSs on the roof-tops and the configuration over the buildings;
- number of Access Points (APs) on the building's façade, in case of being considered WiFi;
- BS's transmission power and gain, for each of the systems;
- receivers' noise figure for UMTS and LTE BSs;
- safety margin, considered in the target received power at the BS;
- MIMO configuration in DL and UL (up to 8×8 in DL, and up to 4×4 in UL);
- signal modulation of the systems being considered;
- MT gain;
- losses in the cable between the BS and the receiver;
- scenario parameters (height of the antennas, height of MT, width of the street and distance of the user to the reference building);
- number of simulator runs and the simulation mode: user static, or user varying the position, including the step and the maximum displacement along the street;
- the output file name.

Regarding the output of the simulator, it comprises the useful parameters for the analysis, which are saved in *.txt files, properly identified and distributed in the file, such that they can be used for the analysis. The parameters are organised by carrier, identifying the system associated to it, and presenting the values corresponding to the several positions, if the simulation mode concerns the user varying his position. The parameters presented in the output file are the following:

- distance from the user's position to his initial position (first point of investigation);
- distance between the user and the BSs considered in the scenario (direct ray);
- indication if the user if in the near- or far-fields of the antenna;
- BS EIRP;

- power available at the MT's receiving antenna;
- power available at the MT's receiving antenna, using the free space model (supplementary);
- MT EIRP;
- BS target power value;
- power available at the BS's receiving antenna;
- path loss;
- DL and UL power densities;
- the total exposure parameter and a verification about compliance with the requirement, as well as the reference levels for each carrier;
- contributions to the global exposure by carrier, link direction and system, including ERs.

When a number of several runs is specified, the simulator generates an output file with the mean and standard deviation values of the statistical parameters.

Figure 3.8 illustrates the overview of the simulator, in terms of the main algorithms involved, as well as its main functions. After the input parameters being configured, they are loaded into the simulator, through the initialisation script, which also executes the simulator. The simulator comprises the DL, UL and the global exposure models: the first one includes the determination of DL exposure, having the MT received power calculation and the conversion to power density as main functions; the second one takes the power control in UL into account, determining the values of the MT radiated power and, consequently, the power density; the third one uses the values obtained by the previous, in order to obtain the total exposure values, as well as to check if ICNIRP's requirements are satisfied, and to determine the contributions to global exposure. Finally, the simulator generates the output files with the relevant values for the analysis, corresponding to each run, and another with the mean and standard deviation of the statistical parameters over the total number of runs.

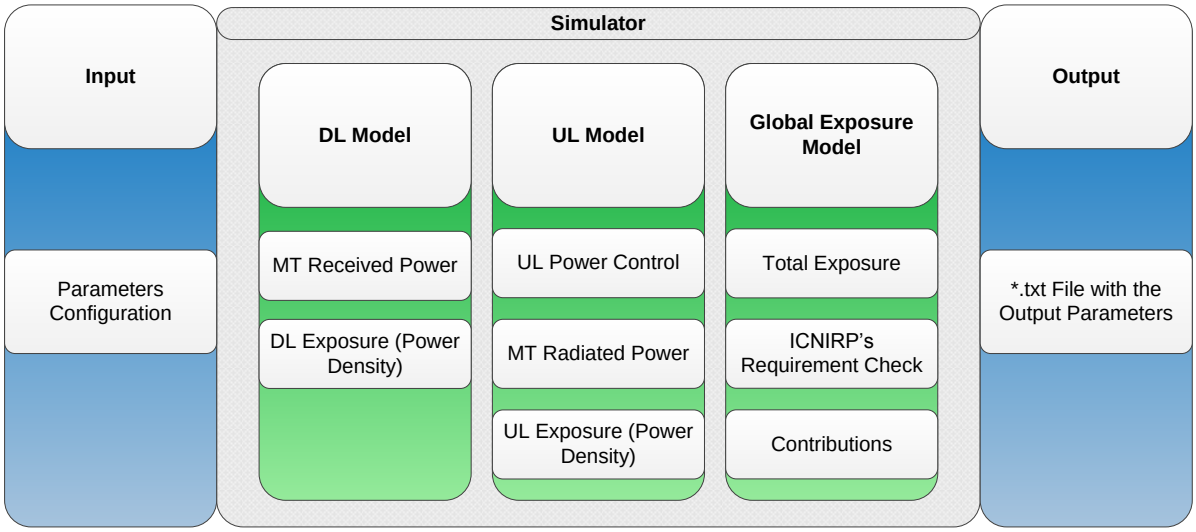

Figure 3.8. Simulator overview.

3.3 Simulator Algorithms

As already mentioned, DL and UL algorithms perform the main functions in order to get the values that are used in the global exposure model. These are used in the main structure of the simulator, which performs the general functions, where the global exposure model is implemented. In this, after all the parameters are initialised according to the parameters configuration for the simulation, it is checked which are the active systems in DL, *i.e.*, the systems that are considered to be transmitting in that direction, and the systems being used in UL; the carriers are assigned to each of the systems, depending on the number of BSs being considered and the number of carriers per BS, for each system. For each BS, a set of carriers is assigned, with its own frequency, according to the system, as one assumes that each BS corresponds to a single operator.

If the simulation mode corresponds to the one where the user is static, the DL and UL models are applied for each carrier corresponding to the active and used systems, taking the number of BSs in the scenario into account. In UL, the values are determined only for one carrier, and corresponding to the reference BS, because the user is assumed to establish the connection only with that BS. For other systems being considered besides the cellular ones, only DL contributions are determined taking into account the free space model, as mentioned in Subsection 3.1.1, as one only considers cellular systems in UL.

When the simulation mode considers the user varying the position, the algorithm is the same as previously described for static mode, being repeated for each position, *i.e.*, at each position, DL and UL models are applied in order to determine the exposure at each point, ceasing the DL calculations when the point corresponding to the maximum displacement over the street is analysed.

Once DL and UL values are obtained for all systems, ICNIRP's requirement is verified, determining the total exposure given by (3.20), as well as the contributions, which include the relative contributions of each system to the total exposure, (3.21), and the ERs, (3.22), which are processes corresponding to the global exposure model. Finally, having all the desired values, the output file is written, with the useful parameters for the analysis. This main algorithm is depicted in Figure 3.9.

The algorithm implemented for the DL model, Figure 3.10, determines the power density corresponding to a given carrier, associated to the system under analysis, starting by loading the useful variables for the calculations. After this, it verifies if the system is LTE, and if so, it determines the power fed to the BS transmitting antenna having the MIMO configuration into account, multiplying (in linear units) the power of a single transmitter by the MIMO order, *i.e.*, the number of transmitters. Then, the lengths of the three rays considered in the DL model are determined, using (3.4), (3.5) and (3.6), so that the differences between the direct ray and the reflected ones can be obtained. The calculation of these parameters depends on the scenario parameters, and also on the distance to the first point of investigation, in the case where the user varies the position, changing his coordinates. With the length of the direct ray, one can verify if the MT is in the near- or far-fields region of the BS, using (3.1).

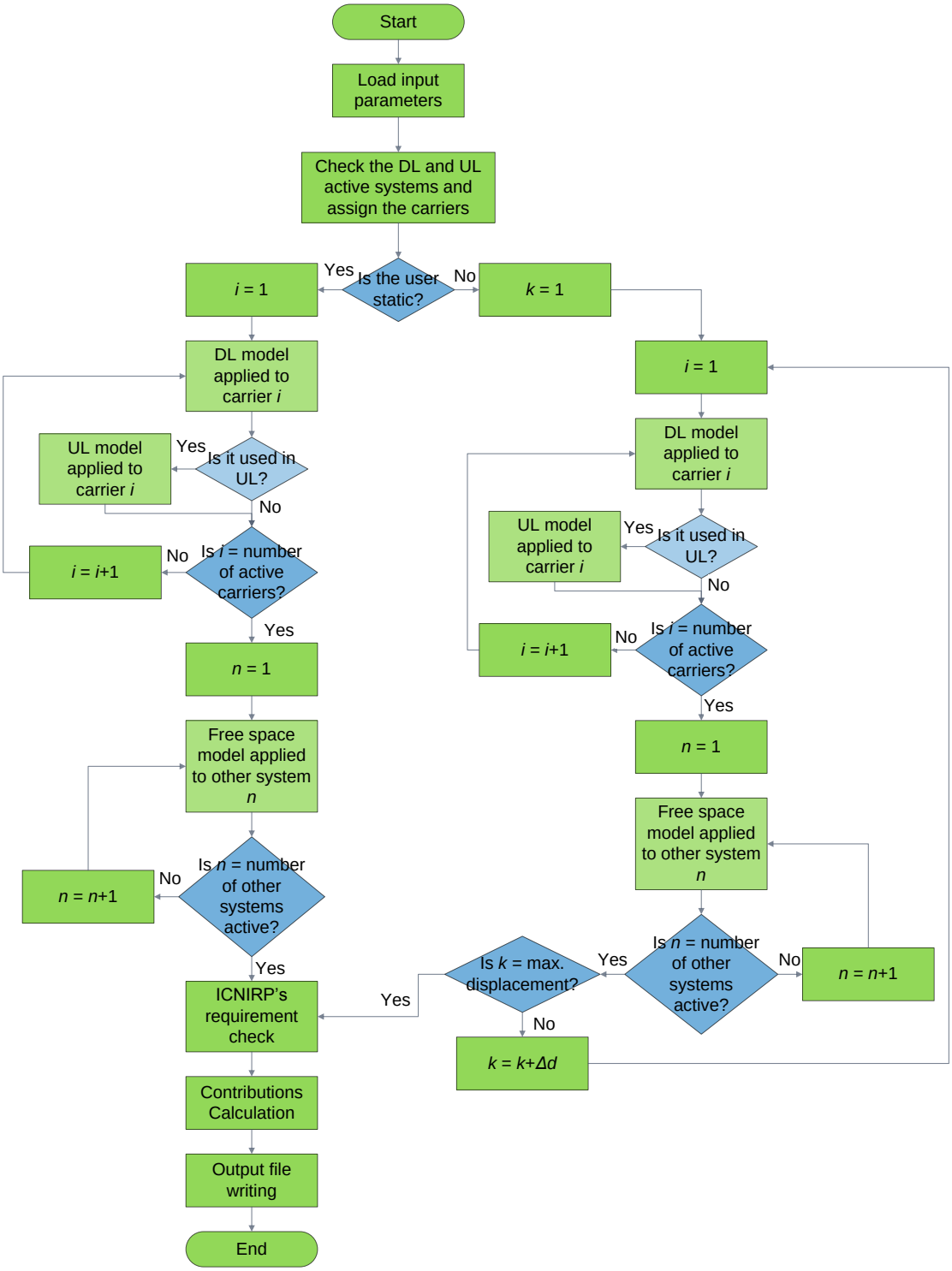

Figure 3.9. Simulator's main algorithm.

Before determine the received power at the MT, through (3.2), a generation of random numbers according to a Uniform Distribution is done, in order to obtain the reflection coefficient for both building and ground surfaces, as defined in Subsection 3.1.1. Then, having the received power at the MT, one can obtain the path loss, (3.11), which is useful for the UL model, for power control purposes. Finally, the conversion to power density is made by (3.10).

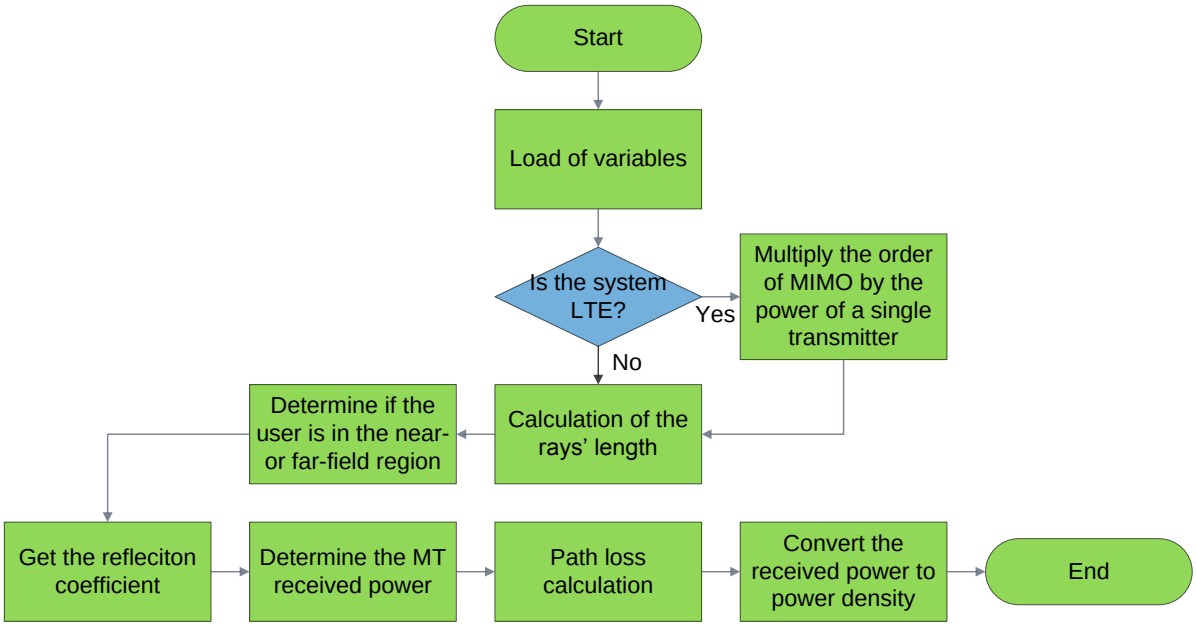

Figure 3.10. DL algorithm.

Regarding the algorithm corresponding to the UL model, Figure 3.11, it does some other verification. Similarly to the DL algorithm, it makes the calculation for a given carrier, also starting with the load of the variables. One of the main parameters that influences the determination of exposure in UL is the user losses, which depend on the type of service being used, Table 3.2, so that a verification is done in order to assign the corresponding value to this parameter.

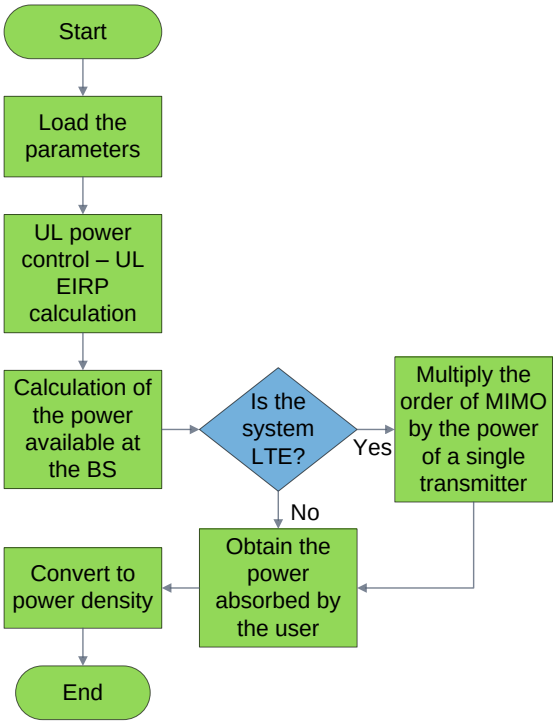

Figure 3.11. UL algorithm.

Then, UL power control determines the MT radiated power, (3.12), as the path loss is known from the DL model. The power available at the BS antenna is determined, which can be useful to observe if the

target power is achieved. If the system is LTE, MIMO is taken into account in the MT radiated power in the same way it is for DL. Finally, having the MT's radiated power and the user losses, one can obtain the power density value, (3.17).

Besides DL and UL algorithms, one should describe the algorithm regarding power control, Figure 3.12, as it performs an important function in the UL model. Basically, this algorithm determines the UL radiated power in order to satisfy the target available power value at the BS receiver, which depends on the receiver's sensitivity. The sensitivity is obtained according to the values presented in Annex C, depending on the system, modulation, service, and on the MIMO configuration being used. It is verified if the system being used is GSM, UMTS or LTE and, according to the system, there are different approaches: for GSM, the values for the sensitivity are according to Table C.1; for UMTS, if the service being used is voice, the values corresponding to R99 are considered, and if the service is data, the type of modulation and the release being considered (R99 or HSPA+) are checked, in order to obtain the SNR values according to Table C.3 and Table C.4, and, then, obtain the sensitivity through (C.6); for LTE, it is also verified the type of modulation being used, as well as the MIMO configuration, with the SNR values being obtained using Table C.5, and, finally, determining the sensitivity according to (C.10).

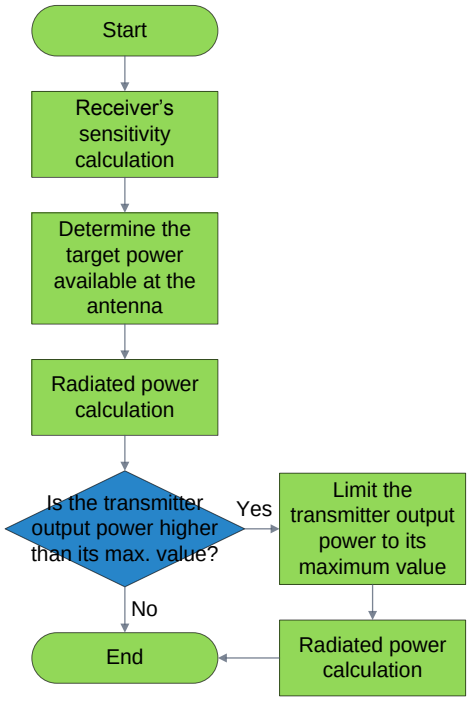

Figure 3.12. Power control process.

Having this value, the target power at the BS is determined, using (3.13), the radiated power being the power such that the target value is satisfied, taking into account that it should not exceed the maximum transmitter output power, being limited to that value. For the UL case, the transmitter output power is limited to 21 dBm for voice, and to 24 dBm for data, in the case of the used system being UMTS or LTE, and to 33 dBm in the case of being GSM, which are the typical maximum values for these services, as already mentioned.

3.4 Simulator Assessment

In order to see if the simulator is working properly, according to the theoretical model, some test cases are done, which allow to validate the algorithms implemented. The first approach is to test the algorithms for extreme situations, defining several test cases, where the expected result is known. In the end, if the results are according to the expected results, one can validate the algorithm, as it is running as desired. This approach is taken for both DL and UL models.

Before defining the test cases for the assessment, the way simulations are performed is firstly described. The simulator generates output values that are not constant over several simulations with the same input parameters, *i.e.*, the values are not exactly the same, presenting some variations. These variations are due to the randomness of the reflection coefficient of the building and ground surfaces, being used to determine the MT received power (3.2), and taken as a Uniform Distribution, as referred in Subsection 3.1.1. Hence, for each test, one should perform several simulations, and determine the average and the standard deviations of the parameters that have randomness associated, over all simulations, in order to have a statistical approach. To determine the number of simulations per test, the average and standard deviations for several sets of simulations were taken, being observed after how many runs the values reach a steady state. In this case, the average and the standard deviations of the MT received power were determined over 1 to 500 simulations, Figure 3.13, allowing to choose the adequate number of simulations.

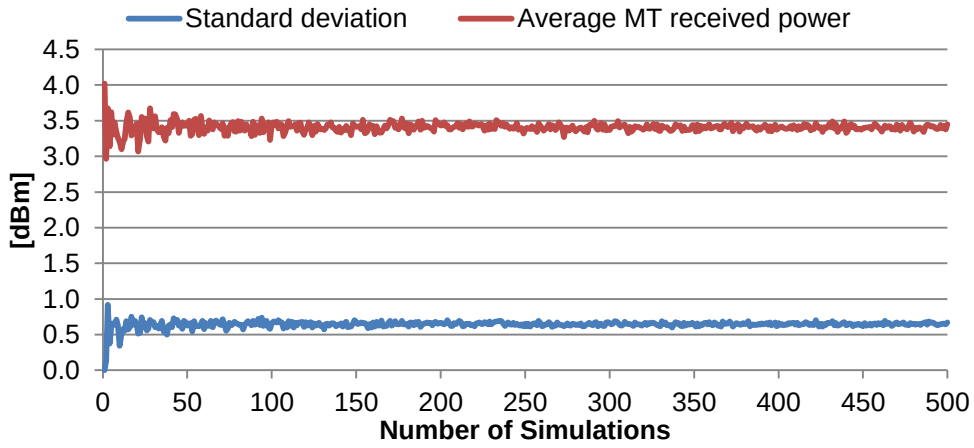

Figure 3.13. Average and standard deviations of the MT received power for different number of simulations.

From Figure 3.13, one can see that both average and standard deviation values show higher oscillations when considering less number of simulations, becoming stable after around 50 simulations. From this value, one can see that the average and standard deviation start to tend to approximately 3.4 and 0.7 dBm, respectively, presenting slight oscillations around it, so that this number of simulations is sufficient, being the one used to make the analysis.

Regarding the test cases, two extreme test cases can be defined for both DL and UL models: when the user is close to the BS, and when the user is at a large distance away from the BS. Concerning

the former, due to the proximity of the user to the BS, high exposure values should be verified in DL, probably exceeding the requirements, and in UL the power radiated by the MT should be low, which leads to a prevalence of the DL component in the total exposure. On the other hand, in the latter case, as the distance from the user to the BS is high, a high path loss is expected and, hence, low exposure values should be observed in DL, and high ones in UL, as the MT needs to compensate the high path loss and to maintain the target power level at the BS.

The tests were done considering only one system in DL and UL, because if the models are valid in this situation, they are also valid when other systems are included. Hence, LTE800 was taken in DL and UL, as data is the service being used. One considered the user in front of the BS, at a distance of 3 m, which is very close to the BS. To do this in the simulator, the height of the BS was defined to be the same of the MT, and the distance from the user to the reference building is 3 m, which was the same as the distance to the BS, in this case. All the other parameters remained by default.

The simulations confirmed the expected results, where, in the first case, the MT received power is very high, leading to a high power density, with the user being in the near-field of the antenna, as confirmed with the output results. On the other hand, in UL, the MT radiated power is low, with the power density having a low contribution to the total exposure, which is dominated by DL, such that the requirement is not satisfied, having a value higher than 1. When the user is at a large distance from the initial position (in the direction of the BS), which is assumed to be 100 m, the results are also according to expectation, and coherent with the previous test: a high path loss is observed, which leads to a low MT received power, so that DL has a low contribution for the total exposure and, on the opposite, UL dominates the contribution, due to the high MT radiated power. Moreover, one can increase even more the distance along the street and observe that the MT radiated power saturates, as the transmitter reaches its limit, which is the case if one considers, for instance, 200 m, as verified in the simulator. For both test cases, one can also observe that LTE800 contributes 100% for the total exposure, being an expected result, as it is the unique system being considered, which means that the contribution calculation is also working as desired.

As the possibility of varying the user's position is one of the operation modes of the simulator, a validation of its operation is also done. In this case, for typical values, and using the default values as for the previous test cases, with only one system active and the data service being used, the displacement of the user along the street is defined and the simulator is ran. One verified that the received power follows the theoretical behaviour given by (3.2), for the assumptions taken into account: it should reach maximum and minimum values, decreasing around a mean value, which corresponds to the free space one, due to the interference between the several rays. On the opposite, in theory, the MT radiated power also oscillates according to this, as it increases when the received power decreases, and decreases when the received power increases. Moreover, it is expected to verify that the MT radiated power increases or decreases exactly at the same amount as the path loss from the previous point to the current one, and the BS received power should be constant, as power control is made in UL, being possible to validate the method responsible for the UL power control.

In this case, a step of 5 m between consecutive points is defined, up to a maximum distance of 100 m

to the BS, at the street level, which is the distance assumed in previous simulations. According to the simulations, the results show that, from point to point, and as the user moves away from the BS, the received and radiated powers have the expected behaviour: on average, the MT received power decreases and, thus, its radiated power increases, as depicted in Figure 3.14, which presents the values of the parameters, averaged over 50 simulations, with the corresponding standard deviations, which are shown to be very low. One can also observe that the MT radiated power increases or decreases in the same amount of path loss, as well as the BS received power is constant and equal to the target value, which confirms that the process implemented for power control is operating correctly. A similar relation can be verified between the increase of path loss and the MT received power, which decreases in the same amount.

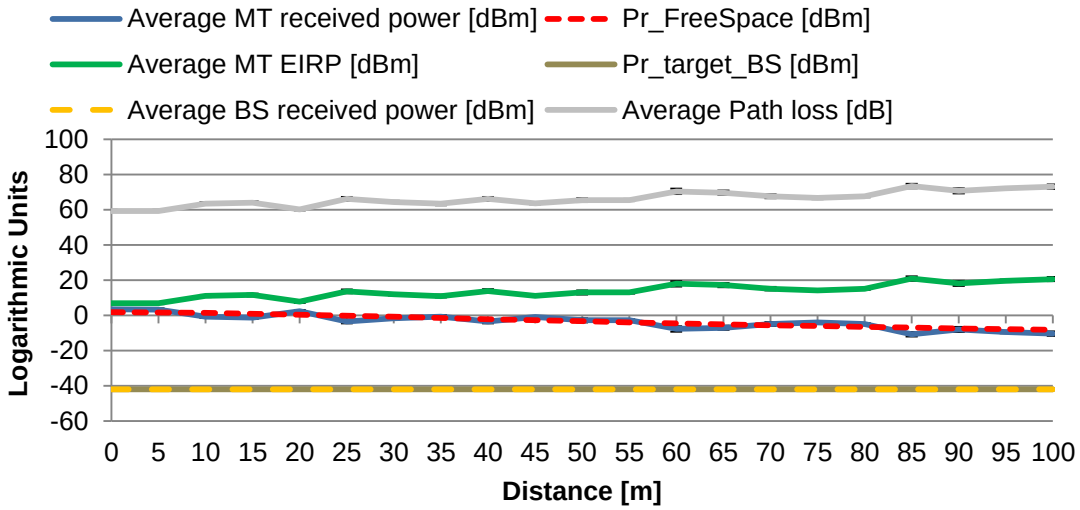

Figure 3.14. Curves representing the parameters' values obtained with the distance.

According to power densities, Figure 3.15, they follow the behaviour of the received and radiated powers, where, on average, DL power density decreases and UL's increases. The contribution of DL is higher in the beginning, then, some oscillations are verified, due to the received and radiated powers oscillations, but, from a given point, the UL contributes the most for the total exposure, which is due to the way the power densities are calculated. Once again, the results obtained by simulations are coherent and according to the expected ones.

One can consider that the user moves up to a large distance from the BS, in order to see the behaviour of the received power, which, from a certain point, decreases without the high oscillations verified in the first hundreds of metres. For a maximum distance of 4 km, with a step of 10 m, the results show that, after a given distance (around 2.4 km), the oscillations are reduced and the power decreases proportionally to $1/r^2$, as one can see, as it is parallel to the free space curve. This behaviour can be observed in Figure 3.16, where the standard deviations are not shown, as they are low compared to the power values and their representation in the graph makes the comprehension less clear, being close to the blue line.

The second approach is based on the comparison between the simulated results and the results obtained manually, *i.e.*, having the inputs of the algorithms, one can get the output values of each,

through the simulation and manually, which should be the nearly the same. To simplify the calculations, only one system can be considered. If it gives the expected values for that system, it would give when other systems are included, as this analysis is from the calculations viewpoint.

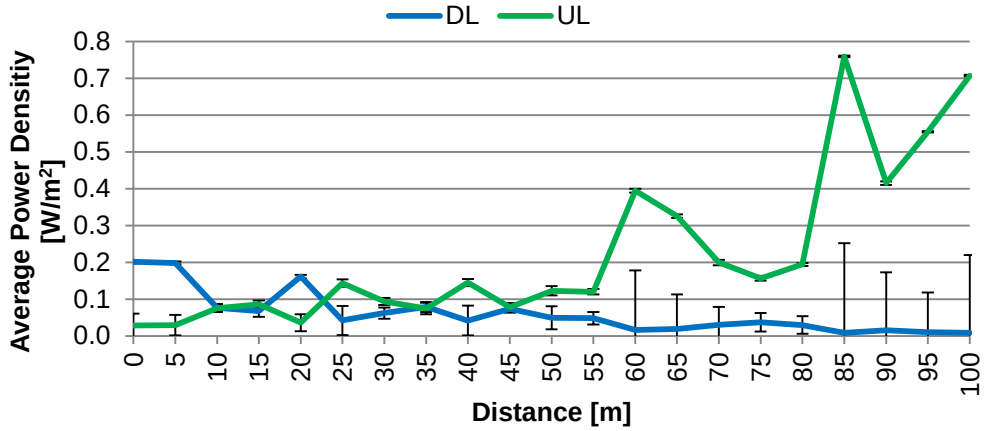

Figure 3.15. DL and UL power density curves along the several positions.

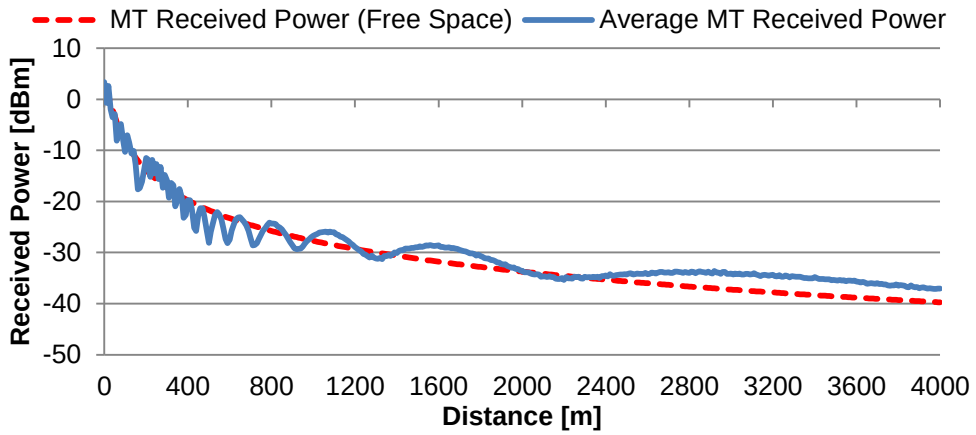

Figure 3.16. Behaviour of MT received power considering a maximum distance of 4 km.

For this purpose, LTE800 is taken into account, and the position of the user is not varied, because it is sufficient for the theoretical models' validation with this approach, as the equations are the same for both modes. Manual calculations include the same calculations performed on the simulator, for this situation under analysis, including the intermediate steps that lead to the output variables. The obtained values of both DL and UL models are close to the values obtained with the simulator, as well as the final results, which depend on these models and are related to the total exposure and the requirement verification. With this approach, one verifies that the simulator is correctly performing the calculations according to the theoretical models and, as the used models are the same, this is also valid for the simulation mode where the user changes his position.

Chapter 4

Results Analysis

In this chapter, the considered scenarios are defined, followed by the description of the measurement procedure, as well as the results obtained experimentally. Then, simulation results, concerning the reference scenario and the parameters under analysis are presented, concluding with a comparison between measured and simulated results.

4.1 Scenarios Description

The analysis is done by considering one reference scenario, and, then, varying the parameters of interest regarding this scenario, in order to assess their influence. In this case, the considered scenario is a typical urban street, with buildings on both sides, the user being located in its centre; a sector BS antenna is located on the roof-top of one of the buildings, as depicted in Figure 4.1.

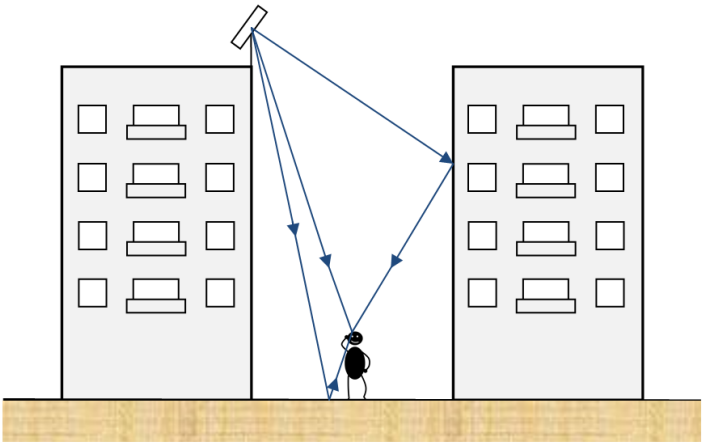

Figure 4.1. Geometry of the reference scenario.

The parameters of the scenario configuration, such as the height of the BS, the number of antennas on the roof-tops, the width of the street and the distance from the user to the reference building are chosen according to typical values presented in [Carr11]. The initial position of the user is such that he/she is in the direction of the BS, at the street level.

Regarding the BS, one assumes that it supports the three cellular systems (GSM, UMTS and LTE), and, although in the reference scenario only one BS is taken into account, more BSs can be considered in the simulations, so that the number of carriers for each system, and per BS, is such that each BS corresponds to a different mobile operator (a maximum of 3 BSs is considered, corresponding to the 3 Portuguese operators). The number of carriers per BS and for each system is assumed to be the typical number of carriers that the operators have, *i.e.*: 4 for GSM, 4 for UMTS, and 1 for LTE; concerning LTE, one carrier is assumed with all the available bandwidth for the system, comprising all the sub-carriers, being 10 MHz for LTE800, and 20 MHz for LTE1800 and LTE2600. One considers that the user is using all the bandwidth, as a worst case approach is taken into account.

In order to have different carriers for each BS, one considers that the carriers are contiguous in the band, *i.e.*, one takes the minimum of the frequency band of a system, and applies (3.3) in order to assign the carriers. This means that, for instance, for the first BS, its 4 GSM900 carriers correspond to the first 0.8 MHz of the 900 MHz band, with the carriers corresponding to the second BS being in the next 0.8 MHz, and the same approach for the third BS. Hence, the carriers for a BS do not necessarily correspond to the carriers of a Portuguese operator, but this is a simple way to assign different carriers to each BS, as interference issues are not taken into account. Table 4.1 presents the

frequencies distribution for each carrier, for the 3 BSs that can be taken into account. One should note that the user uses one fixed carrier in DL and another in UL, assumed to be the first ones of the system's bandwidth, corresponding to the reference BS.

Table 4.1. Centre frequency of the carriers, per system and BS.

Link	BS	Carriers' Centre Frequency [MHz]					
		GSM		UMTS	LTE		
		900 MHz	1800 MHz		800 MHz	1800 MHz	2600 MHz
DL	1	925.2	1805.2	2115	801	1825	2640
		925.4	1805.4	2120			
		925.6	1805.6	2125			
		925.8	1805.8	2130			
	2	926.0	1806.0	2135	811	1845	2660
		926.2	1806.2	2140			
		926.4	1806.4	2145			
		926.6	1806.6	2150			
	3	926.8	1806.8	2155	831	1865	2680
		927.0	1807.0	2160			
		927.2	1807.2	2165			
		927.4	1807.4	2170			
UL	1	890.2	1710.2	1925	842	1730	2520

Typical values are assumed for the BS parameters, where for the transmitter output power the value is 40 W (46 dBm) for all systems, except for LTE800, which is 30 W (44.8 dBm). The losses in the cable between the transmitter and the antenna, as well as the gain of the antenna, are according to [Pire11], and the receiver's noise figure according to [Carr11]. As MIMO is considered for LTE, this means that one has 2×40 W for MIMO 2×2 in the configuration of the reference scenario, a similar approach being taken for other MIMO configurations.

On the other hand, for the MT, as one considers that its radiated power is such that the target power at the BS antenna is achieved, it is only possible to specify the maximum values that the MT transmitter can reach, for voice and data, being based on [Bati11]. An isotropic MT antenna is assumed, as it is the best way to model an MT antenna [NaDA06]. As one considers the maximum throughputs possible, the LTE terminal is of class 5, supporting MIMO up to 4×4, and modulations up to 64QAM [Corr13]. The modulations are used to determine the sensitivity of the BS, so that the maximum possible modulations in UL for UMTS and LTE are taken, being 16QAM and 64QAM, respectively. The sensitivity in GSM is based on typical values, Table C.1, so that it corresponds to the basic GSM modulation, the Gaussian Minimum Shift Keying (GMSK) [Corr13].

In each link, a group of active systems is defined. For DL, one can have all systems active, because it depends on the BS antennas, being different for UL, where only one system is assumed to be active in this link. In the reference scenario, the 3 cellular systems are accounted for (GSM, UMTS and LTE), assuming the 900 MHz band for GSM, and the 2600 MHz one for LTE. For other scenarios, WiFi can also be added, in order to observe its influence, having its own antennas, considering the typical value

for its radiated power of 100 mW [OIMC13]. Also for the reference scenario, and according to the service being used, which can be voice or data, it is assumed that the user uses data with LTE.

The values for the reference scenario are summarised in Table 4.2. Some of these parameters can be varied, in order to obtain the different analysis scenarios.

Table 4.2. Parameters considered in the reference scenario.

<table>
<tr><td rowspan="2">Link/Systems</td><td>DL</td><td colspan="2">GSM900, UMTS (HSPA+) and LTE2600</td></tr>
<tr><td>UL</td><td colspan="2">LTE2600</td></tr>
<tr><td>Service</td><td colspan="3">Data</td></tr>
<tr><td rowspan="7">BS</td><td>Number of BSs</td><td colspan="2">1</td></tr>
<tr><td rowspan="3">Transmitter Output Power [dBm]</td><td>GSM900</td><td rowspan="3">46</td></tr>
<tr><td>UMTS</td></tr>
<tr><td>LTE2600</td></tr>
<tr><td rowspan="3">Antenna Gain [dBi]</td><td>GSM900</td><td rowspan="3">18</td></tr>
<tr><td>UMTS</td></tr>
<tr><td>LTE2600</td></tr>
<tr><td>Noise Figure (LTE UL) [dB]</td><td colspan="2">5</td></tr>
<tr><td>MIMO Configuration</td><td colspan="2">2×2</td></tr>
<tr><td>Cable Losses [dB]</td><td colspan="3">3</td></tr>
<tr><td>Safety Margin [dB]</td><td colspan="3">30</td></tr>
<tr><td>MT</td><td>Antenna Gain [dBi]</td><td colspan="2">0</td></tr>
<tr><td rowspan="4">Scenario Parameters</td><td>BS Height [m]</td><td colspan="2">30</td></tr>
<tr><td>MT Height [m]</td><td colspan="2">1.5</td></tr>
<tr><td>Street Width [m]</td><td colspan="2">35</td></tr>
<tr><td>Distance from MT to the Reference Building [m]</td><td colspan="2">17.5</td></tr>
</table>

Concerning user's mobility, for all the tests, one considers that the user is static, being in the direction of the first BS, the reference BS. The other situation, where the user is varying the position along the street from the initial position, is only considered in the reference scenario, as the objective is to evaluate the behaviour of the parameters with the distance. Tests are done regarding the influence of mobile communications systems, the services, the scenario parameters and MIMO configurations.

Concerning mobile and wireless communication systems, the configuration considers all systems, *i.e.*, GSM, UMTS, LTE and WiFi. For GSM, one considers the system operating in the 900 MHz band, as the 1800 MHz band is assumed to be dedicated to LTE1800, given the trend to use only LTE in this band. As there are 3 possibilities for UL, 3 configurations are considered, one for each of the systems: with LTE800 in UL (AllSyst&LTE800UL), with LTE1800 (AllSyst&LTE1800UL), and with LTE2600 (AllSyst&LTE2600UL), all of them with all the systems operating in DL, as presented in Table 4.3. Regarding WiFi, one considers 4 APs at the building where the BS is installed, where 3 of them can

belong to 3 operators and one being independent. The first AP is located in the direction of the BS, but in the building's façade at a height of 3.5 m, while the other 3 APs are distributed beside this AP, with the distance between them being 1 m.

Table 4.3. DL and UL configurations used in the mobile communication systems analysis.

Designation	**Systems**	
	DL	**UL**
AllSyst&LTE800UL	GSM900, UMTS, LTE800, LTE1800, LTE2600 and WiFi	LTE800
AllSyst&LTE1800UL		LTE1800
AllSyst&LTE2600UL		LTE2600

Another type of analysis concerns the service being used, which can be voice or data. The DL systems are the ones of the reference scenario; the several possibilities for the UL systems supporting these two types of services are taken into account, *i.e.*, one tests GSM with voice, as its main focus is this service, with data and voice being tested with UMTS, where voice is assumed to correspond to R99, with a throughput of 12.2 kbps, and data is tested for both R99 and HSPA+ releases. Lastly, LTE is only tested for data, as there is no voice for LTE. Table 4.4 summarises the systems and services taken into account in this analysis.

Table 4.4. UL systems considered in the services analysis.

Service	**UL Systems**
Voice	GSM900 and UMTS (R99)
Data	UMTS (R99), UMTS (HSPA+), LTE800, LTE1800 and LTE2600

Several scenario configurations are analysed, based on a set of parameters that can be varied: the BS height, the street width, the position of the user regarding the reference building and the number of BS on the roof-tops. Each of these parameters can be varied over a set of values, with the other parameters being fixed, Table 4.5. The exception is when the street width is varied, where the distance of the user to the reference building also varies in order to maintain the user in the centre of the street.

The variation of the number of BSs can give a set of scenarios with different configurations, according to the location of the BSs on the top of the buildings, as the antennas can be disposed in an alternate way or in front of each other, two configurations being depicted in Figure 4.2. In the alternate configuration, Figure 4.2 (a), the BSs are placed alternately on each building, where each BS is assumed to be in a different building, so that the spacing between the BSs in the same side of the street, d_{BS}, is taken as a typical building's façade value (15 m), with the intermediate one being on the front building, in the middle of the other two. For the configuration where the BSs are placed in front of each other, Figure 4.2 (b), the BSs of one side of the street are in front of the BSs of the other side. More specifically, the configurations considered in this analysis are the following:

- 1 BS, only one BS;
- 2 BSs (A), two BSs in the alternate configuration;

- 2 BSs (F), two BSs in front of each other;
- 3 BSs (A), three BSs in the alternate configuration;
- 3 BSs (F), three BSs in front of each other.

When WiFi is considered, the distribution of the antennas on the buildings can also be defined in the same way, with the difference that the antennas are installed on the building's façade, and have a different spacing between them.

Finally, the influence of the MIMO configuration is also evaluated. As in LTE-A MIMO goes up to 8×8 in DL, and 4×4 in UL, these are the configurations that are analysed, impacting on the radiated power and, consequently, on the exposure. One should note that UL does not support MIMO 8×8, but it can be assumed that, in UL, the user is limited to MIMO 4×4 when 8×8 is considered in DL.

Table 4.5. Values used in the scenario parameters analysis.

Adjustable parameter	**Values**	**Fixed Parameters**		
h_b**[m]**	15, 20, 25, 30, 35, 40, 45	w_s **[m]**	d_m **[m]**	**Number of BSs**
		35	17.5	1
w_s**[m]**	20, 25, 30, 35, 40, 45, 50	h_b **[m]**	d_m **[m]**	**Number of BSs**
		30	$\frac{w_s}{2}$	1
d_m**[m]**	2.5, 7.5, 12.5, 17.5, 22.5, 27.5, 32.5	h_b **[m]**	w_s **[m]**	**Number of BSs**
		30	35	1
Number of BSs	1, 2, 3	h_b **[m]**	w_s **[m]**	d_m **[m]**
		30	35	17.5

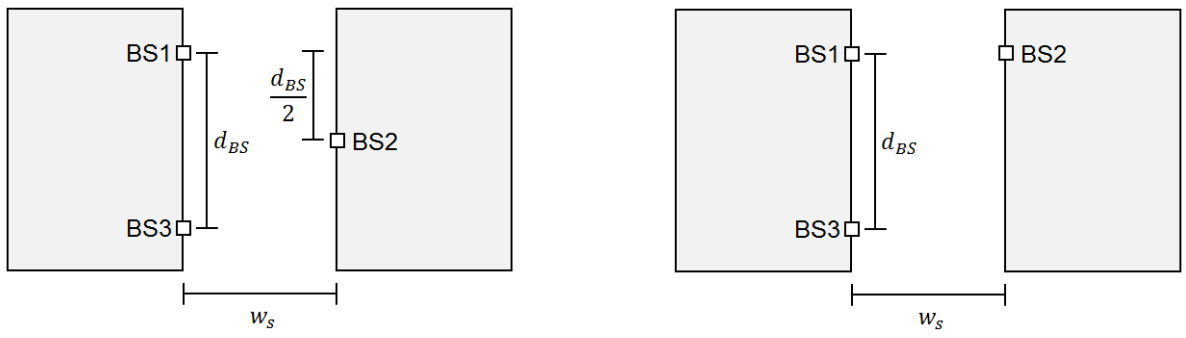

(a) Alternate configuration (b) Configuration with BS in front of each other

Figure 4.2. BS configuration for the BS antennas taken into account.

4.2 Measurements

In this section, the procedure adopted for the measurements is described and the main results are presented.

4.2.1 Procedure

In order to get a better approximation to the theoretical scenario, measurements were made in a street inside the IST *campus*, Figure 4.3, which is surrounded by several buildings, some of them having BS antennas on the roof-top, so that one can evaluate the outdoor exposure in conditions as similar as possible to the theoretical model.

Figure 4.3. General view of measurement scenario (extracted from [Goog13]).

Measurements were made in several points along a street with 3 BS antennas (BS1, BS2 and BS3) and a WiFi AP. The measurements were performed in 25 points separated by 10 m along the entire street, corresponding to a distance of 240 m, approximately. Figure 4.4 shows the scenario configuration with the antennas, and their corresponding orientation, represented with a blue lobe, as well as the measurement points numbered along the street, being represented with white dots.

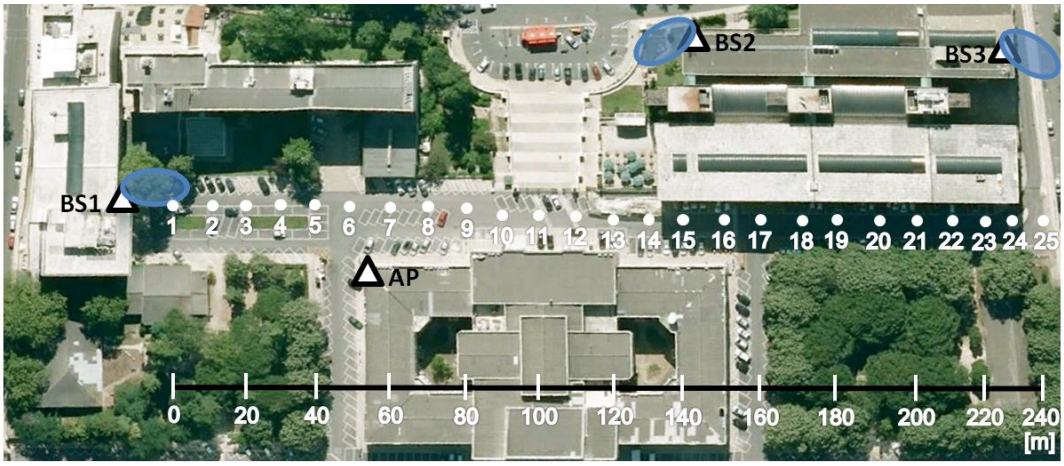

Figure 4.4. Configuration of the scenario and measurement points (adapted from [Goog13]).

The equipment used for the measurements consisted of a Portable Field Meter (PFM), the PMM 8053A [PMM04], Figure 4.5 (a), a wideband equipment with the electric field probe PMM EP-330, analysing in the frequency range of 100 kHz to 3 GHz, and a Selective Radiation Meter (SRM), the Narda SRM-3000 [NARD07], Figure 4.5 (b), which is a spectrum analyser, used with a cable connecting the probe to the basic instrument, and measuring in the [75, 3000] MHz band, with a 0.5 MHz resolution bandwidth.

(a) PMM 8053A [PMM04] (b) Narda SRM-3000 (adapted from [NARD07])

Figure 4.5. Measurement equipment used in the measurements.

The measurement procedure is adapted from the “ECC Recommendation (02)04”, [ECC03], which specifies *in situ* measurement procedures to assess non-ionising electromagnetic levels for the purpose of comparison against reference levels. At each point of investigation, two measurements of 1 minute duration were made, performed simultaneously: with the PFM, which gave the Root-Mean-Square (RMS) electric field value over the 60 s; and with the SRM, which measured the maximum electric field value observed during the same period, for the frequencies over the band, with a frequency resolution of 0.5 MHz. The PFM was mounted on a tripod, with its probe at 1.5 m from the ground, as well as the SRM probe, which was on another tripod at the same height, connected to the handheld basic instrument by cable. The probes were the nearest as possible to each other, in order to measure nearly at the same point. Figure 4.6 presents the equipment configuration used at each measurement point.

Besides the measurements with the aforementioned equipment, the direct distances from the measurement points to the antennas in the environment were also measured, with a laser meter, as well as the points’ coordinates, obtained with a GPS. These values are presented in Annex D.

In the end of the measurements over the street, the distinction between the situations where the MT is performing a voice call or a data connection was made. Hence, for the point where a higher RMS electric field value was verified, the measurements were repeated, only with the PFM, and considering: the simple case, without the MT; the MT performing a GSM voice call; the MT making a UMTS voice call; and, finally, the MT using a UMTS data connection, web browsing, including the download of a file. LTE was not tested, as an LTE terminal was not available, since the terminal used

supports only UMTS (HSPA). Then, this procedure was repeated for two points ± 5 m away from the point where the electric field was higher. One should note that, in this situation, the MT probably was connected to BS1, as it corresponds to the mobile operator of the used MT.

Figure 4.6. Equipment configuration adopted in the measurements.

4.2.2 Results

The values measured by the PFM and SRM can be used to observe the behaviour of the electromagnetic field with the distance. For each of the 25 measurement points, corresponding to the total distance of 240 m, one converts the measured electric field values to power density, through (3.19), as it is the chosen reference parameter considered to assess exposure. One should note that, in some points, the point of investigation can belong to the near-field region of the BS antennas, according to the values from Table 3.1 and the distances to the antennas, presented in Table D.1, so that some of these values can be approximated, due to the use of (3.19) in the near-field region.

The values of the two equipments can be compared, as shown in Figure 4.7, although the measurement band of SRM is lower than the PFM one (*i.e.*, the band from 100 kHz to 75 MHz is not measured by SRM). The power density values obtained through the SRM are one order of magnitude higher than the values obtained through the PFM, in some cases, being almost two orders of magnitude higher. The values obtained with each equipment, for the whole band, are normalised to their respective maximum measured values (*i.e.*, 7.5 mW/m^2 for the PFM, and 98.8 mW/m^2 for the SRM), in order to compare their behaviour along the distance, as depicted in Figure 4.7.

In general, there is a very similar trend on the measurements done by both equipments. The differences between the values obtained with each equipment are mainly due to the fact that SRM measures the maximum electric field values over the measurement period, while the PFM measures the RMS ones, *i.e.*, in some cases, due to the dynamics/randomness of the scenario, a peak value could have occurred, being filtered in the PFM mean value, but registered by the SRM, so that higher

values of power density are verified with the SRM. This is intensified with the fact of the electric field values being converted to power density, meaning that, the difference between the electric field values are much more noticeable, as power density depends on the square of the electric field, so that the error is also squared. However, although the obtained value could be overestimated, it is 20 times below the ICNIRP's most restrictive value (2 W/m^2) for the frequencies of analysis, so that the requirements are fulfilled. These reasons also justify the fact of the distance corresponding to the highest value does not coincide to the one corresponding to the highest obtained with the PFM, *i.e.*, for the SRM one has the highest value at a distance of 80 m, whereas the maximum for the data acquired with the PFM was registered at 90 m.

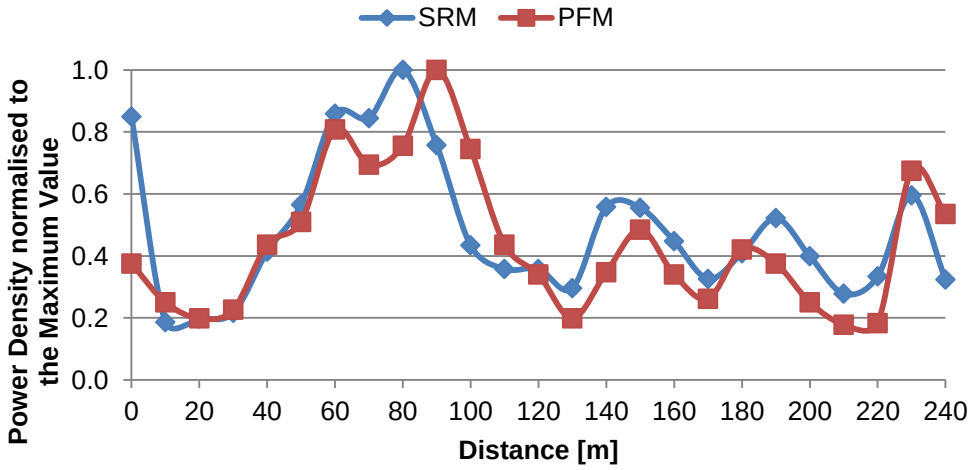

Figure 4.7. Trend of measured power density along the street.

Regarding the evolution of power density over distance, according to Figure 4.7, one observes that in the first point of investigation it presents a higher value than the following points, as it is the closest point to the BS1. As the distance increases, the values decrease up to a minimum value, as the path loss increases with the distance. Then, although the distance increases, the power density values increase up to a maximum value. This behaviour can be explained by getting near to the maximum of the radiation pattern of the BS1, corresponding to its maximum radiated power, but also by getting near to BS2, meaning that at this point the distance to each of the BSs is such that the contributions of each one lead to the maximum value of exposure. After this maximum value, the values decrease up to a minimum value, as the point of investigation is beyond the maximum of the radiation pattern of BS1, and BS2 also starts to have less influence. For the remaining points, lower exposure values are obtained, with the trend to decrease with the distance. The oscillations in the values can be justified by the antenna's radiation pattern, whose gain varies depending on the measurement position regarding the antenna, as well as with the interference between the direct and the reflected rays, the effect of multipath. At the distance of 220 m, a high variation of power density is observed, which is explained with the fact getting near the direction of BS3.

Concerning data acquisition with the spectrum analyser, SRM, it allows one to identify the systems operating in the scenario. Over the 25 points of investigation, a set of systems was identified in most

of the points, while some other systems are only detected in certain points, as it depends on the position regarding the antennas. One presents the spectrum obtained for [75, 3000] MHz in Figure 4.8, representing the measurement made in one point where all systems identified over all the points are detected, so that it is the one chosen to show the several spectral stripes. One can observe that the dominant stripes correspond to cellular systems, namely: in 800 MHz, corresponding to LTE800; 900 MHz, which is the GSM band; 1800 MHz, being possible to be either GSM or LTE; 2100 MHz, associated to UMTS, and 2600 MHz, being also an LTE band. Besides these systems, also in 75 MHz a minor stripe is observed, corresponding to FM broadcasting systems, as well as near 3000 MHz, being in the band of air traffic and military radars [OIMC13], their values being much lower.

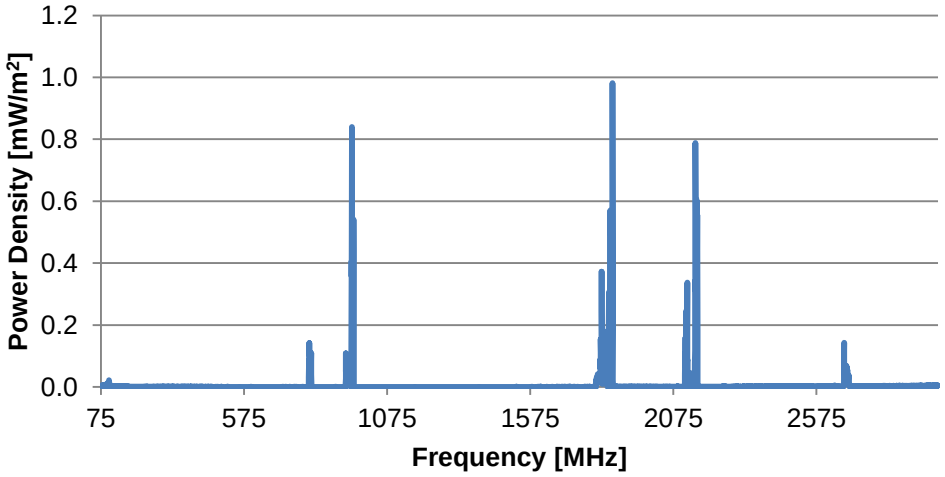

Figure 4.8. Power density for the frequency range of [75, 3000] MHz, obtained with SRM.

The focus is to evaluate the exposure in between the bands of LTE, *i.e.*, in [800, 2600] MHz, so that the systems that were detected in the measurements inside this band are identified and analysed in terms of their contributions. From the systems mentioned before, the only ones that are not considered are FM broadcasting and air traffic and military radars. Annex F presents a detailed analysis of the evolution of power density values of each system with the distance.

Regarding the contributions of the signals, one can obtain the values corresponding to all the frequencies in the band of interest, *i.e.*, as the SRM acquires with a frequency resolution of 0.5 MHz, the values for the frequencies in the band of interest, spaced by 0.5 MHz, are used in (3.20). The contribution of each system to the total exposure is obtained through the sum of the signals contribution corresponding to each system, being a particular case of (3.20). The total exposure is, then, determined through (3.20), which sums all the contributions, *i.e.*, the contributions of all the signals in the band of interest, being represented in Figure 4.9. Furthermore, the relative contributions of each system are also determined, through (3.21). With these, it is possible to have a general view of the systems contributions to the total exposure at each point, Figure 4.9, showing a similar evolution with the distance to the one obtained for power density values, where it is possible to observe the low contribution of LTE2600, which is only detected in two points, as well as of WiFi, which has low power density values associated, as detailed in Annex F. Furthermore, it is possible to verify that the total

exposure satisfies the requirement, where the highest value (0.022) is 45 times below the maximum admissible, being 2.2% of it, observed for the distance of 80 m. Regarding the contributions of each of the systems, considering their operation bands and summing all their contributions, for the distance of 80 m, GSM900 is the system that contributes the most to the total exposure, with a relative contribution of 50.3%, with GSM/LTE1800 contributing 26.5%, UMTS with a relative contribution of 11.5%, and LTE800 having 9.3%. WiFi and LTE2600 are the ones with residual relative contributions, being 0.3% and 0.5%, respectively. These values, as well as the highest power density ones, are summarised in Table 4.6.

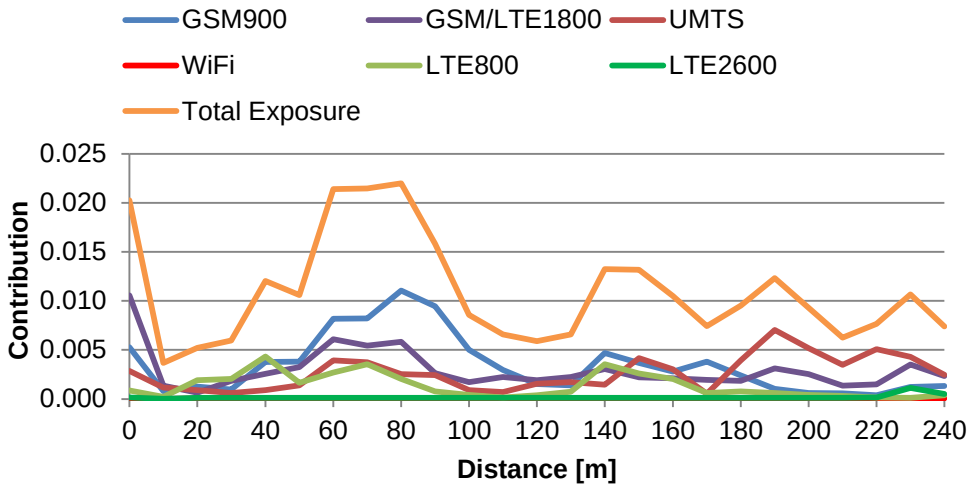

Figure 4.9. System contribution to the total exposure, obtained through the SRM data.

Table 4.6. General average values obtained in the measurements.

System	Relative Contribution	Max. Power Density [mW/m^2]		Max. Total Exposure
		PFM	SRM	
GSM900	50.3%	7.5	98.8	0.022
UMTS	26.5%			
LTE2600	9.3%			

Finally, concerning the distinction between the service and the system being used, the measurements were repeated with the PFM for the point at 90 m and in two intermediate points, corresponding to 85 and 95 m. The results presented in Figure 4.10 show that, in general, the values of power density increase with the distance to the first point of investigation, with the exception being UMTS at a distance of 85 m, which is higher than the others. For 95 m, one verifies that the value without MT is higher than the one for 90 m, the maximum obtained for the 25 points along the street with the PFM, as this is an intermediate point, so that this is the maximum value verified over all the measurements without the MT in the street, corresponding to 8.5 mW/m^2, being much lower (235 times) than the most restrictive reference value.

Regarding the comparison between the services being used, it is shown that using voice GSM leads to a high increase in power density, meaning that it almost doubles the value regarding the situation

without MT, with the maximum value being registered for 95 m, corresponding to 18.9 mW/m^2 (106 times below the most restrictive level). On the other hand, no significant differences are observed when using voice UMTS, which can be justified with the fact that UMTS power control is faster than in GSM, not showing higher radiated values when establishing a connection, as it happens with GSM. For data UMTS, the most relevant difference is at the distance of 85 m, where the variation is around 23% regarding the situation without MT, which might not be directly related to the MT of the measurements, as it could have been the influence of other users near the measurement point. The values concerning this analysis are summarised in Table 4.7.

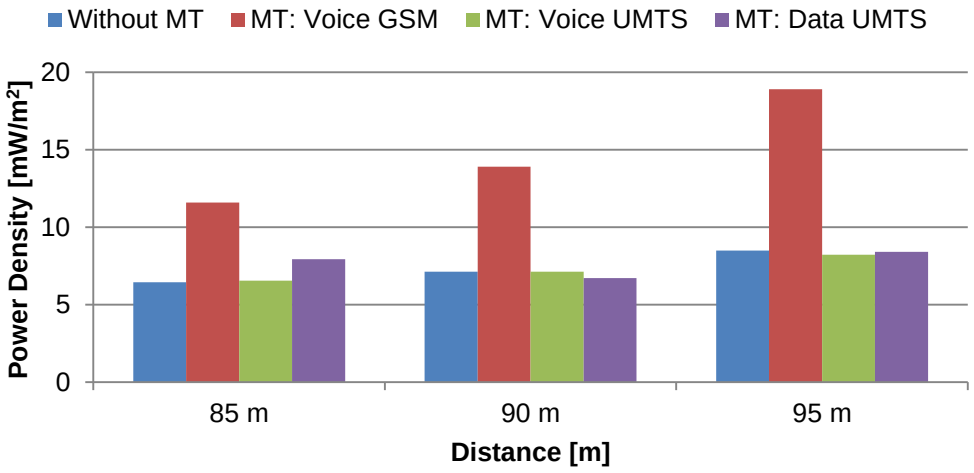

Figure 4.10. Comparison of the power density values between several usage types.

Table 4.7. General average values obtained in the measurements, for the several usage types.

Usage Type	Power Density [mW/m^2]		
	85 m	**90 m**	**95 m**
Without MT	6.4	7.1	8.5
Voice GSM900	11.6	13.9	18.9
Voice UMTS	6.5	7.1	8.2
Data UMTS	7.9	6.7	8.4

4.3 Simulations

This section presents the results obtained for the reference scenario, as well as for the different scenarios that are obtained through the variation of the parameters to be analysed.

4.3.1 Reference Scenario

The simulations regarding the reference scenario, whose parameters are defined in Section 4.1, are

done with the three cellular systems active being GSM900, UMTS (HSPA+) and LTE2600. These systems were chosen by taking into account that LTE2600 is the most common in urban scenarios, providing more capacity than the other LTE ones; GSM900 is the version chosen for GSM, as the 1800 MHz version is being used in LTE, and the trend is to have 1800 MHz only for LTE; for UMTS, the HSPA+ version is considered, as it is the latest one.

In the situation where the user is static, in front of the reference BS, at the level of the street, the direct distance between the BS and the MT is 33.4 m, meaning that the user is in the near-field of the BS for all cellular systems, according to Table 3.1; hence, one should take into account that the use of the expressions of far-field leads to approximate values, as mentioned in Subsection 3.1.3. From Figure 4.11, one can see that the power density values in DL are higher for LTE2600, with UMTS carriers presenting the lowest values. This can be explained by the path loss, which increases with frequency, so that the power values of UMTS at the point of investigation are lower than the GSM900 ones. The same is not verified when comparing the values of LTE2600 with the others: although the frequency of LTE is the highest of all operating systems, it uses MIMO 2×2, meaning that the radiated power is twice the one without MIMO, which would lead to the lowest values of power density comparing to the others. Although the frequency of the carriers increases with their number, it is observed that the average DL power density does not always decrease with the number of carriers, some oscillations being verified, as, depending on the frequency, the interference between the reflected rays can be constructive or destructive, reinforcing or fading the signal.

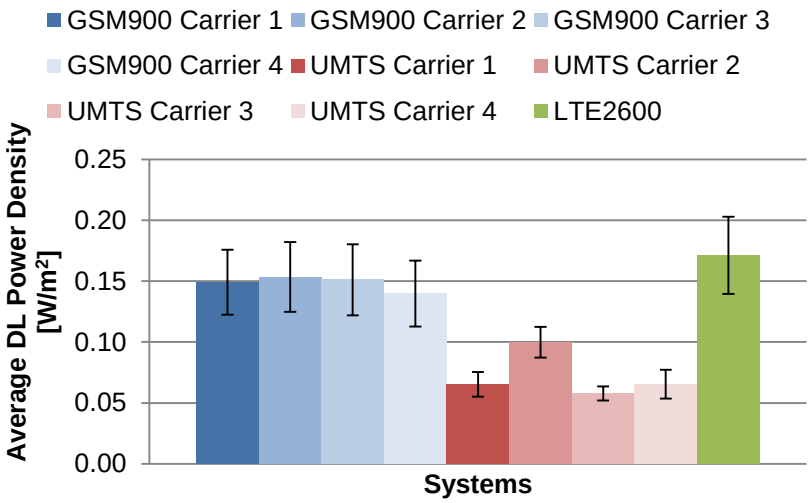

Figure 4.11. Average DL power density for each system in the reference scenario.

The highest average DL power density is observed for LTE2600, with a value of 0.171 W/m^2, being 58 times below the reference level, which is 10 W/m^2 for this frequency, according to Table 2.7, having an ER of 1.7%. The highest value for GSM900 (0.153 W/m^2) is 30 times below the corresponding reference level (4.6 W/m^2), with an ER of 3.3%, and the higher value of UMTS (0.1 W/m^2) is 100 times below the reference level (ER of 1%). The values of the GSM carriers are approximately the same, as the standard deviations are higher than the difference between the respective values for DL.

Regarding UL, the values of power density only correspond to LTE2600, as it is the unique system

being used by the user. The average value obtained for this component is 0.707 W/m^2, with a standard deviation of 0.129 W/m^2, being 14 times below the reference level (ER of 7.1%). This value is 4 times higher than the DL one, which can be explained with the MT EIRP being high, mainly due to the higher path loss and BS target value. This is different from what is observed in the assessment, for LTE800, where the path loss is lower, due to its lower frequency, and the BS sensitivity is higher, *i.e.*, the receiver requires less power, as it has half of the LTE2600 bandwidth, requiring a lower MT radiated power.

In order to compare the average contributions of DL and UL to the total exposure, the contributions of all DL systems are summed in order to obtain the DL contribution, the same being applied to UL, which only corresponds to LTE2600. The average DL contribution corresponds to 0.174, with a standard deviation of 0.015, with the UL value being the one corresponding to LTE2600, 0.071 and standard deviation of 0.013. Hence, the average total exposure is the sum of the average DL and UL contributions, leading to a value of 0.245, with standard deviation of 0.0198, which is 4 times below the requirement (24.5% of the maximum admissible for the total exposure). The DL contribution corresponds to 71.2% of this value, and 28.8% for the UL contribution, where it is verified that, at the point of investigation, the DL component is dominant, as it comprises the 3 systems operating in that direction, whereas UL only comprises one system, corresponding to an LTE2600 carrier.

Furthermore, it is possible to obtain the average contribution of each of the systems to the average total exposure, in order to assess about their influence. The total contribution of a system is obtained by summing the average contributions of the DL and UL carriers of that system. The average contributions of each system are shown in Figure 4.12, where the LTE2600 contribution corresponds to 0.088 (35.9% of the total exposure), with UMTS ones being 0.029 (11.8%), and the GSM contribution being 0.128 (52.3%), having the highest contribution to the total exposure. The dominance of GSM900 is associated to lower path loss values, which lead to the values of DL power density presented in Figure 4.11. The fact of having a lower reference level (4.5 W/m^2) and 4 carriers, each of them with the maximum power values, leads to is prevalence over LTE2600. The general average values obtained in the simulations of the reference scenario are summarised in Table 4.8.

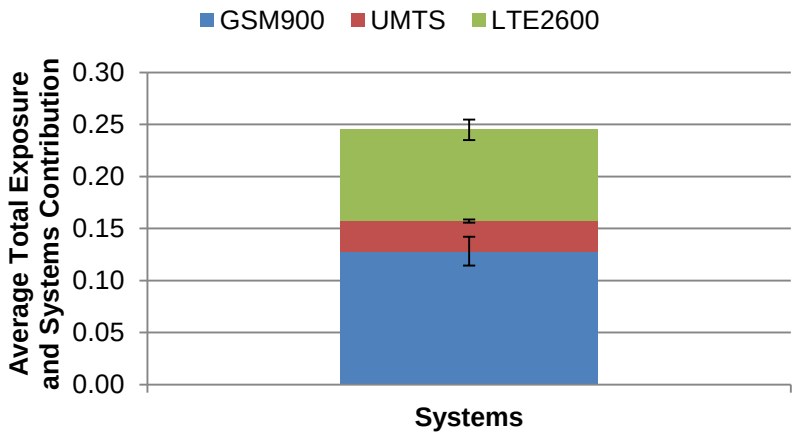

Figure 4.12. Average total exposure with the contribution of each system.

Table 4.8. General average values obtained for the reference scenario.

System	Max. DL Power Density [W/m^2]	UL Power Density [W/m^2]	Relative Contribution	DL Relative Contribution	UL Relative Contribution	Total Exposure
GSM900	0.153	-	52.3%	71.2%	28.8%	0.245
UMTS	0.010	-	11.8%			
LTE2600	0.171	0.707	35.9%			

When considering the user moving along the street, a maximum distance of 240 m from the initial position is assumed, with steps of 10 m, corresponding to the distances of the measurements. In this case, one can observe the behaviour of the parameters previously presented with the distance, starting with the average DL power density, Figure 4.13, being verified that the trend is to decrease with the distance, presenting some oscillations in the first points, due to the interference between the several rays. This is an expected behaviour, as the radiation pattern of the antenna is not taken into account, *i.e.*, the maximum gain is considered for all the directions, as mentioned in Subsection 3.1.1.

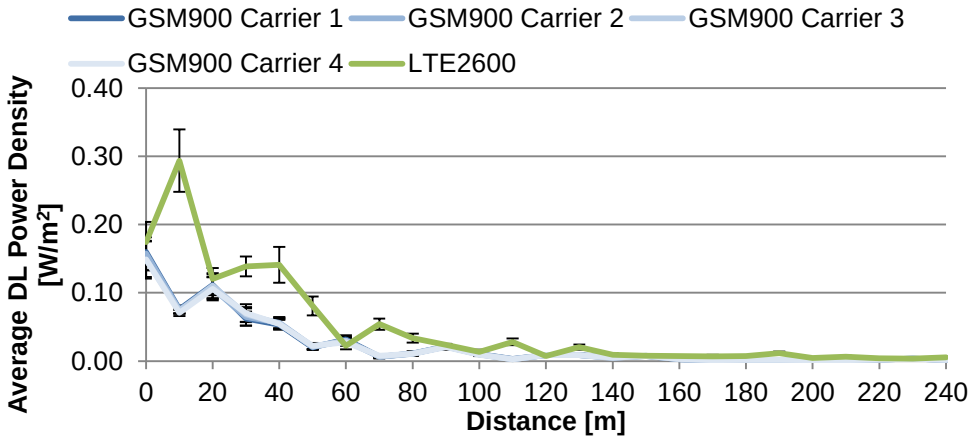

(a). GSM900 and LTE2600

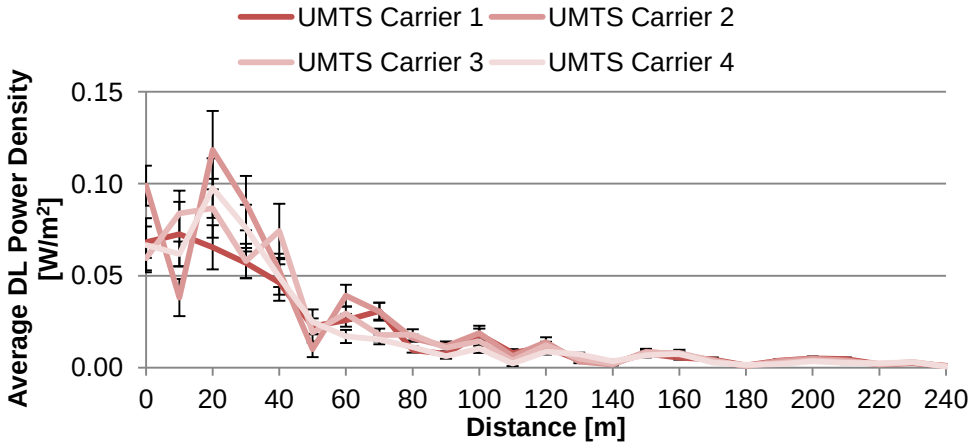

(b). UMTS

Figure 4.13. Average DL power density over the distance.

The overall behaviour is the same for all systems, where for UMTS the oscillations differ between the carriers, as the interference between the rays can reinforce or fade the signal depending on the frequency, besides the distance. UMTS Carrier 2 is the one that presents higher oscillations and, thus, can reach higher values of power density in the first points, confirming the results of the situation where the user is static. LTE2600 has the highest DL power density values, Figure 4.13 (a), with the maximum value of 0.294 W/m^2, observed at a distance of 10 m, being 34 times below the reference level (ER of 2.9%); in GSM900, Figure 4.13 (a), the maximum is 0.160 W/m^2, obtained at the initial position, being 29 times below the reference level (ER of 3.5%); in UMTS, Figure 4.13 (b), the maximum value of 0.118 W/m^2 is verified at 20 m, which is 85 times below the reference level (ER of 1.2%).

In UL, the results suggest that the UL power density increases with the distance, as shown in Figure 4.14. This is due to the increase of path loss, meaning that the MT radiated power should also increase, in order to compensate for the increase in path loss and to satisfy the target value at the BS. As the distance increases, the MT radiated power increases up to the moment that the transmitter reaches its maximum transmission power, being observed that the UL power density saturates at 2.584 W/m^2 for a distance of 90 m, being the maximum power density value in UL, a value that is much closer to the reference level, as it is 4 times below the reference value (ER of 25.8%).

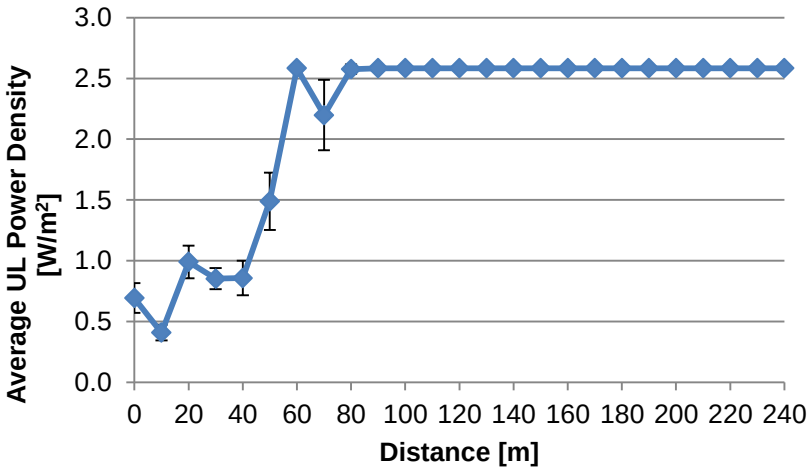

Figure 4.14. Average UL power density over the distance.

The high requirements in terms of BS target value, which have to do with the consideration of the maximum possible throughput, that leads to a high SNR (24 dB), as well as with the maximum bandwidth (20 MHz), have impact on the BS sensitivity, also contributing to the higher values of UL power density. Hence, when the MT reaches the maximum radiated power and the user continues to move away from the BS, it happens that the BS target value is not satisfied, as path loss increases.

The average DL and UL contributions to the total exposure, Figure 4.15, have opposite behaviours, justified by the evolution of DL and UL power densities over the distance. One can observe that the contributions of DL decrease with the distance, and the UL ones increase, surpassing the contribution of DL. More specifically, DL has an average relative contribution to the total exposure of 72.2% in the

initial position, against 27.8% of UL. Some oscillations are verified in the contributions, which depend on the oscillations of path loss from a point to another, and, from 40 m, the UL starts to have higher contributions compared to DL, contributing in 50.3% to the total exposure, against 49.7% of DL at this point. From the distance where the MT radiated power saturates, the average contribution of UL becomes constant, being 0.258 (relative contribution of 91.4%), and 0.024 (8.6%) for DL. From this point on, although the UL contributions remain constant, the DL ones decrease, as the DL power density becomes lower.

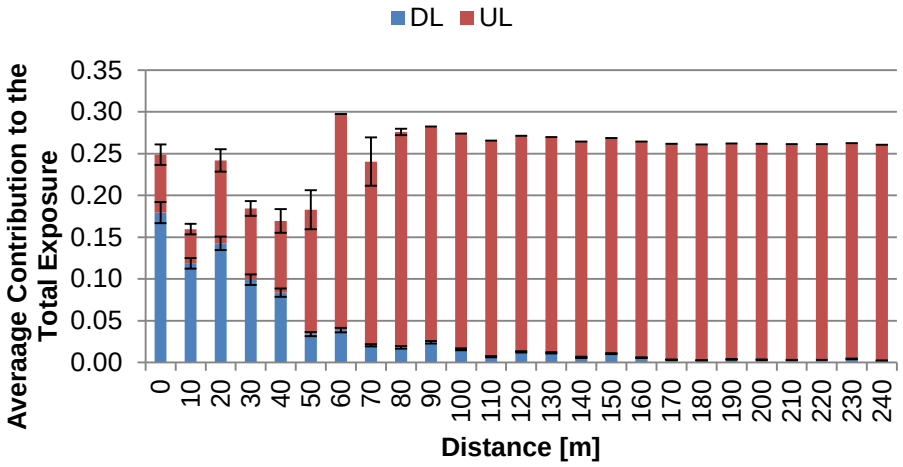

Figure 4.15. Average DL and UL contributions to the total exposure over the distance.

Finally, the average contributions of each system over the distance are analysed, Figure 4.16. Results show that LTE2600 is the system that contributes the most to the total exposure, motivated by the high contribution of the UL component. The only exception is in the initial position, where GSM900 has a higher contribution, because of its higher DL power density. GSM900 has a higher contribution than UMTS, as the power density due to GSM900 is higher than in UMTS, as already seen. Moreover, it is observed that the total exposure closely follows the LTE2600 contributions curve after the initial 50 m, due to the fact of LTE2600 becoming the system highly dominating the contributions.

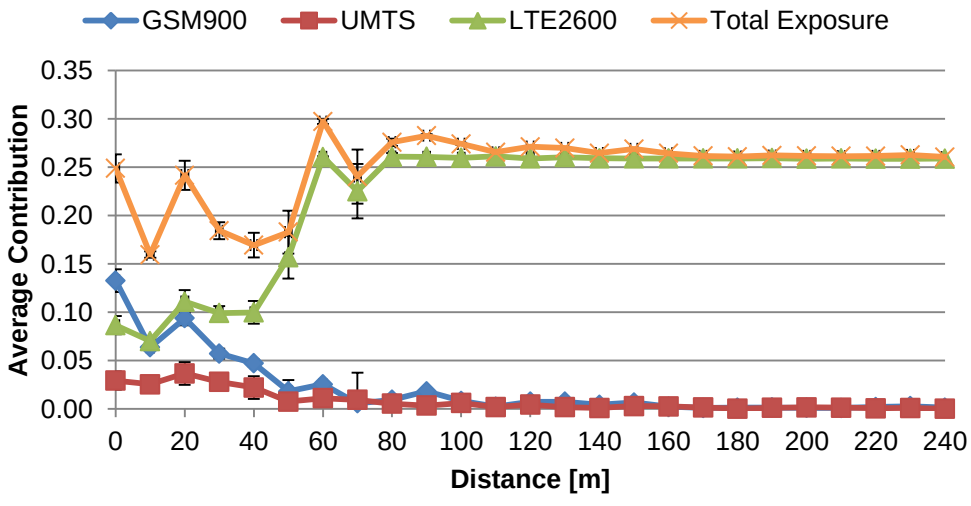

Figure 4.16. Average systems contributions to the total exposure over the distance.

Regarding the values of the contributions, the average total exposure complies with the requirements, being always lower than 1. More specifically, the maximum value of the average total exposure is verified at a distance of 60 m, corresponding to 0.297, 3 times below the reference value (29.7% of reference value), due to the high contribution of the UL component. For this maximum value, the average contribution of GSM900 is 0.026 (contributing 8.6% to the total exposure), and the UMTS one is 0.011 (3.7%), with the LTE2600 being 0.260 (87.7%).

The general average values obtained in the simulations of the reference scenario considering the user varying the position along the street are presented in Table 4.8, the highest values of DL and UL obtained power density being shown, the highest total exposure and the systems relative contribution to this value, as well as the DL and UL relative contributions in several points of investigation.

Table 4.9. General average values for the reference scenario, considering the user's mobility.

System	Max. DL Power Density [W/m^2]	Max. UL Power Density [W/m^2]	Relative Contribution	DL Relative Contribution	UL Relative Contribution	Max. Total Exposure
GSM900	0.160	-	8.6%	72.2% (0 m) 50.3% (40 m) 8.6% (90 m)	27.8% (0 m) 49.7% (40 m) 91.4% (90 m)	0.297
UMTS	0.118	-	3.7%			
LTE2600	0.294	2.584	87.7%			

4.3.2 Mobile Communication Systems

The evaluation of the mobile communication systems is done considering all systems, *i.e.*, GSM, UMTS, LTE and WiFi, based on the scenario configuration described in Section 4.1, as well as on the set of systems detailed in Table 4.3. Regarding the reference scenario, the differences in DL concern the number of LTE systems, LTE800 and LTE1800 being also considered, as well as WiFi. As GSM and UMTS remain the same, the analysis concerning the DL power density is the same for the reference scenario for these two systems. From Figure 4.17, it is suggested that LTE1800 is the system that leads to the highest value of DL power density, even when compared with the other two LTE systems. The value for LTE800 is lower than the LTE1800, as its transmitter output power is 30 W, lower than the value for the other LTE systems, which is 40 W. Hence, as the LTE2600 signal suffers the highest path loss, LTE1800 is the one with the maximum DL power density, whose value is 0.251 W/m^2, 40 times below the reference value (ER of 2.5%).

Although WiFi values consider the total power coming from the 4 APs taken into account, WiFi presents negligible values of power density compared to the ones corresponding to cellular systems, being 2 150 times below the lowest value obtained for DL, which is associated to the carrier 3 of UMTS. This is due to the difference in radiated powers, which are very low for WiFi (around 0.1 W), compared to cellular systems (30/40 W), as well as due to path loss, being higher than most of the cellular systems (the only exception is LTE2600), because of its frequency of 2400 MHz, which decreases even more the power of the WiFi signals.

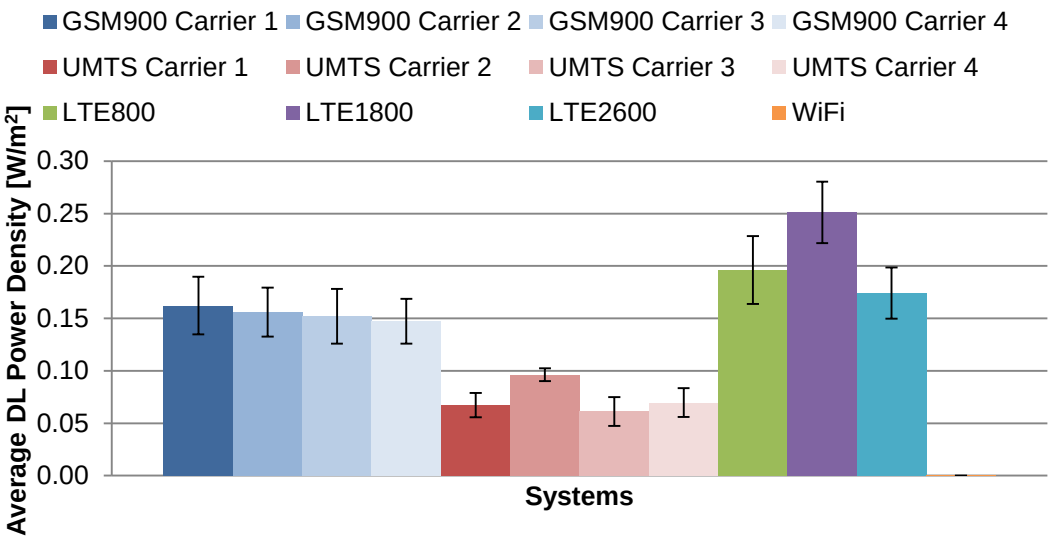

Figure 4.17. Average DL power density for each of the mobile communication systems.

Concerning UL, the results of the simulations varying the UL system over the 3 LTE technologies, Figure 4.18, show that the average UL power density increases with the frequency of operation, a behaviour that is due to the increase of path loss. As for LTE2600 the path loss is higher, the MT needs to radiate more power in order to maintain the same target power at the BS. This explains the fact of UL power density being the highest for LTE2600, and the lowest when LTE800 is used, with a decrease of 95.7% with respect to the LTE2600, with the value of LTE1800 being 63.2% below the LTE2600 one. As the conditions are the same of the reference scenario for UL, the values of LTE2600 are nearly the same obtained in that scenario, being 14 times below the reference level.

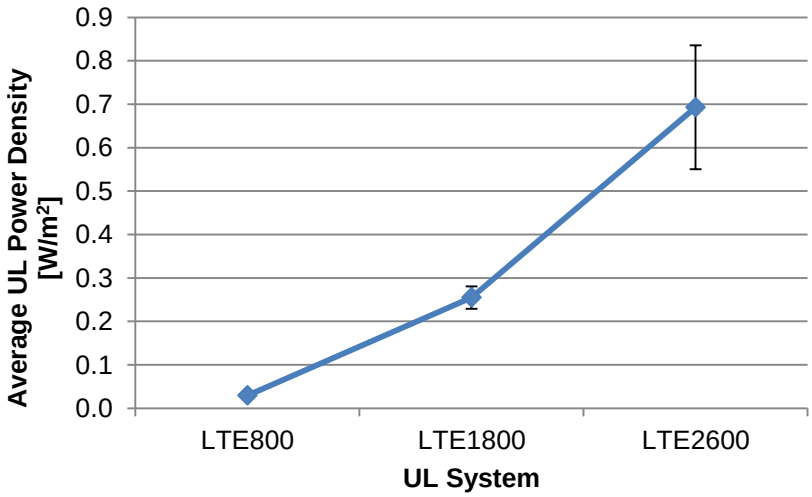

Figure 4.18. Average UL power density for each LTE technology.

DL and UL contributions for the 3 DL/UL configurations are presented in Figure 4.19. One can see that the value of the average DL contribution remains nearly constant (0.257), as the DL systems are the same for all the tests, although their relative contribution to the total exposure decreases, due to the increase of the UL contribution. This allows to confirm the trend previously observed: the contributions

of UL increase with frequency, *i.e.*, in the LTE800 UL test, the UL contribution to the total exposure is the lowest (0.007, 2.7% of the total exposure), followed by the contribution of LTE1800 UL, being 0.03 (10.4%); with LTE2600 UL, the highest contribution is observed, corresponding to a value of 0.069 (21.5%). Moreover, one can see that the UL contribution in LTE800 is 10 times less than the LTE2600, which is twice the LTE1800 UL contribution.

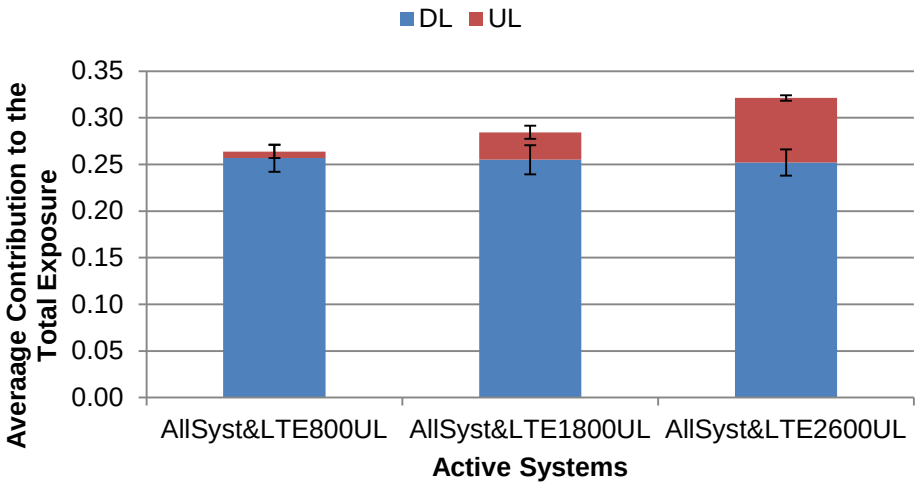

Figure 4.19. Average DL and UL contributions to the total exposure, for the 3 configurations.

The average contribution of each of the systems to the total exposure is presented in Figure 4.20, where it is shown that the contribution of each system increases when it is used in UL, which is not the case of GSM900, UMTS and WiFi, each one remaining nearly the same for the 3 tests. It is verified that the total exposure complies with the requirements, with its maximum value occurring for the case of LTE2600 UL (0.321), which is 3 times below the maximum admissible for the total exposure, corresponding to 32.1% of its value. The system that contributes the most for this value is GSM900, with a contribution of 0.130 (40.5% of the total exposure value), followed by LTE2600, due to the contribution of the UL component, having a contribution of 0.087 (27.1%). The remaining systems have lower contributions: LTE800 has a contribution of 0.049 (15.3%); UMTS contributes 0.029 (9%), and LTE1800 contributes with 0.026 (8.1%), with the contribution of WiFi being negligible, as it is virtually null. The higher contributions of GSM900 can be explained by the number of carriers that this system has and by the lower reference level, so that it contributes more than the LTE2600 system, although it uses MIMO, as observed in the reference scenario.

Although LTE1800 presents the highest values of DL power density, when determining the contributions of each signal, one obtains higher values for LTE800, as the reference level for this frequency is lower, which can be confirmed by the fact of LTE2600 UL signal contributing 21.5% to the total exposure, meaning that only 5.6% corresponds to the LTE2600 DL signal.

Considering the maximum value obtained for the total exposure, one can also conclude that the introduction of LTE in the network, regarding the already existing systems, approximately doubles the total exposure, with the 3 LTE technologies in DL and LTE2600 in UL.

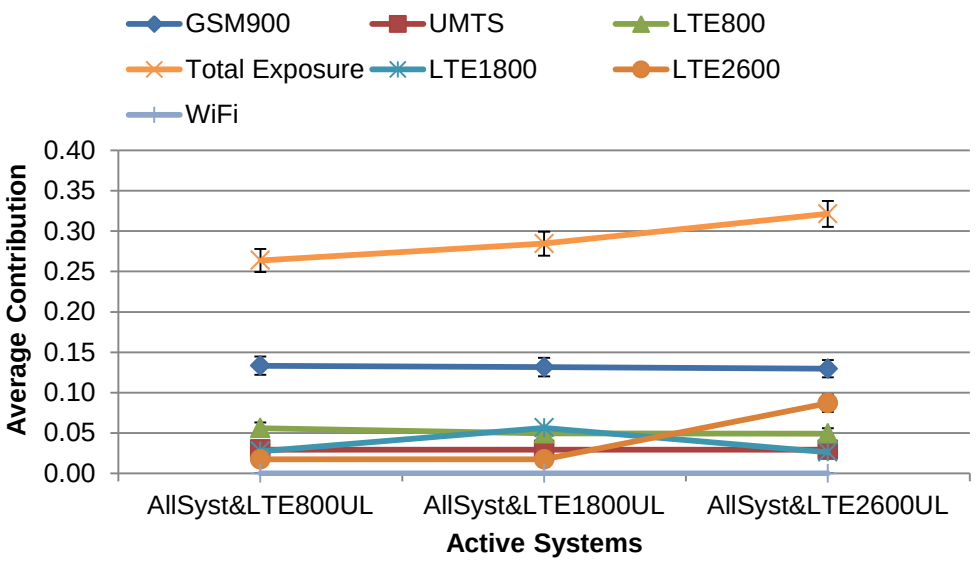

Figure 4.20. Average system contribution to the total exposure, for the 3 configurations.

The general average values obtained in this analysis, regarding the exposure, are presented in Table 4.10.

Table 4.10. General average values obtained for the mobile communication systems analysis.

System	Max. DL Power Density [W/m^2]	UL Power Density [W/m^2]	Relative Contribution	DL Relative Contribution	UL Relative Contribution	Max. Total Exposure
GSM900	0.162	-	40.5%	78.5%	21.5%	0.321
UMTS	0.096	-	9.0%			
LTE800	0.196	0.030	15.3%			
LTE1800	0.251	0.255	8.1%			
LTE2600	0.174	0.693	27.1%			
WiFi	2.837×10^{-5}	-	0.0%			

4.3.3 Services

The analysis of the services consists of varying the service being used (voice or data) for the several systems in UL, maintaining only one technology per system, *i.e.*, GSM, UMTS and LTE only have one version active at each test, meaning that, for instance, when data LTE800 or data LTE1800 are used, LTE2600 is not taken into account, the same approach being taken for the other services.

The objective is to distinguish between voice and data, taking into account the UL systems as indicated in Table 4.4. The results of the average UL power density, Figure 4.21, suggest that the largest variations of the UL power density occur when using data LTE, namely LTE1800 and LTE2600. If one looks only to the behaviour of data LTE, one can verify the same evolution as the one obtained in Figure 4.18, so that the conclusions about their relation are the same.

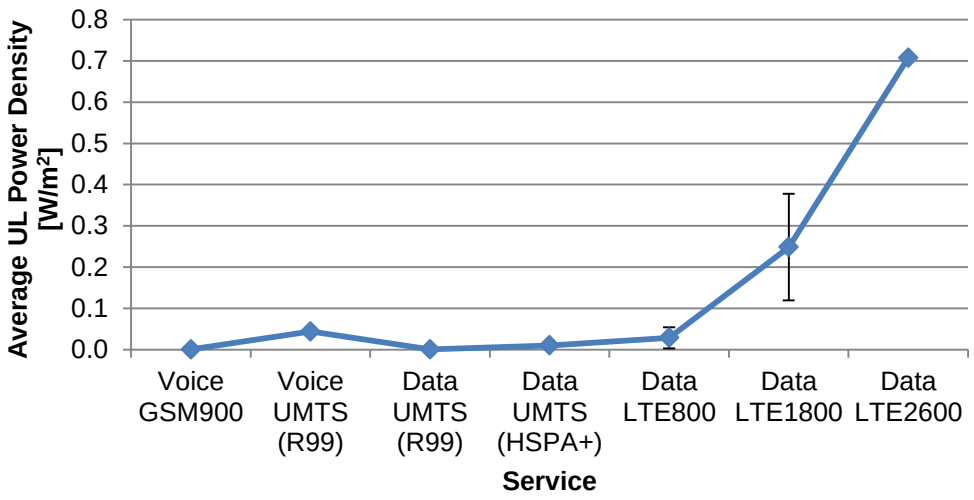

Figure 4.21. Average UL power density in each service scenario.

Besides LTE, the service that shows a higher value when compared to the other services, although much lower than the LTE1800 and LTE2600, is voice UMTS, being 0.044 W/m^2 (227 times below the reference value), which is 44 times higher than the one observed for voice GSM900 (0.001 W/m^2), and 73 times higher than the one of data UMTS (R99), 0.6 mW/m^2, which mainly have to do with the considered value for the SNR, used in the sensitivity calculation, which increases the BS target value for voice UMTS, leading to the increase of the MT radiated power.

The service that has a major impact in the exposure viewpoint is data LTE, mainly LTE1800 and LTE2600, the average values of UL power density being 6 and 16 times higher than the one for voice UMTS, respectively, and 23 and 67 times higher than data UMTS (HSPA+). Concerning data LTE800, it is 3 times the value of data UMTS (HSPA+), LTE800 being the LTE system with the lowest UL power density.

However, in order to assess the influence of each service on the total exposure, one should focus on the UL contributions, which are presented in Figure 4.22. Although the variations in between the power density values concerning each of the services can vary substantially in some of them, when observing the values of the UL contributions, one concludes that only data LTE1800 and data LTE2600 have relevant contributions to the total exposure value, 0.029 (13.2% to the total exposure) and 0.071 (28.8%), respectively, meaning that the other systems do not have relevant influence in the total value of the total exposure, as one can observe from Figure 4.22.

Furthermore, one can see that the average DL contribution is higher for LTE800, as it has lower path loss than the other LTE systems, with LTE2600 being the one with the lowest contribution in DL. The UL analysis is the same as the one done for the mobile communication systems analysis, as the systems in UL are the same, so that data LTE2600 has the highest contribution to the total exposure.

Regarding the contribution of each system to the total exposure, Figure 4.23, it is observed that for GSM900 and UMTS the value of the contribution does not show relevant variations, as UL contributions are much smaller than DL ones, so that the contribution of the system remains nearly

constant, the same being verified for the total exposure. A similar behaviour is observed between data LTE800 and data LTE1800, where the value of the total exposure also remains nearly the same due to the approximate values of the LTE800 and LTE1800 contributions. Although the UL power density of LTE1800 is higher than the LTE800 one, its reference value is higher than for the latter, so that, in this case, one cannot directly compare the power density values to conclude about the contributions. This is also observed in Figure 4.22, where, although the UL contributions are different, the contribution of the system (DL and UL) is approximately the same.

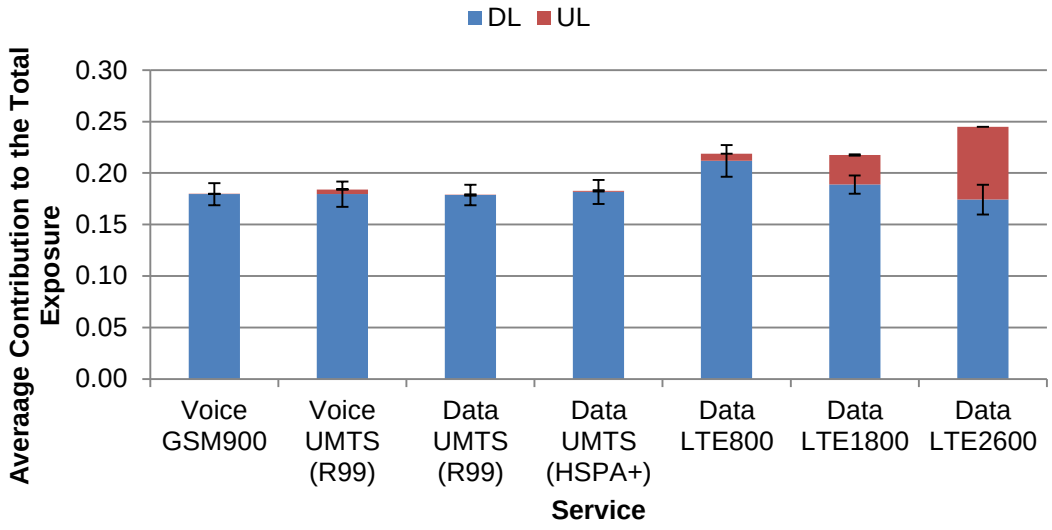

Figure 4.22. Average DL and UL contributions, depending on the service.

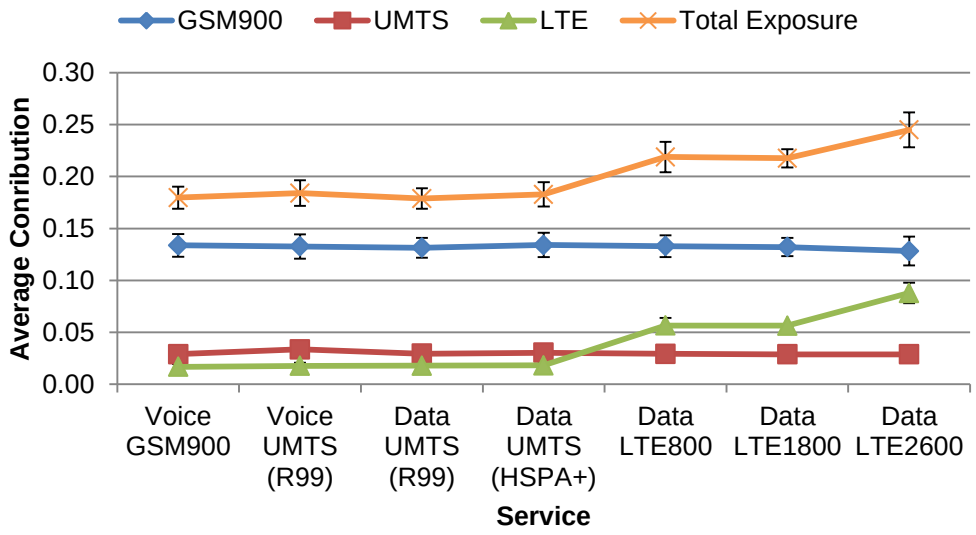

Figure 4.23. Average system contribution to the total exposure, depending on the service.

The highest value of the total exposure is 0.245, being 4 times below the reference value (24.5% of the maximum value), which corresponds to the reference scenario, being shown in Table 4.11, as well as the most relevant general parameters previously referred.

Table 4.11. General average values obtained for the services analysis.

Service	UL Power Density [W/m^2]	UL Relative Contribution	Max. Total Exposure
Voice GSM900	0.001	0.10%	0.245
Voice UMTS (R99)	0.044	2.50%	
Data UMTS (R99)	0.001	0.04%	
Data UMTS (HSPA+)	0.010	0.51%	
Data LTE800	0.029	3.20%	
Data LTE1800	0.249	13.20%	
Data LTE2600	0.707	28.80%	

4.3.4 Number of BSs

This analysis comprises the variation of the number of BS antennas on the roof-tops, taking into account the parameters presented in Table 4.5, and the configurations also described in Section 4.1. In each configuration, as the DL power density is, on average, equal for the same BS, one presents the DL power density of the system carrier that has the highest value, for each BS and for the two configurations, Figure 4.24. The UL power densities are not presented, as they are the same as for the reference scenario, as it is assumed that the MT is always connected to BS1.

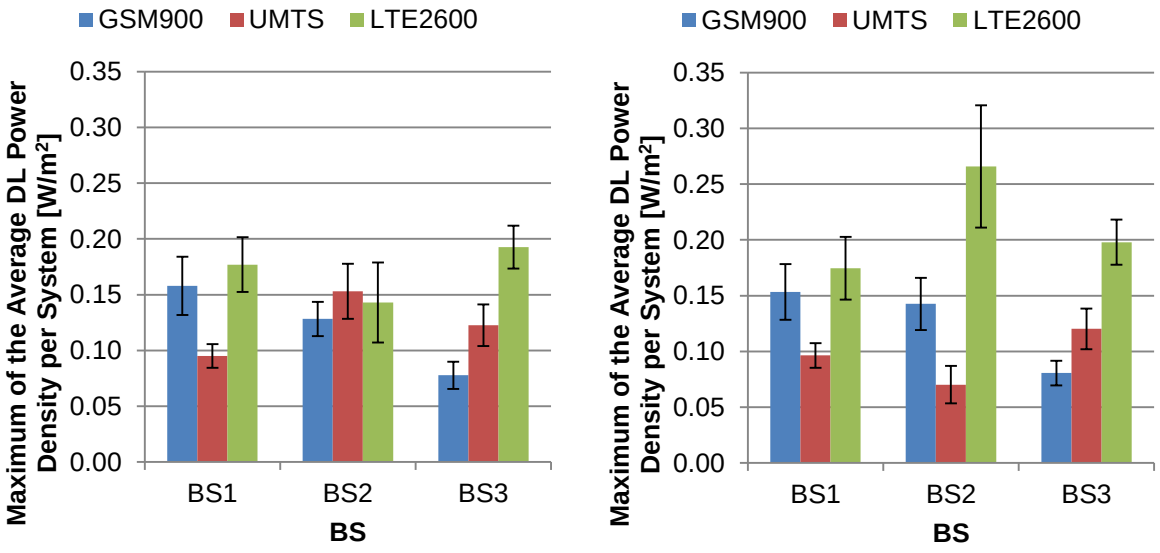

(a) BSs in the alternate configuration (b) BSs in front of each other

Figure 4.24. Maximum values of the average DL power density for each system, for the 3 BSs.

As expected, the values corresponding to BS1 and BS3 are the same for the 2 configurations, as their position on the roof-top is the same from one configuration to another, only changing the position of BS2. The values from one configuration to the other can oscillate, as the distances to BS2 change, and as the DL model accounts for the interference between the several rays.

Concerning exposure to BS2, the values of GSM900 remain approximately the same, as the standard deviation of the values of the configuration where the BS are in front of each other includes the ranges of values obtained in the alternate configuration. The values of UMTS decrease approximately 54.2% from the alternate configuration, Figure 4.24 (a), to the other configuration, Figure 4.24 (b), which might be due to the decrease of the distance from the MT to BS2, such that the interference between the rays is more destructive. On the other hand, LTE2600 values of BS2 increase approximately 86% when the configuration is changed, which might be due to the same reason, but for the frequency of LTE2600 the interference can be constructive, so that the signal is reinforced.

The most relevant results in this analysis, which allow a more specific comparison between configurations, are the ones corresponding to the contributions to the total exposure. When the configuration is varied, maintaining the number of BSs, the average DL contributions for the 2 configurations, Figure 4.25, do not have significant differences, being nearly the same, approximately 0.350 (84% of the total exposure) with 2 BSs, and approximately 0.470 (86%) with 3 BSs. This is due to the fact that only BS2 changes the position, with a displacement of 7.5 m on the buildings' roof-top, to change to the alternate configuration, increasing the direct ray only by less than 1 m (from 33.4 m to 34.3 m), which can be neglected compared to the distance by the direct ray. Therefore, to verify a significant difference in the two configurations, the distance between BSs should be higher.

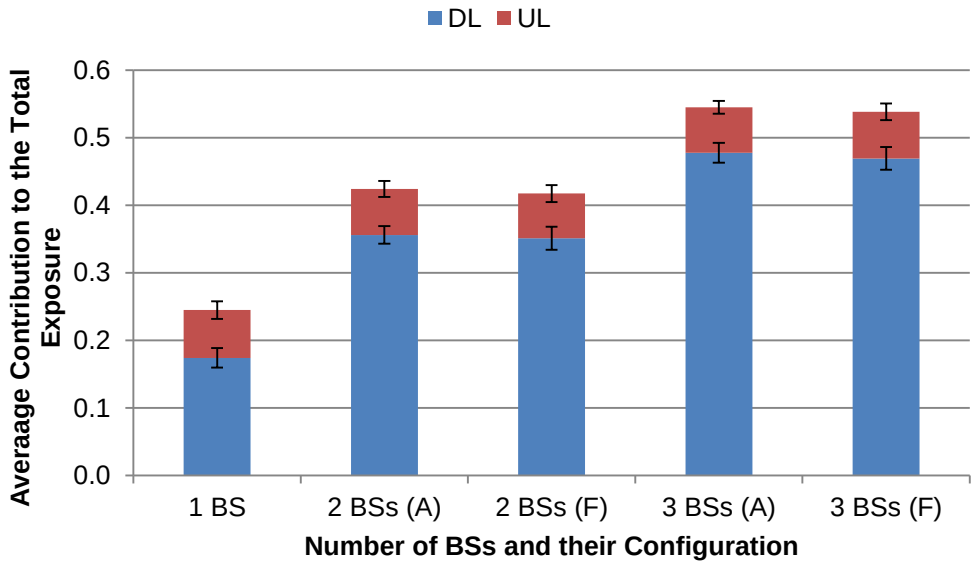

Figure 4.25. Average DL and UL contributions to the total exposure, depending on the number of BSs and their configuration on the roof-tops of the buildings.

However, the main differences in the DL contributions are observed when the number of BSs increases, with the UL contribution being approximately constant, as there are no changes in UL. From the obtained results, one can see that the average DL contribution is approximately doubled and tripled when the number of BSs increases from 1 to 2 and to 3, respectively. This can be explained due to the number of carriers being 2 and 3 times higher, respectively. When the number of BSs increases from 2 to 3, there is an increase of 34.3% regarding the value with 2 BSs for the alternate

configuration, and 33.6% for the other, which is a lower increase than from 1 BS to 2 BSs, probably due to the position of the BS3 being further, having a less contribution.

The behaviour of the total exposure is presented in Figure 4.26, where one can see the contribution of each of the systems, being shown that GSM900 is the one that contributes the most, followed by LTE2600, with UMTS presenting more accentuated oscillations. The total exposure value follows the behaviour previously described for the different number of BSs, and respective configurations, *i.e.*, compared to only 1 BS, the total exposure double and tripled for 2 and 3 BSs, respectively. Although for the GSM900 and LTE2600 there is a slightly increase in the contributions, from the alternated configuration to the one where the BSs are in front of each other, the total exposure does not vary significantly, as the UMTS contribution decrease, cancelling the increase of the other contributions. The maximum value of the average total exposure is obtained for the configuration with 3 alternated BSs, having a value of 0.545, 2 times below the maximum admissible value (54.5% of this value), where GSM900 has an average contribution of 56.5%, UMTS of 21.7% and LTE2600 of 21.8%. GSM900 dominates the contributions, due to the lower path loss that its signals suffer as well as due to its number of carriers (12 carriers, 4 per BS). The contributions of UMTS and LTE are closer, as the UMTS path loss is higher than in GSM900, and LTE2600 uses MIMO 2×2 and has the UL component, so that its contribution approximates the UMTS one.

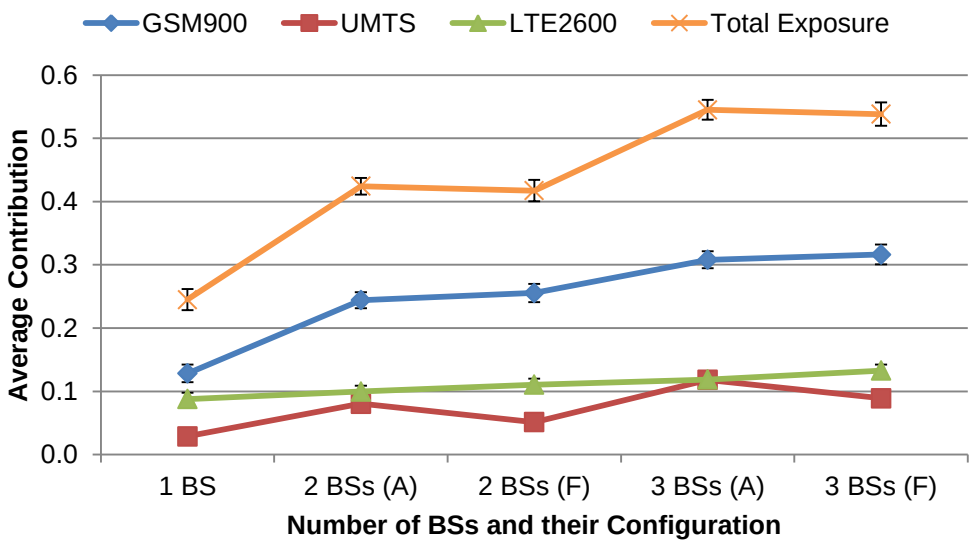

Figure 4.26. Average system contribution to the total exposure, depending on the number of BSs and their configuration on the roof-tops of the buildings.

The values obtained, regarding the highest value of the total exposure, are summarised in Table 4.12, as well as the highest values obtained for DL and UL power densities.

The number of BSs is the scenario parameter that presents the most relevant results with its variation. The other scenario parameters, the height of the BS, the width of the street and the distance to the reference building, are also analysed in terms of their influence, being part of additional simulation results, which are presented in Annex E.

Table 4.12. General average values obtained for the analysis of the number of BSs.

System	Max. DL Power Density [W/m^2]	UL Power Density [W/m^2]	Relative Contribution	DL Relative Contribution	UL Relative Contribution	Max. Total Exposure
GSM900	0.158	-	56.5%	87.6%	12.4%	0.545
UMTS	1.153	-	21.7%			
LTE2600	0.266	0.707	21.8%			

4.3.5 MIMO

As in LTE, more specifically in LTE-A, there is the possibility of having MIMO up to 8×8 in DL and 4×4 in UL, a comparison between these configurations is made, in order to assess their impact on exposure. The study of the impact of MIMO is done considering the reference scenario, only varying the MIMO configuration, so that the average DL power densities concerning GSM and UMTS are, on average, nearly the same as the ones presented in the reference scenario.

The behaviour of LTE2600 with the MIMO configuration is shown in Figure 4.27, showing that DL and UL power densities increase with the increase of the MIMO order, more precisely, from 2×2 (reference scenario) to 4×4, the DL and UL power densities increase by 2, as the radiated power is doubled. Regarding the 8×8 configuration, in DL it is observed that the average power density is 4 times the value when MIMO 2×2 is used, whereas for UL the value remains the same as with MIMO 4×4, as it is assumed that the UL is limited to MIMO 4×4, because this is the maximum defined for LTE-A UL, meaning that, in practice, when MIMO 8×8 is taken into account, only the BS use it, transmitting 8 times the power of a single transmitter, with the MT supporting the maximum of 4×4. The maximum value of power density is observed for MIMO 8×8 in UL, corresponding to 1.342 W/m^2, which is 7 times below the reference level (ER of 13.4%).

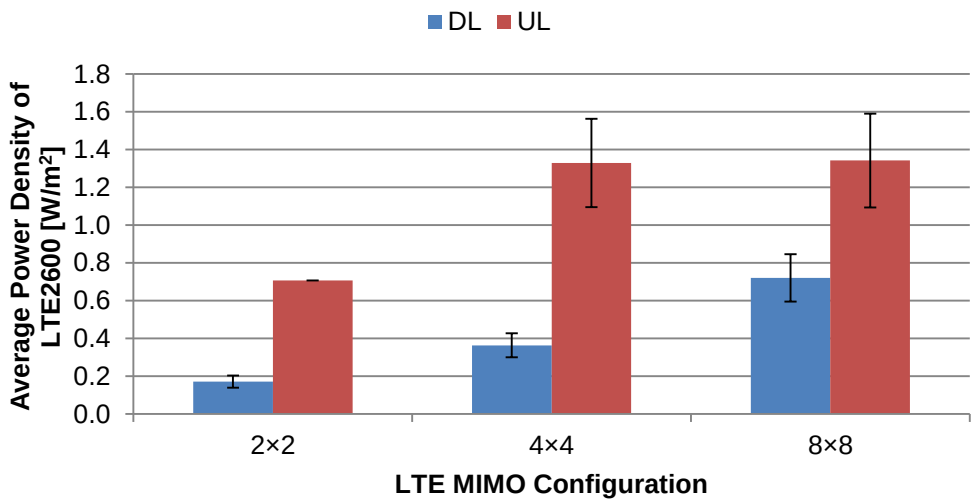

Figure 4.27. Average DL and UL power densities of LTE2600 for different MIMO configurations.

The average contributions of DL and UL to the total exposure, Figure 4.28, are coherent with behaviour of DL and UL power densities. For MIMO 4×4, the average contribution to the total exposure is 0.194 (59.6% of the total exposure) for DL, and 0.133 for UL (40.4%). In the case of MIMO 8×8, the average DL contribution is 0.233 (63.6%) and the UL remains nearly the same as it is expected, with a value of 0.134 (36.4%). It is noticed that the DL contributions do not double and triple for MIMO 4×4 and 8×8, respectively, regarding the reference scenario, which is expected, as in DL, contrarily to UL, other systems exist and maintain their values, so that DL contributions increase by the same amount that LTE DL increases.

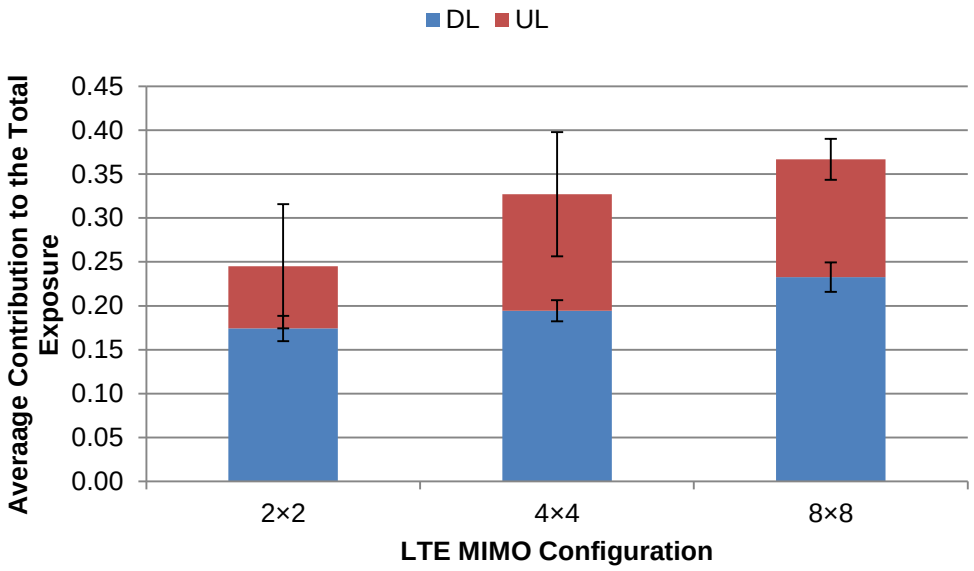

Figure 4.28. Average DL and UL contributions to the total exposure for different MIMO configurations.

According to the results of the average system contribution, Figure 4.29, the GSM900 and UMTS contributions remain constant, as expected, because MIMO is solely used in LTE2600. When MIMO 4×4 is used, it is observed that LTE2600 becomes the system that contributes the most to the total exposure. This is due to the fact of the BS radiated power being doubled, by doubling the number of transmitting antennas. The contribution is even higher when MIMO 8×8 is used, leading to the maximum value of the total exposure, corresponding to 0.367, 3 times below the maximum admissible (36.7% of the maximum value allowed), with LTE2600 having an average contribution to the total exposure of 56.2%, followed by GSM900, which has an average contribution of 36%, with the lower contribution corresponding to UMTS, contributing 7.8% to the total exposure. One can also obtain the values that express the total exposure variation, according to the MIMO configuration. From MIMO 2×2 to 4×4, the total exposure increases around 33.6%; from MIMO 2×2 to 8×8, the total exposure increases approximately 49.8%, with the variation between MIMO 4×4 and 8×8 being 12.1%, less than the one from 2×2 to 4×4, because UL is limited to MIMO 4×4.

The values obtained regarding the highest value of the total exposure, which corresponds to MIMO 8×8, as well as the respective DL and UL relative contributions, and the highest values of DL and UL power densities, are summarised in Table 4.13.

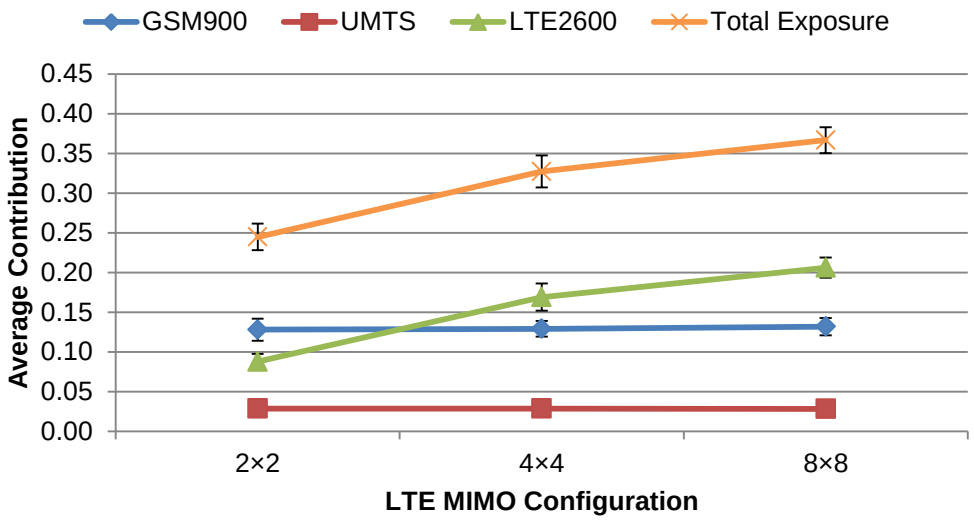

Figure 4.29. Average system contribution to the total exposure for different MIMO configurations.

Table 4.13. General average values obtained for the MIMO analysis.

System	Max. DL Power Density [W/m^2]	UL Power Density [W/m^2]	Relative Contribution	DL Relative Contribution	UL Relative Contribution	Total Exposure
GSM900	0.156	-	36.0%	63.6%	36.4%	0.367
UMTS	0.100	-	7.8%			
LTE2600	0.721	1.342	56.2%			

4.4 Comparison of Results

The measurements and the simulations do not exactly correspond to the same scenario, *i.e.*, there are some differences, such as the street configuration, which is not exactly the same as the one theoretically defined, having buildings of different heights and not being surrounded by buildings in the two sides, for all its length. Hence, the comparison of the simulation results is done between the most similar tests to the type of results obtained in the measurements, which basically are two: the one where the user varies his position, for the reference scenario, and the one where it is made a differentiation between the services being used.

Concerning the situation where the user varies his/her position along the street, although the systems being considered do not exactly agree with the systems operating in the measurement scenario, the comparison of the behaviour of the total exposure over the distance can be done. One of the main differences from the simulated to the measured results has to do with the radiation pattern of the antennas. As in the theoretical model it is considered the maximum BS gain for all the directions, the behaviour of the total exposure presents some differences, as the power density in DL has the trend to

decrease, whereas in the real scenario one observes a maximum in the first dozens of metres, which corresponds to the maximum of the radiation pattern. Moreover, as the distance increases, the influence of the radiation pattern can be seen, with the values presenting some peaks, which is not verified in the simulated results, as DL decreases. This comparison is shown in Figure 4.30, where it is possible to compare the trend of the measured and simulated power density along the street, with the power density values normalised to their respective maximum values, and the simulated corresponding to LTE2600, as the behaviour is similar to the other simulated systems.

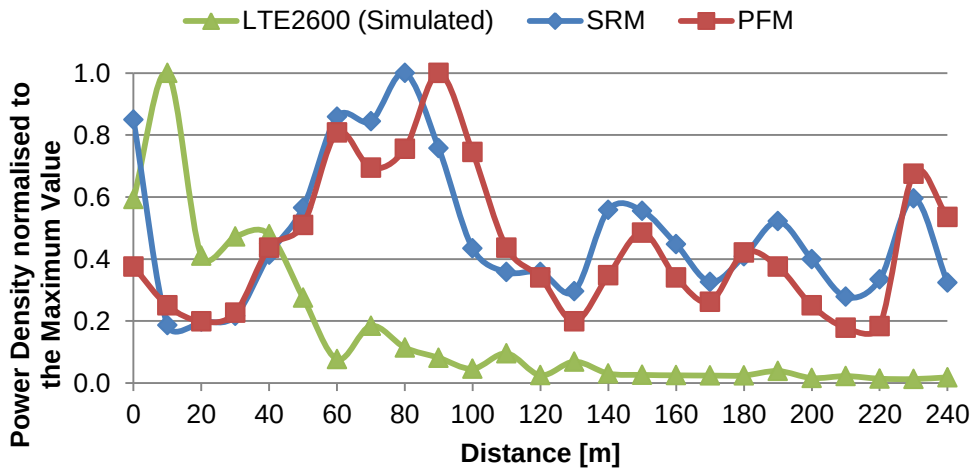

Figure 4.30. Trend of the measured and simulated power density along the street.

In spite of these differences, one can observe some similarities in the relative contributions of each of the systems to the total exposure, comparing the simulation values of the reference scenario, in the situation where the user is varying the position along the street, with the real scenario ones. In the simulated scenario, as for the initial position one has, in theory, the maximum of radiation, one can compare the simulated contributions at this position with the measured contributions at the distance of approximately 80 m, where the maximum radiation is verified (with the SRM), so that the comparison is made in similar conditions, with the values being summarised in Table 4.14. The difference is that, in the real scenario, GSM/LTE1800 and LTE800 are taken into account, while in the reference one, besides GSM900 and UMTS, there is only LTE2600. One can observe that the relative contributions are close in the two scenarios for GSM900 and UMTS. Moreover, one can notice that the sum of the relative contributions of LTE800 (9.3%) with the ones of GSM/LTE1800 (26.5%) gives a value of 35.8%, which is much close to the value of the LTE2600 relative contribution in the reference scenario (34.8%). The values of the total exposure have a difference of, approximately, one order of magnitude, Table 4.14, which might be due to the fact of being considering a worst case approach in the theoretical scenario.

The other result that was obtained for both measurements and simulations is the test of the services being used, which can only be compared in a relative way, as in the measurements the values comprise the overall band measured by the equipment. The main difference is that in the real scenario it is observed that voice GSM shows higher values than other systems, Figure 4.10, which is not

verified in the simulations, as its UL contribution is much lower than the DL one, Figure 4.22, not having a relevant influence in the total exposure. However, it is observed that UL contributions of UMTS systems are also much lower than the DL ones, so that it does not influence substantially the value of the total exposure, which is what happens in the measurements when using UMTS. Hence, the main disagreement from the measurements is in voice GSM900, where one does not observe an increase of the UL contribution, which might be due to the fact that the implemented power control does not exactly represent what happens in a real scenario, being a simplified approach, directly adapting the MT power to the value that is required.

Table 4.14. Exposure values and systems relative contributions in the reference and real scenarios.

System	Relative Contribution	
	Reference Scenario (Simulation)	Real Scenario
GSM900	53.4%	50.3%
UMTS	11.8%	11.5%
LTE800	-	9.3%
GSM/LTE1800	-	26.5%
LTE2600	34.8%	0.5%
Total Exposure	0.249	0.022

Finally, besides the differences identified to the real scenario, which might be due to the assumptions of the theoretical model concerning the reference parameters, so that only some results can be compared in a relative way, it is observed that, in both cases, the exposure requirements are satisfied, with the total exposure being higher in the simulations results, as a worst case approach is taken into account.

Chapter 5

Conclusions

This chapter concludes the work, summarising the main results obtained, and presenting some suggestions for future work.

The main objective of this thesis was to analyse the implementation of LTE-A in a low exposure perspective, evaluating the exposure of LTE considering the presence of signals from other networks, such as GSM and UMTS. To achieve this goal, a model was developed in order to assess the exposure from both DL and UL in a typical urban scenario, which includes DL and UL models.

Chapter 2 presents the fundamental concepts concerning LTE, the central system of the work. The first section gives a description of the LTE network architecture, its main elements and their functions. Then, the basic aspects of the LTE radio interface are mentioned, including the frequency bands, the multiple access techniques, power levels and system's main features, including the ones corresponding to LTE-A. The third section presents a description of the services and applications, where the different classes of services are identified. The coexistence of other systems with LTE is referred in the fourth section, where GSM and UMTS have a major relevance, being described their main characteristics and radio aspects. Finally, the last section starts with a basic description of the exposure parameters and their reference levels, followed by an overview of the most relevant works in the context of LTE exposure.

Chapter 3 details the developed models and their implementation. The purpose of the DL model is to determine the exposure in DL, being based on a propagation model that gives the received power, such that it accounts for the rays reflected on the surrounding buildings. The conversion to the reference parameter, in order to evaluate exposure and to compare it with reference levels, is done through the MT received power and its relation with power density: one considers the MT antenna effective area to obtain an estimation of the power that reaches the user. For the UL exposure, a model with the same purpose of the DL one was developed, taking the MT radiated power such that the required value at the BS is achieved, power control being considered. Then, with the MT radiated power, the power that is absorbed by the user is estimated through the user losses, and converted to power density, taking the surface of absorption as the lateral area of the head, or the torso's front area, depending on the service being used (voice or data, respectively).

The outcome of both DL and UL models is used by the global exposure model, which aims to obtain the total exposure, given by a parameter that sums the contributions of all the signals in the band of interest, derived by ICNIRP's requirement for simultaneous exposure to multiple frequency fields [ICNI98]. This model is also responsible to assess if the requirements are complied, as well as for determining the signals' and systems' contributions to the total exposure. These models were implemented in a simulator, developed in MATLAB [Math10].

In Chapter 4, the analysis of the measurements and simulations results is done. The measurements were made in order to assess the exposure in a real scenario, a street inside the IST *campus* being chosen, having some buildings surrounding it, some of them with BS antennas on the roof-tops. Over 240 m, two equipments were used to measure the electric field strength in 25 points (with a step of 10 m): a broadband meter (PFM), which analysed from 100 kHz to 3 GHz, giving the RMS electric field value over 60 s, and a spectrum analyser (SRM), [75, 3000] MHz, which measured the maximum electric field value observed during the same period.

The results obtained with both PFM and SRM show a similar trend, expressing the influence of the

antenna's radiation pattern, being observed that power density increases with the distance to the first point of investigation up to a maximum value, then with the trend to decrease. The maximum value was obtained with the SRM, at a distance of 80 m, being approximately 98.8 mW/m^2, 20 times below the most restrictive level in the band under analysis. The values obtained with the SRM are verified to be one order of magnitude higher than the ones obtained with the PFM, and could reach two orders of magnitude in some points, which is the case of the maximum value.

The contributions of each system to the total exposure, in the band of [800, 2600] MHz, were obtained through the data acquired by the SRM. GSM900 contributes the most (50.3%), followed by GSM/LTE1800 (26.5%), UMTS (11.5%), and LTE800 (9.3%). The contributions of LTE2600 and WiFi are very low, the former due to the fact of only being detected in the last two points, and the latter due to its low radiated power compared with cellular ones, not having significance.

Measurements were also made to assess the influence of service usage in exposure, comparing to the situation without using the MT with the use of voice GSM and UMTS, and data UMTS, using the PFM. The most significant difference is verified when using voice GSM, almost doubling the values of power density regarding the situation without MT, with UMTS does not showing this influence. The maximum value observed when using GSM corresponds to 18.9 mW/m^2, being 106 times below the most restrictive level.

The simulations were done for a reference scenario, and then varying the parameters under analysis, in order to evaluate their influence. The results obtained in the simulations refer to the average values obtained by 50 runs, as the parameters of interest are statistical. The analysis of the reference scenario comprised the 3 cellular systems: GSM900, UMTS (HSPA+) and LTE2600, considering data LTE2600 in UL. For the situation where the user is static in front of the BS, at the level of the street (33.4 m from the MT to the BS, by direct ray), a DL power density of 0.171 W/m^2 (58 times below the reference level and ER of 1.7%) is observed for LTE2600, even higher than GSM900, showing that MIMO have an increasing impact in the received signal. However, the main contribution of LTE2600 is in the UL, where its power density value is 4 times higher than the DL one (0.707 W/m^2), 14 times below the reference level (ER of 7.1%). In spite of the power density values of LTE2600, GSM900 is the system that contributes the most to the total exposure, with a contribution of 53.4%, due to its lower reference level (4.5 W/m^2) and to the higher number of carriers, with LTE2600 contributing 34.8% and UMTS 11.8%, with the total exposure being 0.245, 4 times below the requirement value. When comparing the contributions of each system to the total exposure, obtained by simulation, with the ones obtained with the data acquired by the SRM, previously mentioned, one observes that the contributions are close for GSM900 (50.3%) and UMTS (11.5%) and that the joint contribution of GSM/LTE1800 (26.5%) with LTE800 (9.3%) is 35.8%, which is much close to the value of the LTE2600 contribution of the simulated reference scenario (34.8%).

The analysis in the situation where the position of the user is varied up to 240 m in the street shows the relevance that LTE2600 UL can have in the total exposure. It is observed that the UL contribution increases with the distance, surpassing the DL one and leading to a saturation in 2.584 W/m^2 at a distance of 90 m, when the maximum transmitter output power is reached, being 4 times below the

reference level (ER of 25.8%), which is very near the reference level. The maximum value verified for the total exposure (0.297) is 3 times below the requirement, with LTE2600 dominating the contributions to this value (87.7%), due to the high values of the UL component.

The consideration of all mobile communication systems provides a general view on the impact of each system in a network comprising several technologies. The 3 LTE systems were tested in UL, with the influence of the LTE systems increasing with the frequency of operation. UL contributions increase 10 times from the use of LTE800 to LTE2600 in UL, with LTE2600 being twice the LTE1800 UL contribution, being confirmed that LTE2600 is the system that leads to the worst case exposure value in UL. The maximum total exposure verified is 0.321, 3 times below the reference value (32.1% of it), with GSM900 contributing the most to the total exposure (40.5%). LTE2600 contributes 27.1%, LTE800 having 15.3% of contribution, UMTS 9% and LTE1800 8.1%. Although LTE1800 presents the higher DL power density, LTE800 has higher contribution, as the reference level for its frequency is 4 W/m^2, lower than the one for 1800 MHz (9 W/m^2), being the LTE system with higher DL contribution. WiFi is verified to have no such influence, its values being negligible. Finally, the introduction of LTE in the network, regarding the already existing systems, approximately doubles the total exposure, considering the 3 LTE technologies in DL and LTE2600 in UL.

The analysis of the type of service being used was also performed. The main results show that the largest variations of the UL power density occur when using data LTE, namely LTE1800 and LTE2600, being the services that have a major impact in the exposure, and whose relation between the LTE UL contributions are the same as the ones obtained for the analysis concerning the mobile communications systems, as the UL systems are the same. Regarding their relation to other services, LTE1800 and LTE2600 have UL power density values 6 and 16 times higher than the one with voice UMTS, respectively, and 23 and 67 times higher than data UMTS (HSPA+). LTE800 exposure is 3 times higher the value of UMTS (HSPA+). The UL values concerning other services besides data LTE1800 and data LTE2600 are much lower than their corresponding DL component, so that they do not have significant influence in the total exposure, which are according to the measurements, as the UMTS services do not added significant exposure, except for the case of voice GSM900, where measurements show a significant increase of the exposure when using this service.

In terms of the variation of the number of BSs on the buildings' roof-tops, results show that the total exposure approximately duplicates and triplicates, when the number of BSs is set from 1 to 2 and to 3, respectively. With the small distances considered between the BSs, there are no such differences between using an alternate configuration or a configuration where the BSs are in front of each other. The maximum values obtained for the total exposure correspond to the configuration with 3 BSs, having a value of around 0.545, 2 times below the maximum admissible value (54.5% of this value), with GSM900 having the highest contribution (56.5%), UMTS and LTE2600 having approximate contributions, 21.7% and 21.8%, respectively. Other scenario parameters were varied, where one can see the parameter dependence with the height of the BS, the width of the street, and the distance to the reference building, acting as additional results, the first could be compared to the approach where the distance is being changed, and the other two present results that are specifically dependent on the

geometry of the scenario, not allowing to draw much relevant conclusions.

The analysis of the influence of MIMO was studied taking into account new configurations: MIMO 4×4 and MIMO 8×8. Results show that the DL and UL power densities increase by a factor equal to the number of transmitting antennas that is added from one configuration to another, except for the UL, which is limited to MIMO 4×4, as it is the maximum defined for LTE-A UL. It is also verified that, from MIMO 4×4, LTE2600 becomes the system that contributes the most to the total exposure. The highest value of total exposure is 0.376, with MIMO 8×8, 3 times below the maximum admissible (36.7% of this value), with LTE2600 having a contribution of 56.2%, GSM900 of 36% and UMTS of 7.8%. The change from MIMO 2×2 to 4×4 leads to an increase in the total exposure of 33.6%, and of 49.8% when changing to MIMO 8×8.

Summarising, it is observed that MIMO has a significant impact on the influence of LTE to the total exposure. LTE UL has also a relevant influence on the total exposure, with LTE2600 having the highest contributions in UL, being 10 and 2 times higher from the LTE800 and LTE1800, respectively. On the other hand, LTE800 is the one contributing the most in DL. Moreover, it is observed that the introduction of the 3 LTE systems in the network, with other mobile systems, and using LTE2600 in UL, approximately doubles the total exposure. The total exposure approximately duplicates and triplicates with the configurations of 2 and 3 BSs, regarding the reference scenario, with 1 BS. Finally, MIMO increases the total exposure in 33.6% and 49.8% when changing from MIMO 2×2 to MIMO 4×4 and 8×8, respectively. All the scenarios comply with the reference levels, with the maximum power density value being 2.584 W/m^2, in the reference scenario, varying the position of the user, which is 4 times below the reference value (ER of 25.8%); the maximum value of the total exposure, obtained for the configuration with 3 BSs, is 0.545, approximately 2 times below the limit level (54.5% of it).

The developed model allows an evaluation of the exposure in a specific urban scenario, taking a worst case analysis into account. However, some limitations can be pointed out: firstly, although the number of rays considered in the DL model correspond to the most relevant, it constitutes a limitation, not supporting a high number of rays, which could reproduce the scenario in a more realistic way; secondly, it does not support the 3D radiation pattern of the antenna, considering the maximum gain, which would add a realistic approach to the antenna; finally, the simulator does not support other systems besides the cellular ones in UL, not being possible to test, for instance, WiFi UL.

Concerning future work, it is suggested to improve the model functionalities, such as adding the 3D radiation pattern of the antenna, and analysing the influence of the electrical and mechanical tilts in the exposure, focusing on the parameters of the antennas. An exposure assessment, similar to this work, in indoor scenarios would also be interesting, as in these environments the antennas are closer to people, as well as in other specific scenarios where the exposure can be high, such as the focus on heterogeneous networks. The support of other functionalities in UL, such as WiFi or Bluetooth could also be analysed, considering more systems operating at the same time. Finally, the study of exposure in conjunction with other parameters, such as interference, coverage and capacity, balancing them in order to optimise the network parameters such that exposure could be reduced, would be also interesting, although having a higher level of complexity.

Annex A

LTE Frequency Bands

In this annex, the frequency bands available for LTE, according to 3GPP Release 11, are detailed, as well as the bands' usage by each world's region. It is also specified the respective frequency assignment in Portugal, by each telecommunications operator, with the results of the auction held by ANACOM

The assigned frequency bands for E-UTRA are detailed in Table A.1, according to 3GPP Release 11.

Table A.1. E-UTRA frequency bands (adapted from [3GPP13c], [3GPP13b] and [HoTo11]).

E-UTRA Operating Band		**Uplink operating band BS receive UE transmit [MHz]**	**Downlink operating band BS transmit UE receive [MHz]**	**Duplex Mode**
1	2100	[1920, 1980]	[2110, 2170]	FDD
2	1900	[1850, 1910]	[1930, 1990]	FDD
3	1800	[1710, 1785]	[1805, 1880]	FDD
4	1700/2100	[1710, 1755]	[2110, 2155]	FDD
5	850	[824, 849]	[869, 894]	FDD
6[1]	800	[830, 840]	[875, 885]	FDD
7	2600	[2500, 2570]	[2620, 2690]	FDD
8	900	[880, 915]	[925, 960]	FDD
9	1700	[1749.9, 1784.9]	[1844.9, 1879.9]	FDD
10	1700/2100	[1710, 1770]	[2110, 2170]	FDD
11	1500	[1427.9, 1447.9]	[1475.9, 1495.9]	FDD
12	US700	[699, 7169]	[729, 746]	FDD
13	US700	[777, 787]	[746, 756]	FDD
14	US700	[788, 798]	[758, 768]	FDD
15	Reserved	Reserved	Reserved	FDD
16	Reserved	Reserved	Reserved	FDD
17	US700	[704, 716]	[734, 746]	FDD
18	Japan800	[815, 830]	[860, 875]	FDD
19	Japan800	[830, 845]	[875, 890]	FDD
20	EU800	[832, 862]	[791, 821]	FDD
21	1500	[1447.9, 1462.9]	[1495.9, 1510.9]	FDD
22	3500	[3410, 3490]	[3510, 3590]	FDD
23	S-Band	[2000, 2020]	[2180, 2200]	FDD
24	L-Band	[1626.5, 1660.5]	[1525, 1559]	FDD
25		[1850, 1915]	[1930, 1995]	FDD
26		[814, 849]	[859, 894]	FDD
27		[807, 824]	[852, 869]	FDD
28		[703, 748]	[758, 803]	FDD
29		N/A	[717, 728]	FDD
...				
33	UMTS TDD1	[1900, 1920]	[1900, 1920]	TDD
34	UMTS TDD2	[2010, 2025]	[2010, 2025]	TDD
35	US1900 UL	[1850, 1910]	[1850, 1910]	TDD
36	US1900 DL	[1930, 1990]	[1930, 1990]	TDD
37	US1900	[1910, 1930]	[1910, 1930]	TDD
38	2600	[2570, 2620]	[2570, 2620]	TDD
39	UMTS TDD	[1880, 1920]	[1880, 1920]	TDD
40	2300	[2300, 2400]	[2300, 2400]	TDD
41	2600 US	[2496, 2690]	[2496, 2690]	TDD
42		[3400, 3600]	[3400, 3600]	TDD
43		[3600, 3800]	[3600, 3800]	TDD
44		[703, 803]	[703, 803]	TDD
Note 1: Band 6 is not applicable.				

The FDD frequency bands available for each of the world's regions are illustrated Table A.2, namely for Europe, Asia, Japan and Americas.

Table A.2. FDD Frequency bands' usage by world's region (adapted from [HoTo11]).

Band	Europe	Asia	Japan	Americas
2100	×	×	×	
1900				×
1800	×	×		
1700/2100				×
850		×		×
800			×	
2600	×	×		
900	×	×		
1700			×	
1500			×	
US700				×
Japan800			×	
EU800	×			
3500	×	×	×	×
S-Band				×
L-Band				×

The results of the auction held by ANACOM for the 450, 800, 900, 1800, 2100 and 2600 MHz are shown in Table A.3, with the assigned frequency bands and corresponding bandwidth for each Portuguese operator.

Table A.3. Results from ANACOM auction for frequency bands (adapted from [ANAC13]).

Frequency Band [MHz]	Bandwidth [MHz]	Assigned Operator
450	2 × 1.25	-
800	2 × 5	TMN
800	2 × 5	TMN
800	2 × 5	Vodafone
800	2 × 5	Vodafone
800	2 × 5	Optimus
800	2 × 5	Optimus
900	2 × 5	-
900	2 × 5	Vodafone
1800	2 × 5	TMN
1800	2 × 5	TMN
1800	2 × 5	Vodafone
1800	2 × 5	Vodafone
1800	2 × 5	Optimus
1800	2 × 5	Optimus
1800	2 × 5	-
1800	2 × 5	-

Table A.3. (cont.) Results from ANACOM auction for frequency bands (adapted from [ANAC13]).

Frequency Band [MHz]	Bandwidth [MHz]	Assigned Operator
1800	2 × 4	TMN
1800	2 × 4	Vodafone
1800	2 × 4	Optimus
2100	5	-
2100	5	-
2600	2 × 5	TMN
2600	2 × 5	TMN
2600	2 × 5	TMN
2600	2 × 5	TMN
2600	2 × 5	Vodafone
2600	2 × 5	Vodafone
2600	2 × 5	Vodafone
2600	2 × 5	Vodafone
2600	2 × 5	Optimus
2600	2 × 5	Optimus
2600	2 × 5	Optimus
2600	2 × 5	Optimus
2600	2 × 5	-
2600	2 × 5	-
2600	25	Vodafone
2600	25	-

Annex B

Systems Coexisting with LTE

This annex provides a detailed list of the systems operating in the bands of LTE, being useful for the identification of the systems for a given frequency in these bands.

LTE systems operate in [800, 2600] MHz, so that it is useful to identify the other systems coexisting in the same band when assessing exposure. Hence, Table B.1 presents the list of systems operating in [800, 2600] MHz, in order to simplify the identification of the systems coexisting with LTE.

Table B.1. Systems operating in the frequency band of [800, 2600] MHz (adapted from [OIMC13]).

Frequency [MHz]	**Services**
[791, 821]	LTE800 UL
[832, 862]	LTE800 DL
[862, 890]	Wireless Applications 800 (Radio Microphones, Hearing Aids, Alarms)
[865, 868]	RFID800
[880, 915]	GSM900 UL
[925, 960]	GSM900 DL
[960, 1215]	Navigation and Flight Security Systems
[1215, 1240]	Global Positioning System (GPS)
[1240, 1260]	Amateur Radio
[1270, 1300]	Amateur Radio
[1300, 1350]	Radars
[1452, 1480]	T-DAB - Radio Broadcasting
[1525, 1544]	Satellite Mobile Communications (IRIDIUM) DL
[1621, 1626]	Satellite Mobile Communications (IRIDIUM) UL
[1710, 1785]	GSM1800 UL
[1795, 1800]	Wireless Applications 1800 (Radio Microphones, Hearing Aids)
[1805, 1880]	GSM1800 DL
[1880, 1900]	Cordless Phone (DECT)
[1920, 1980]	UMTS (IMT-2000) UL
[2110, 2170]	UMTS (IMT-2000) DL
[2300, 2400]	Amateur Radio
[2400, 2484]	Industrial Scientific and Medical (ISM) Band (WiFi b/g/n, Bluetooth)
[2500, 2570]	LTE2600 UL
[2620, 2690]	LTE2600 DL

Annex C

Link Budget

This annex presents a description of the expressions used in link budget.

The calculations of link budget allow to estimate the path loss, an important parameter to determine the power levels in a link, whose expressions are used in the models developed in this work.

Firstly, one starts to define the path loss, which is given by [Corr13]:

$$L_{p[\mathrm{dB}]} = P_{EIRP[\mathrm{dBm}]} - P_{r[\mathrm{dBm}]} + G_{r[\mathrm{dBi}]} \quad \text{(C.1)}$$

where:

- P_{EIRP}: Effective Isotropic Radiated Power.

The value of EIRP depends on the link. In DL, one should account with the losses in the cable between the BS transmitter and the antenna, so that the EIRP in DL is given by [Corr13]:

$$P_{EIRP[\mathrm{dBm}]}^{DL} = P_{Tx[\mathrm{dBm}]} - L_{c[\mathrm{dB}]} + G_{t[\mathrm{dBi}]} \quad \text{(C.2)}$$

where:

- P_{Tx}: transmitter output power.

In UL, although the losses in this direction correspond to the losses due to the user, the EIRP simply comprises the output power of the transmitter and the gain of the transmitting antenna, as the losses due to the user do not influence the antenna radiated power, meaning that, after having the EIRP value, this value is reduced by the losses due to the user [Corr13]:

$$P_{EIRP[\mathrm{dBm}]}^{UL} = P_{Tx[\mathrm{dBm}]} + G_{t[\mathrm{dBi}]} \quad \text{(C.3)}$$

The power at the receiver also depends on the link. In DL, it is given by [Corr13]:

$$P_{Rx[\mathrm{dBm}]}^{DL} = P_{r[\mathrm{dBm}]} - L_{u[\mathrm{dB}]} \quad \text{(C.4)}$$

where:

- P_{Rx}^{DL}: power at the input of the receiver, considering DL.

In UL, it is calculated by [Corr13]:

$$P_{Rx[\mathrm{dBm}]}^{UL} = P_{r[\mathrm{dBm}]} - L_{c[\mathrm{dB}]} \quad \text{(C.5)}$$

where:

- P_{Rx}^{UL}: power at the input of the receiver, considering UL.

The sensitivity of the receiver depends on the system. For GSM, the values are according to Table C.1 [Corr13].

Table C.1. GSM BS receiver sensitivity (extracted from [Corr13]).

Class	**Receiver Sensitivity [dBm]**					
	BS				**MT**	
	Macro-Cell		**Micro-Cell**			
	900 MHz	**1800 MHz**	**900 MHz**	**1800 MHz**	**900 MHz**	**1800 MHz**
1	-104	-104	-97	-102	-104	-102
2			-92	-97	-102	
3			-87	-92		

In UMTS, the sensitivity depends on the service [Corr13]. The receiver sensitivity can be determined by (C.6), which depends on the processing gain, due to use of a coding scheme as multiple access technique:

$$P_{Rx\,min[\mathrm{dBm}]} = N_{[\mathrm{dBm}]} - G_{P[\mathrm{dB}]} + \rho_{N\,[\mathrm{dB}]} \quad \text{(C.6)}$$

where:

$$N_{[\mathrm{dBm}]} = N_{th[\mathrm{dB}]} + F_{[\mathrm{dB}]} \quad \text{(C.7)}$$

$$N_{th[\mathrm{W}]} = k_{B[\mathrm{m^2 kg\,s^{-2}K^{-1}}]} T_{[\mathrm{K}]} \Delta f_{[\mathrm{Hz}]} \quad \text{(C.8)}$$

$$G_{P[\mathrm{dB}]} = 10 \log\left(\frac{R_c}{R_b}\right) \quad \text{(C.9)}$$

- N: total noise power;
- G_P: processing gain;
- ρ_N: Signal-to-Noise Ratio;
- N_{th}: thermal noise power;
- F: noise figure, whose values are presented in Table C.2;
- k_B: Boltzmann constant;
- T: noise temperature;
- Δf: signal bandwidth; in UMTS, it is taken as the chip rate, R_c;
- R_b: throughput.

Considering the typical values for the noise temperature (290 K), its product with the Boltzmann constant, converted in dBm, gives a typical value of -174 dBm.

For LTE, the sensitivity does not account for the processing gain used for the case of UMTS, hence, it can be calculated in the following way:

$$P_{Rx\,min[\mathrm{dBm}]} = N_{[\mathrm{dBm}]} + \rho_{N\,[\mathrm{dB}]} \quad \text{(C.10)}$$

Table C.2. Noise Figure for UMTS and LTE (adapted from [Carr11]).

Noise Figure [dB]			
UMTS		**LTE**	
DL	**UL**	**DL**	**UL**
9	7	7	5

The SNR values can be obtained through expressions that relate the SNR with the throughput. The considered SNR values are the ones from which the corresponding throughput saturates and becomes constant, *i.e.*, corresponding to the maximum throughput, which is the value that leads to a higher SNR, being the worst case in terms of power requirements.

For UMTS, there are different values depending on the release. For R99, the SNR intervals for voice and for several data throughputs are presented in Table C.3, where the values taken into account are the maximum of the interval, corresponding to the maximum possible throughput, taken into account for both DL and UL. For HSPA+, the values of SNR for DL and UL, for the maximum throughout and for the three types of modulation are presented in Table C.4.

Table C.5 presents the considered values of SNR, depending on the MIMO configuration and on the modulation scheme. These values correspond to 10 MHz bandwidth, using normal CP and considering the EPA5Hz channel model [Carr11]. The coding rate is 1/3 for QPSK, 3/4 for 16QAM and 5/6 for 64QAM. The values for 2×2 MIMO are based on [Carr11], being taken as reference for obtaining the values for MIMO 4×4, whose throughput values are twice the MIMO 2×2 ones, with SNR ones remaining the same. As the worst case is considered, the bandwidth assumed to the user is the maximum possible, *i.e.*, 20 MHz, so that the throughput, whose values corresponds to a single RB, needs to be multiplied by the number of RBs of the considered band (100 RBs for 20 MHz bandwidth and 50 RBs for 10 MHz).

Table C.3. SNR for UMTS R99 (extracted from [Corr13]).

Service	R_b **[kbps]**	ρ_N **[dB]**
Voice	12.2	[4.8, 8.8]
Data	64	[1.1, 3.8]
	128	[0.9, 3.5]
	384	[0.4, 3.2]

Table C.4. SNR for HSPA+ (adapted from [Bati11]).

Modulation	**Link**	R_b**[Mbps]**	ρ_N**[dB]**
QPSK	**DL**	7.2	16
	UL	5.5	6
16QAM	**DL**	14.4	16
	UL	11.0	14
64QAM	**DL**	21.6	20

Table C.5. SNR for LTE UL (adapted from [Carr11]).

MIMO configuration	**Modulation**	R_b/RB **[bps]**	R_b **(100 RBs) [Mbps]**	R_b **(50 RBs) [Mbps]**	$\rho_{N[\mathrm{dB}]}$
2×2	QPSK	95 899	9.59	4.79	8
	16QAM	429 084	42.91	21.45	18
	64QAM	716 032	71.60	35.08	24
4×4	QPSK	191 798	19.18	9.59	8
	16QAM	858 168	85.82	42.91	18
	64QAM	1432 064	143.20	71.60	24

Annex D

Measurement Data

This annex presents the auxiliary data obtained in the simulations, such as the coordinates of the measurement points and the distances to the BSs.

In the 25 measurement points, done along 240 m, one got the coordinates for each one, which are presented in Table D.1. The values of the distance to the antenna were obtained with a laser meter, so that only the distances corresponding to points in line of sight with the BSs are presented

Table D.1. Measured points and auxiliary parameters.

Measure Point	**Coordinates**		**Distance to antenna (direct ray)**				**Electric Field RMS [V/m]**
			BS1	**BS2**	**BS3**	**AP**	
1	N 38º 44' 08.8'	W 09º 08' 22.9''	25.0	-	-	60.0	0.95
2	N 38º 44' 09.6'	W 09º 08' 23.0''	30.0	-	-	50.5	0.84
3	N 38º 44' 09.7'	W 09º 08' 23.1''	37.5	-	-	41.5	0.75
4	N 38º 44' 09.6'	W 09º 08' 22.8''	48.0	-	-	34.0	0.80
5	N 38º 44' 09.9'	W 09º 08' 23.0''	56.0	-	-	26.5	1.11
6	N 38º 44' 10.3'	W 09º 08' 22.7''	67.5	105.5	-	23.0	1.20
7	N 38º 44' 10.6'	W 09º 08º 22.9''	77.0	97.5	-	23.0	1.51
8	N 38º 44' 10.7'	W 09º 08' 22.8''	86.5	88.5	-	27.0	1.40
9	N 38º 44' 11.1'	W 09º 08' 22.8''	97.5	79.5	-	35.5	1.46
10	N 38º 44' 12.2'	W 09º 08' 23.6''	107.0	71.5	-	43.5	1.68
11	N 38º 44' 12.5'	W 09º 08' 23.8''	116.5	66.0	-	51.5	1.45
12	N 38º 44' 12.9'	W 09º 08' 23.5''	127.5	-	-	62.0	1.11
13	N 38º 44' 12.7'	W 09º 08' 22.7''	137.0	-	-	71.5	0.98
14	N 38º 44' 13.1''	W 09º 08' 22.9''	146.5	-	-	80.5	0.75
15	N 38º 44' 13.0''	W 09º 08' 22.9''	156.0	-	-	90.5	0.99
16	N 38º 44' 13.8''	W 09º 08' 22.8''	167.0	-	-	99.5	1.17
17	N 38º 44' 13.6''	W 09º 08' 21.5''	176.5	-	-	-	1.10
18	N 38º 44' 14.6''	W 09º 08' 23.4''	186.5	-	-	-	0.86
19	N 38º 44' 14.7''	W 09º 08' 23.4''	197.0	-	-	-	1.09
20	N 38º 44' 15.0''	W 09º 08' 22.8''	205.0	-	-	-	1.03
21	N 38º 44' 15.2''	W 09º 08' 23.0''	217.5	-	-	-	0.84
22	N 38º 44' 15.8''	W 09º 08' 23.4''	226.5	-	-	-	0.71
23	N 38º 44' 15.7''	W 09º 08' 22.4''	236.5	-	-	-	0.72
24	N 38º 44' 16.7''	W 09º 08' 23.8''	247.5	-	63.3	-	1.38
25	N 38º 44' 16.5''	W 09º 08' 23.4''	257.0	-	64.9	-	1.23

Table D.2 presents the values obtained for the situation where the several types of services are compared. Three measurements points are obtained, corresponding to the measurement point 10, and two other measurement points, -5 m and $+5$ m from it (measurement points 10a and 10b, respectively).

Table D.2. Measured points for the service influence.

	Coordinates		Distance to the antenna (direct ray) [m]				MT Measurement Mode			
			BS1	BS2	BS3	AP	No MT	Voice GSM	Voice UMTS	Data UMTS
10	N 38º 44' 11.5''	W 09º 08' 22.7''	97.0	107.0	-	71.5	1.64	2.29	1.64	1.59
10a	N 38º 44' 11.6''	W 09º 08' 23.0''	112.5	69.5	-	47.5	1.79	2.67	1.76	1.78
10b	N 38º 44' 12.4''	W 09º 08' 23.0''	102.0	77.0	-	38.0	1.56	2.09	1.57	1.73

Annex E

Additional Simulations Results

This annex presents some additional results obtained by simulation, regarding the variation of scenario parameters, being the height of the BS, the distance to the reference building and the width of the street.

Additional results are obtained for other scenario parameters, which, although not being the most relevant, present a complementary role in the analysis.

The first parameter corresponds to the BS height. Figure E.1 shows that the highest values of the average DL power density are for 15 and 20 m, which tend to decrease with the increase of the height of the BS, being a similar behaviour to the one when the user moves away from the BS, also presenting the oscillations due to the interference between the several rays, as the distance from the BS to the user increases in both of the situations, so that the same analysis regarding the systems is applicable.

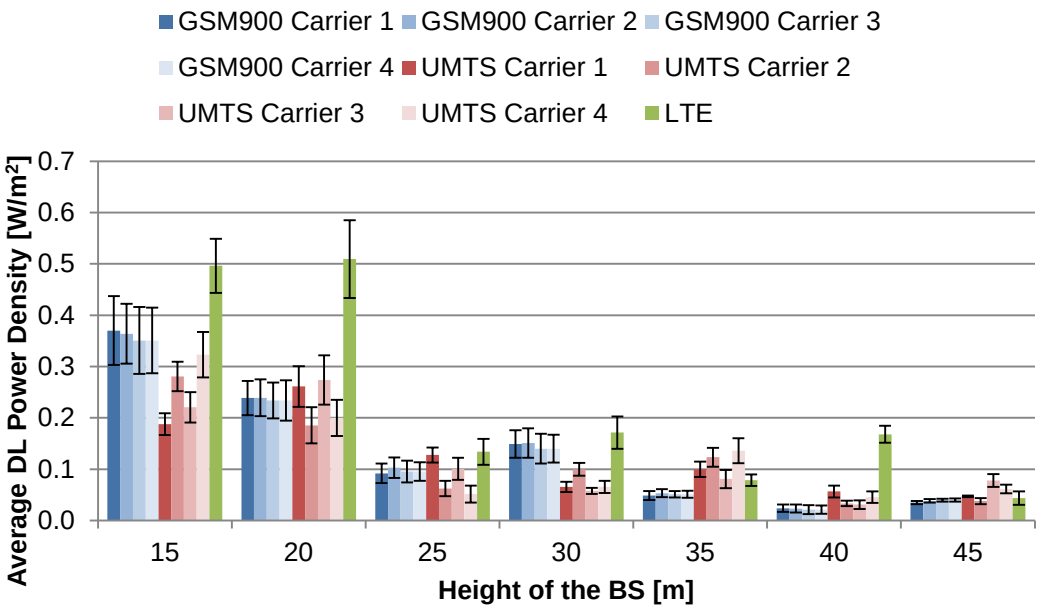

Figure E.1. Average DL power density for different BS heights.

LTE2600 presents the highest values of DL power density for a height of 20 m, with a value of 0.509 W/m^2, 3 times higher than the value obtained for the reference scenario (BS height of 30 m), being 20 times below the reference value (ER of 5%), with UMTS having the lowest ones.

The same can be concluded about the behaviour of the average UL power density, Figure E.2, which tends to increase with the height of the BS, in opposite to the DL power density, as the distance between the MT and the BS increases, similarly to the situation where the user is moving away from the BS. The oscillations of the UL power density are also verified, also due to the interference between the several rays, which can reinforce or fade the received power, influencing the path loss, being used to determine the MT radiated power. The higher value is observed for a BS height of 45 m, 15 m (50%) higher than the reference BS height, with a value of 2.378 W/m^2, 3 times higher than the value obtained for the reference scenario, being 4 times below the reference level (ER of 23.8%). This high value in UL has to do with the distance from the MT to the BS, increasing the path loss, so that the MT radiated power needs to be high, in order to satisfy the required values at the BS. This is similar to what is verified in the situation where the user is moving away from the BS, as what changes is the distance.

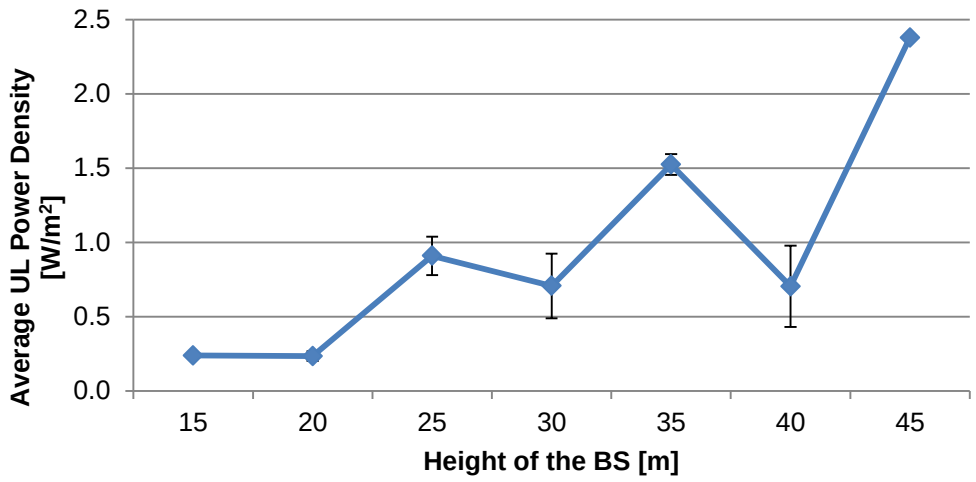

Figure E.2. Average UL power density for different BS heights.

The contributions of DL and UL, Figure E.3, also present a similar behaviour when increasing the height of the BS, regarding to the situation where the user is moving away from the BS. The average UL contribution has its lowest values for the BS heights of 15 and 20 m, where the influence of the DL is the highest, due to the proximity of the user to the BS. As the height is increased, the UL contribution tends to increase, and, on the other hand, the DL ones to decrease. In the extreme values, *i.e.*, for 15 and 45 m of BS height, the values of DL and UL contributions for the height of 15 m are 0.464 (95.1% of the total exposure) and 0.024 (4.9%), respectively, and 0.059 (20%) and 0.238 (80%) for 45 m, respectively.

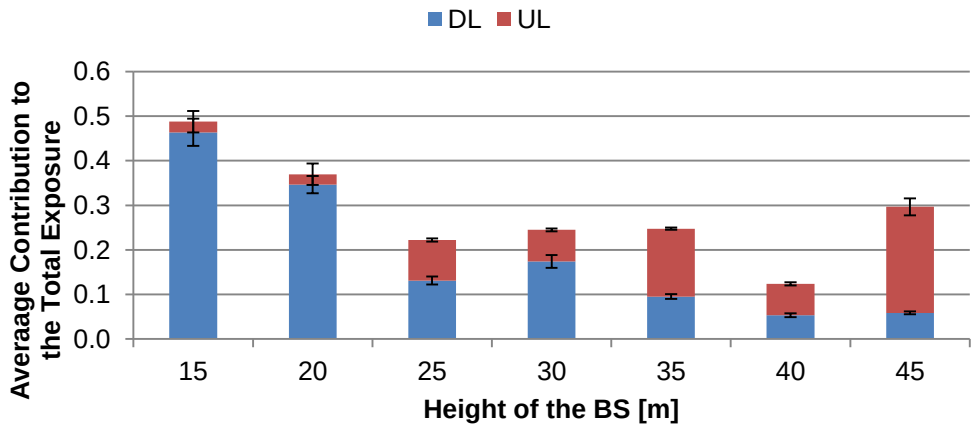

Figure E.3. Average DL and UL contributions to the total exposure for different BS heights.

Lastly, the average contribution of each of the systems to the total exposure, Figure E.4, has the tendency to decrease, following the behaviour of the DL power density, except for the case of LTE2600, as it has the UL component, so that the contribution tends to increase, with a clearer evidence from the height of 35 m, where the UL contribution surpasses the DL one. The maximum value of the total contribution coincides with a BS height of 15 m, being 0.488, 2 times below the maximum admissible value (48.8% of this value). Concerning the values of the contribution of each

system to the total exposure, for the highest average total exposure obtained, GSM900 contributing with 0.313 (64.1%), UMTS with 0.101 (20.8%), and LTE2600 with 0.073 (15.1%) to the total exposure.

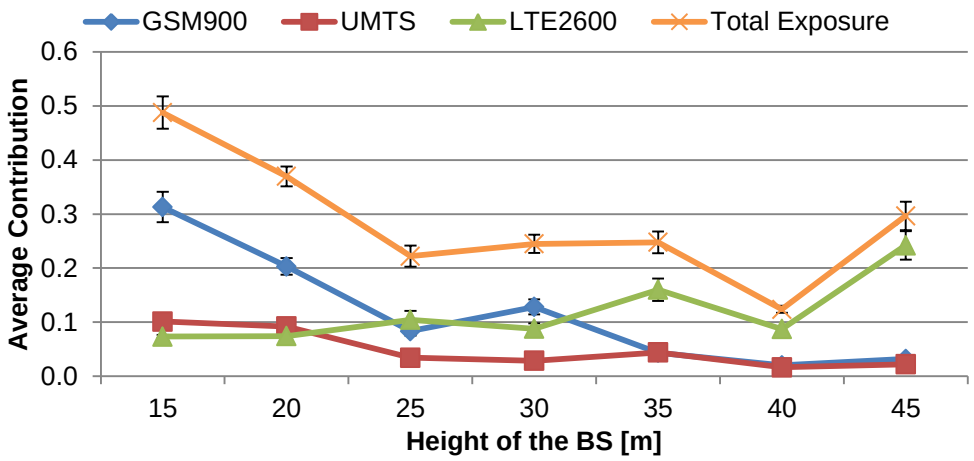

Figure E.4. Average system contribution for different BS heights.

The second parameter to be evaluated is the distance to the reference building, which is varied according to what is defined in Table 4.5. Figure E.5 shows the behaviour of DL power density corresponding to each of the carriers, where one can see that the distance to the reference building influences the DL power density, without presenting a trend. As the received power depends on the geometry of the scenario, and the radiation pattern of the antenna is not considered, it depends on the interference between the rays, which can be constructive or destructive depending on the distances, so that the results show that this is highly specific of the geometry of the scenario.

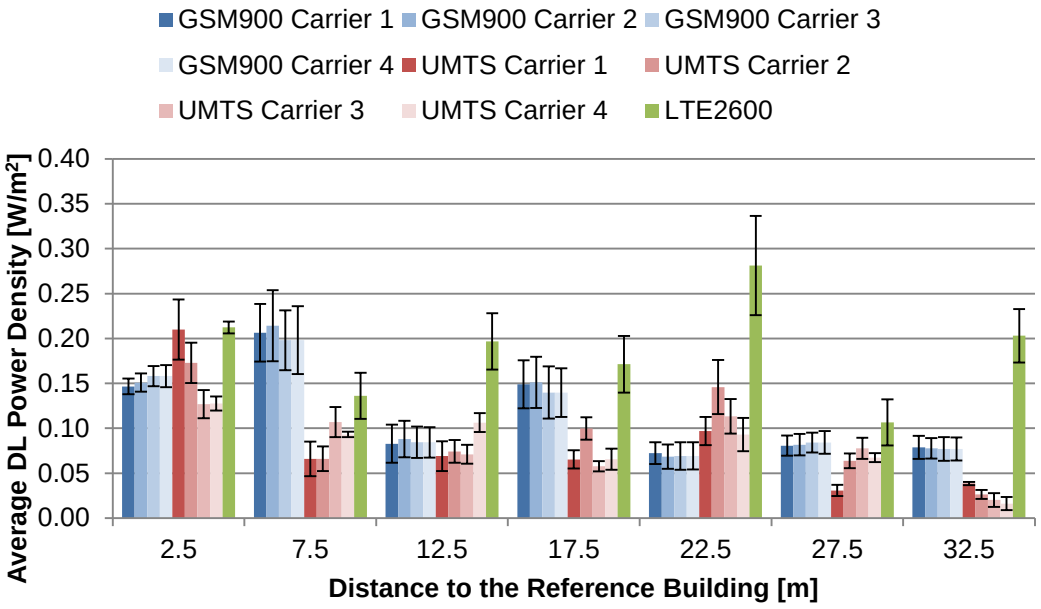

Figure E.5. Average DL power density depending on the distance to the reference building.

Regarding the values, one can see that GSM900 carriers have higher values for the distance of 7.5 m, with UMTS having its highest values at a distance of 2.5 m. The maximum value of DL power density

obtained correspond to LTE2600, at a distance to the reference building of 22.5 m, being 0.281 W/m^2, being 36 times below the reference level (ER of 2.8%), so that it is far from it, although the value is nearly twice the one verified for the reference scenario.

On the other hand, the evolution of the average UL power density with the distance to the reference building, Figure E.6, is complementary of the DL ones, because when DL exposure increases, it means that the path loss is lower, so that the MT can reduce its radiated power. Hence, one can observe that the higher the values of DL power density, the lower the UL ones. The highest value obtained for the UL power density corresponds to the distance to the reference building of 27.5 m, with a value of 1.181 W/m^2, being 8 times below the reference level (ER of 11.8%), which is nearer to the maximum admissible value than the maximum value obtained for DL, and twice the value obtained for the reference scenario.

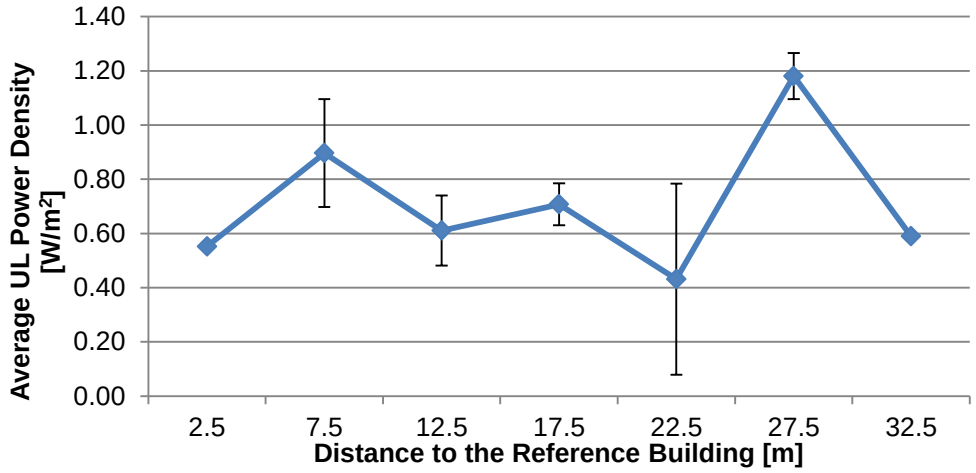

Figure E.6. Average UL power density depending on the distance to the reference building.

The average contributions to the total exposure, Figure E.7, also follow the behaviour of the DL and UL power densities, with the highest DL contribution being of 0.224 (71.6%) at the distance to the reference building of 7.5 m, justified with the highest contribution of GSM900, as one can see in Figure E.7, and the UL one is observed at the distance of 27.5 m, contributing 0.118 (51.8%) to the total exposure.

For the majority of the points, the system that contributes the most to the total exposure is GSM900, with UMTS having the less contribution. The maximum of the average total contribution is verified at a distance of 7.5 m, with a value of 0.314, 3 times below the maximum admissible value (3.14% of it), where GSM900 contributes 56.6%, followed by LTE2600, which contributes 32.8%, and UMTS contributing 10.6%.

A similar approach is made when analysing the influence of the variation of the street width, considering that the user remains in the centre of it. As for the distance to the reference building, the results regarding this parameter do not show a trend, being also specific of each position, which defines a different scenario configuration. The highest value of DL power density is observed for LTE2600, for a street width of 20 m, with a value of 0.255 W/m^2, 39 times below the reference value, as can be seen in Figure E.8.

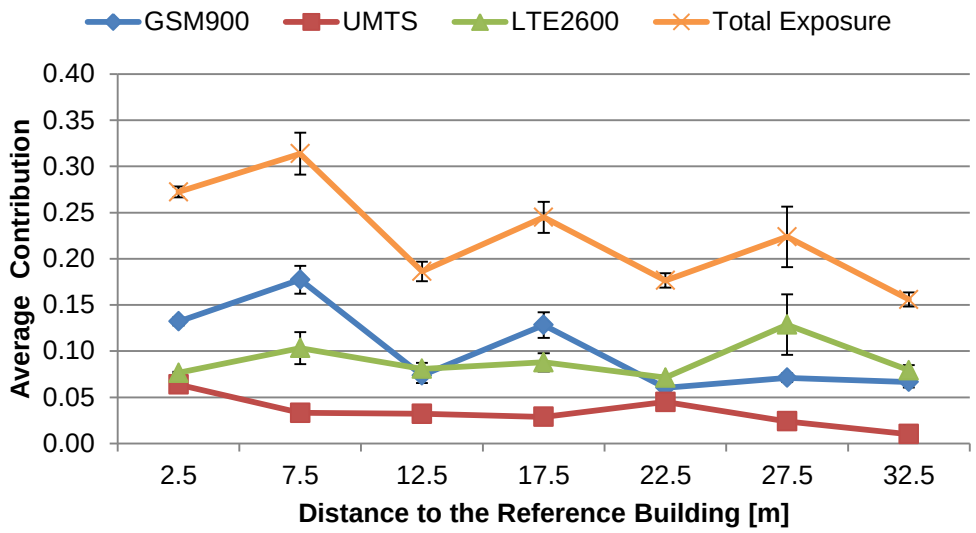

Figure E.7. Average system contribution to the total exposure, depending on the distance to the reference building.

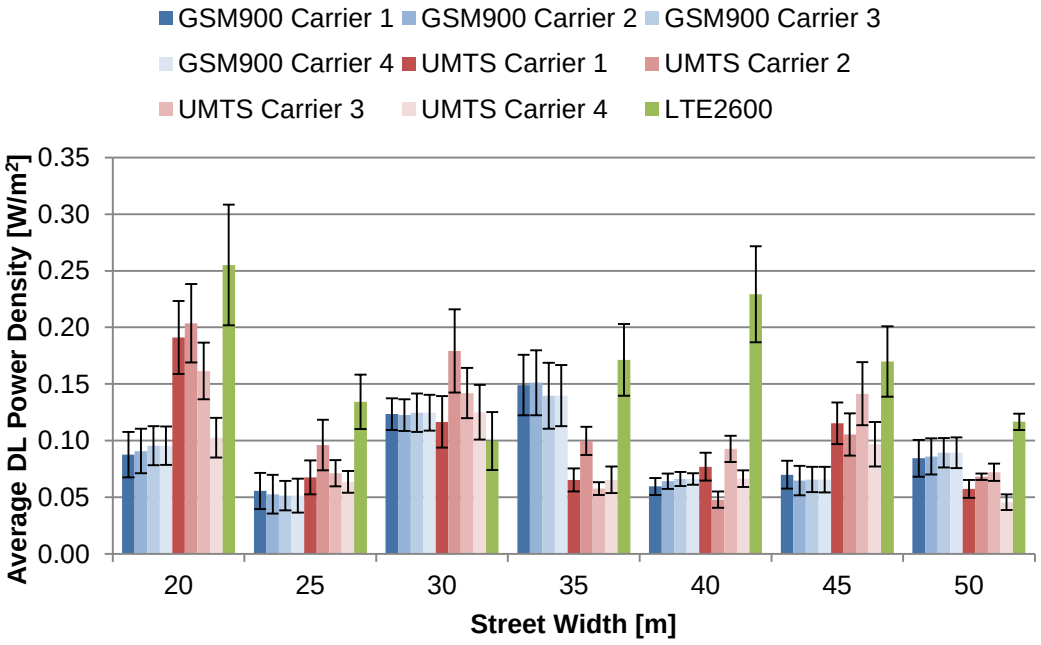

Figure E.8. Average DL power density, depending on the street width.

The average UL power density, Figure E.9, also shows a complementary behaviour, when compared to the DL values, increasing up to the street width of 30 m, reaching the maximum value of 1.27 W/m^2, 8 times below the reference value (ER of 12.7%).

According to the results, the contribution of DL to the total exposure is maximum for the street width of 35 m, with a value 0.174 (71.2%), and the UL having the maximum value of 0.127 (41.4%) for the street width of 30 m, where the average contribution of DL is approximate to the one corresponding to 35 m (in absolute values), Figure E.10.

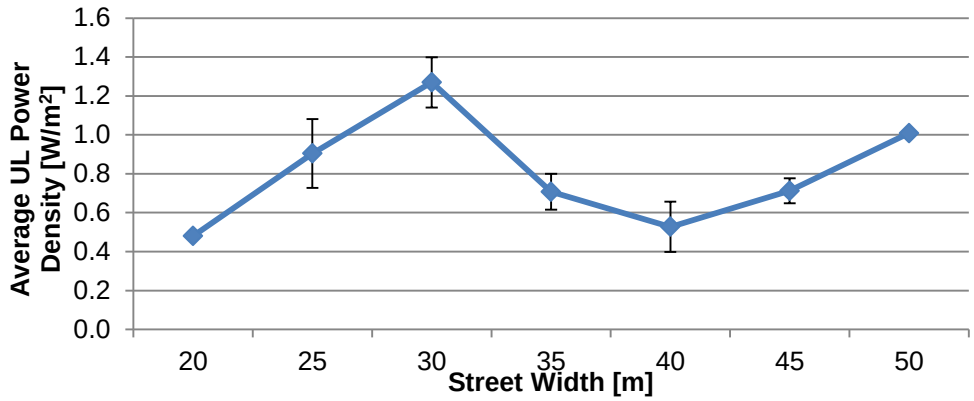

Figure E.9. Average UL power density, depending on the street width.

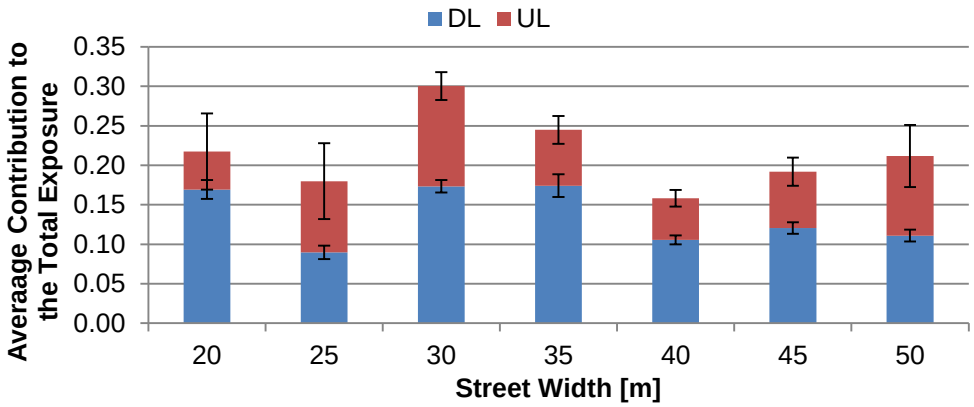

Figure E.10. Average DL and UL contributions to the total exposure, depending on the street width.

Finally, concerning the total exposure and the contributions of each of the systems, Figure E.11 shows that the contributions to the total exposure of UMTS are the lowest, with GSM900 and LTE2600 alternating their dominance, depending on the street width. The highest value of the total exposure is observed for the street width of 30 m, with a value of 0.3, 3 times below the maximum admissible value (3.3% of the maximum value). For this value, LTE2600 has the highest contribution to the total exposure, 44.9%, with GSM900 contribution 36.1%, and UMTS 19%.

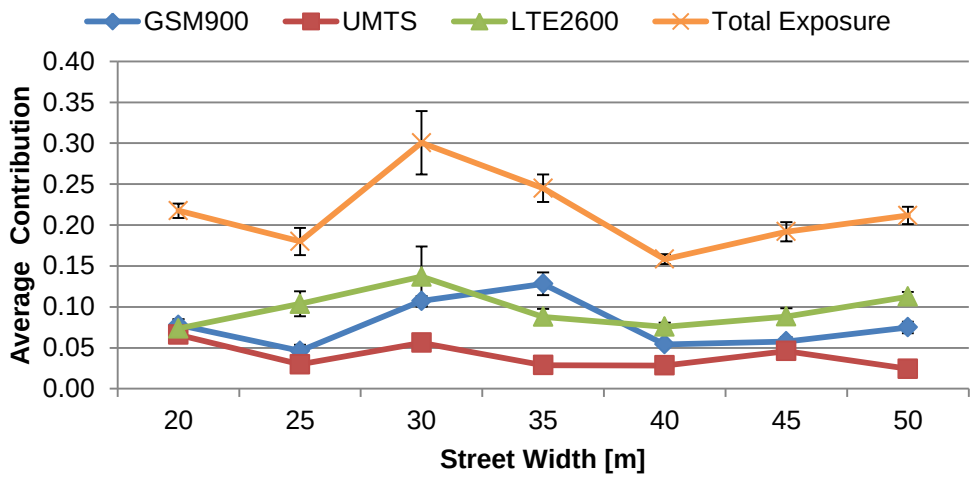

Figure E.11. Average system contribution to the total exposure, depending on the street width.

Annex F

Additional Measurements Results

In this annex, it is provided a description about the evolution of the measured maximal power density values with the distance, obtained with the SRM, for the systems being considered in the band of LTE.

Through the data acquired by the SRM at each measurement point, one can obtain the evolution of the maximal power density values with the distance for each of the systems, where it is possible to verify that the behaviour of power density with the distance is not exactly the same for each of them. Between GSM900, GSM/LTE1800 and UMTS, Figure F.1 (a), the main difference is observed in GSM900: the behaviour is similar to the one presented in Figure 4.7, an increase of the values up to a maximum value being verified, related to the radiation pattern of the antenna; after that maximum, the values tend to decrease, as the point of investigation moves away from the direction of the maximum of the radiation pattern, as well as due to path loss, which becomes higher. It is also possible to observe oscillations on the signal, which is due to multipath, but also to the radiation pattern.

In the case of UMTS, the behaviour differs from the previous. The higher values are registered at higher distances, do not coinciding with the GSM900 behaviour, where the maximum is at lower distances, closer to the BS. The main reason for this is the radiation pattern for UMTS being different, as it depends on frequency, so that the distance where the maximum of the radiation pattern is observed could be higher, which also depends on the tilt of the antenna. This is also applicable to the values obtained for the 1800 MHz DL band, which can correspond to GSM or LTE. Moreover, an increase of the values nearly 60 m might be due to the influence of BS2, where it starts to be in line of sight with the measurement equipment.

In Figure F.1 (b), one can observe the behaviour of the maximum power density values for the band corresponding to WiFi. From the first point of investigation to the following one, a decrease from approximately 8.6 $\mu W/m^2$ to around 1.3 $\mu W/m^2$ is shown, which corresponds to the minimum value verified. The fact of the first value being the second largest value observed can be due to another WiFi transmitter closer than the AP to the investigation point. Then, the values increase up to an extreme value (4.6 $\mu W/m^2$), as the point of investigation gets closer to the AP, being registered at a distance of 40 m from the initial position, in the fifth point of investigation. After this point, the values of power density decrease, which might has to do with the direction of the radiation pattern of the AP, and remain approximately the same, without high variations, before reaching the largest verified value (17.2 $\mu W/m^2$), which corresponds to the distance of 160 m from the initial position. At this point, the AP has no influence, so that this might be due to a WiFi transmitter belonging to the indoor WiFi network installed inside the building beside the point of investigation, as the measurement was made in front of its main entrance, composed of glass doors, where the losses are much lower, easily allowing the signal propagation to outdoors. After this maximum, another extreme value is verified (5.15 $\mu W/m^2$), which also might be due to the WiFi installed in the surrounding buildings.

The values obtained for WiFi are in the order of $\mu W/m^2$, which are 3 orders of magnitude below the ones obtained for cellular systems, which is due to the fact of the power radiated by WiFi antennas being much lower than by the cellular ones. Additionally, the largest value verified for the maximum WiFi power density (17.2 $\mu W/m^2$) is 6 orders of magnitude below the ICNIRP reference level, so that the exposure requirement is satisfied.

Concerning the LTE systems, Figure F.1 (c), LTE800 shows a similar behaviour to the GSM900 one, with a maximum value for the distance of 80 m, which might be due to the radiation pattern being

similar to the GSM900 one, as the frequencies are nearer. The LTE2600 exhibits low values of power density, the higher ones being verified in the last two points of investigation, where another BS antenna starts to be in line of sight, so that it suggests that the BS1 and BS2 do not have LTE2600 operating.

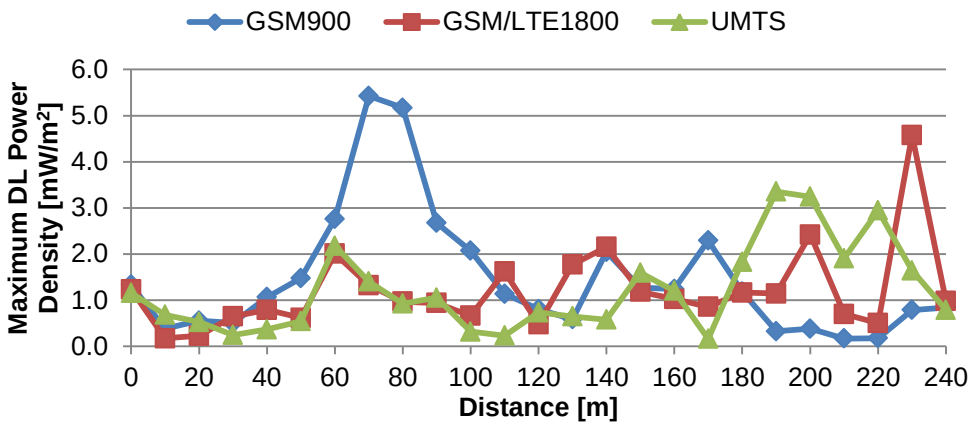

(a) GSM900, GSM/LTE800 and UMTS

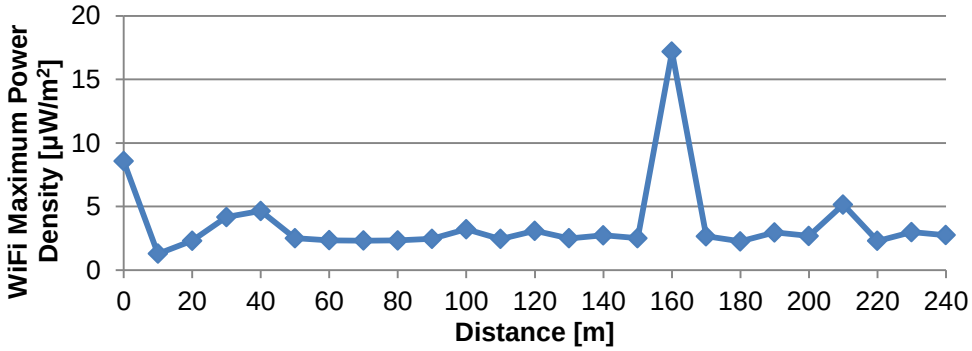

(b) WiFi

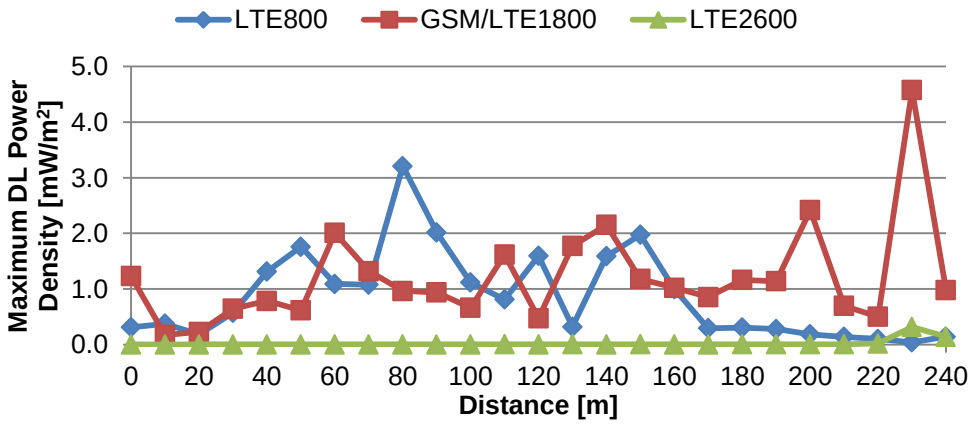

(c) LTE800, GSM/LTE1800 and LTE2600

Figure F.1. Maximum DL power density for the systems identified in the band of interest, in the points of investigation.

References

[3GPP09] 3GPP, Technical Specification Group Radio Access Network, *User Equipment (UE) radio transmission and reception (FDD) (Release 7)*, Report TS 25.101, V7.18.0, Sep. 2009 (http://www.3gpp.org/ftp/Specs/html-info/25-series.htm).

[3GPP12] 3GPP, Technical Specification Group Services and System Aspects, *Quality of Service (QoS) concept and architecture (Release 11)*, Report TS 23.107, V11.0.0, June 2012 (http://www.3gpp.org/ftp/Specs/html-info/23107.htm).

[3GPP13a] 3GPP, Technical Specification Group Services and System Aspects, *Policy and charging control architecture (Release 12)*, Report TS 23.203, V12.0.0, Mar. 2013 (http://www.3gpp.org/ftp/Specs/html-info/23203.htm).

[3GPP13b] 3GPP, Technical Specification Group Radio Access Network; Evolved Universal Terrestrial Radio Access (E-UTRA), *User Equipment (UE) radio transmission and reception (Release 11)*, Report TS 36.101, V11.4.0, Mar. 2013 (http://www.3gpp.org/ftp/Specs/html-info/36101.htm).

[3GPP13c] 3GPP, Technical Specification Group Radio Access Network; Evolved Universal Terrestrial Radio Access (E-UTRA), *Base Station (BS) radio transmission and reception (Release 11)*, Report TS 36.104, V11.4.0, Mar. 2013 (http://www.3gpp.org/ftp/Specs/html-info/36104.htm).

[Agil09] Agilent Technologies, *Agilent 3GPP Long Term Evolution: System Overview, Product Development, and Test Challenges*, Application Note, USA, 2009 (http://cp.literature.agilent.com/litweb/pdf/5989-8139EN.pdf).

[Agil11] Agilent Technologies, *Introducing LTE-Advanced*, Application Note, USA, 2011 (http://cp.literature.agilent.com/litweb/pdf/5990-6706EN.pdf).

[ANAC13] http://www.anacom.pt/render.jsp?contentId=1105917, Apr. 2013.

[Antu12] Antunes,M.G., *Estimation of exclusion regions in LTE base stations co-located with GSM/UMTS*, M.Sc. Thesis, Instituto Superior Técnico, Lisbon, Portugal, Oct. 2012.

[Bati11] Batista,R., *Performance Evaluation of UMTS/HSPA+ Data Transmission for Indoor Coverage*, M.Sc. Thesis, Instituto Superior Técnico, Lisbon, Portugal, Oct. 2011.

[BoSc11] Bornkessel,C. and Schubert,M., “Exposure of the General Public to LTE Base Stations”, in *Proc. of EBEA 2011 - 10th International Congress of the European Biolectromagnetics Association*, Rome, Italy, Feb. 2011 (http://proceedings.ebea2011.org/modules/request5397.pdf?module=oc_program&action=view.php&id=5174).

[Carr11] Carreira,P., *Data Rate Performance Gains in UMTS Evolution to LTE at the Cellular Level*, M.Sc. Thesis, Instituto Superior Técnico, Lisbon, Portugal, Oct. 2011.

[Comm13] http://www.commscope.com/andrew/eng/product/antennas/index.html, Apr. 2013.

[Corr13] Correia,L.M., *Mobile Communication Systems – Lecture Notes*, Instituto Superior Técnico, Lisbon, Portugal, 2013.

[DaPS11] Dahlman,E., Parkvall,S. and Sköld,J., *4G LTE/LTE-Advanced for Mobile Broadband*, Elsevier, Oxford, UK, 2011.

[ECC03] Electronic Communications Committee (ECC) European Conference of Postal and Telecommunications Administrations (CEPT), *Measuring Non-Ionizing Electromagnetic Radiation (9 kHz – 300 GHz)*, ECC Recommendation (02)04, Oct. 2003.

[Ekst09] Ekström,H., "QoS Control in the 3GPP Evolved Packet System", *IEEE Communications Magazine*, Vol. 47, No. 2, Feb. 2009, pp. 76-83.

[Eric13] Ericsson, *Ericsson Mobility Report – On the Pulse of the Networked Society*, Stockholm, Sweden, June 2013 (http://www.ericsson.com/res/docs/2013/ericsson-mobility-report-june-2013.pdf).

[FeAm03] Ferreira,S. and Amaral,P., *Evaluation of Propagation Models in UMTS* (in Portuguese), Graduation Thesis, Instituto Superior Técnico, Lisbon, Portugal, Nov. 2003.

[FeGW11] Feliachi,R., Gati,A. and Wiart, J., "Methods for measuring in-situ exposure induced by non-regular signals like WLAN and LTE", in *Proc. of EUCAP 2012 - 5th European Conference on Antennas and Propagation*, Rome, Italy, Apr. 2011.

[FiFe03] Figanier,J. and Fernandes,C.A., *Aspects of Propagation in the Atmosphere* (in Portuguese), AEIST, IST, Lisbon, Portugal, 2003.

[Goog13] Google Inc., *Google Earth*, Software Version 7.1.1.1888, July 2013 (http://earth.google.com/).

[HoTo04] Holma,H. and Toskala,A., *WCDMA for UMTS: Radio Access for Third Generation Mobile Communications*, John Wiley & Sons, Chichester, UK, 2011.

[HoTo11] Holma,H. and Toskala,A., *LTE for UMTS: Evolution to LTE-Advanced*, John Wiley & Sons, Chichester, UK, 2011.

[ICNI98] ICNIRP, "ICNIRP Guidelines for Limiting Exposure to Time-Varying Electric, Magnetic and Electromagnetic Fields (up to 300 GHz)", *Health Physics*, Vol. 74, No. 4, Apr. 1998, pp. 494-522, (http://www.icnirp.de/documents/emfgdl.pdf).

[JVGV10] Joseph,W., Verloock,L., Goeminne,F., Vermeeren,G. and Martens,L., "Assessment of General Public Exposure to LTE and RF Sources Present in an Urban Environment", *Bioelectromagnetics*, Vol. 31, No. 7, Oct. 2010, pp. 576-579.

[JVGV12a] Joseph,W., Verloock,L., Goeminne,F., Vermeeren,G. and Martens,L., "In Situ LTE

Exposure of the General Public: Characterization and Extrapolation", *Bioelectromagnetics*, Vol. 33, No. 6, Sep. 2012, pp.466-475.

[JVGV12b] Joseph,W., Verloock,L., Goeminne,F., Vermeeren,G. and Martens,L., "Assessment of RF Exposures from Emerging Wireless Communication Technologies in Different Environments", *Health Physics*, Vol. 102, No. 2, Feb. 2012, pp. 161-172.

[Kath12] Kathrein-Werke KG, *698 – 6000 MHz Base Station Antennas, Filters, Combiners and Amplifiers for Mobile Communications*, Catalogue, Rosenheim, Germany, Jan. 2012 (http://www.romkatel.ro/cataloage/img/comob/kathrein_698-6000.pdf)

[LEXN13] http://www.lexnet-project.eu/, Sep. 2013.

[Luo11] Luo,F., *Digital Front-End in Wireless Communications and Broadcasting: Circuits and Signal Processing*, Cambridge University Press, NY, USA, 2011.

[Math10] The Mathworks, *MATLAB*, Software Version 7.10.0.499 (R2010a), Feb. 2010 (http://www.mathworks.com/products/matlab/).

[Moli11] Molisch,A.F., *Wireless Communications*, John Wiley & Sons, Chichester, UK, 2011.

[NaDA06] Nawrocki,M.J., Dohler,M. and Aghvami,A.H., *Understanding UMTS Radio Network Modelling, Planning and Automated Optimisation: Theory and Practice*, John Wiley & Sons, Chichester, UK, 2006.

[NARD07] Narda Safety Test Solutions, *SRM-3000 Selective Radiation Meter – Operating Manual*, Pfullingen, Germany, Nov. 2007 (http://www.narda-sts.de/pdf/hochfrequenz/OM_SRM3000_EN.pdf).

[NASA10] NASA, *Human Integration Design Handbook (HIDH)*, NASA/SP-2010-3407, Washington, DC, USA, Jan. 2010 (http://ston.jsc.nasa.gov/collections/TRS/_techrep/SP-2010-3407.pdf).

[OlMC13] Oliveira,C., Mackowiak,M. and Correia,L.M., *State of the Art on Current Metrics for EMF Exposure Evaluation*, EC LEXNET Project, Report LEXNET-WP2-INOV-024-04-State_Art_Metrics, Ver. 4, INOV, Lisbon, Portugal, May 2013.

[PFKP10] Pelosi,M., Franek,O., Knudsen,M.B., Pedersen.G.F. and Andersen,J.B., "Antenna Proximity Effects for Talk and Data Modes in Mobile Phones", *IEEE Antennas and Propagation Magazine*, Vol. 52, No. 3, June 2010, pp. 15-27.

[Pire11] Pires,R., *Coverage and Efficiency Performance Evaluation of LTE in Urban Scenarios*, M.Sc. Thesis, Instituto Superior Técnico, Lisbon, Portugal, Oct. 2012.

[PMM04] PMM 8053A The Solutions for Every Electrosmog Problems, Catalogue, PMM Safety Products, Segrate, Italy, July 2004 (http://www.pmm.it/narda/emc_radiated_immunity_en.asp).

[PyMu12] Pythoud,F. and Mühlemann,B., *Measurement Method for LTE Base Stations*, Technical Report, Federal Office of Metrology METAS, Bern-Wabern, Switzerland, 2012

(http://www.metas.ch/2012-218-808).

[SeBC12] Sebastião,D., Branco,M. and Correia,L.M., *Measures in Nearby Areas of Antennas* (in Portuguese), monIT Project, Report monIT_1084_05_Ext_Tec_ReportNearFields, Ver. 5, Instituto de Telecomunicações, Lisbon, Portugal, Jan. 2012.

[SeTB11] Sesia,S., Toufik,I. and Baker,M., *LTE – The UMTS Long Term Evolution*, John Wiley and Sons, Chicester, UK, 2011.

[ShGD12] Shi,D., Gao,Y. and Du,X., "The SAR Value Analysis of LTE Terminals", in *Proceedings of EMC EUROPE 2012 - International Symposium on Electromagnetic Compatibility"*, Rome, Italy, Sep. 2012 (http://ieeexplore.ieee.org/stamp/stamp.jsp?tp=&arnumber=6396821).

[Tang12] Tang,.A, "Introductions of SAR reduced solution and LTE antenna design", in *Proc. of APMC 2012 - Asia-Pacific Microwave Conference*, Kaohsiung, Taiwan, Dec. 2012 (http://ieeexplore.ieee.org/stamp/stamp.jsp?tp=&arnumber=6421761).

[Telc13] www.telcoantennas.com.au, Apr. 2013.

[VJGV12] Verloock,L., Joseph,W., Gati,A., Varsier,N., Flach,B., Wiart,J. and Martens,L., "Low-Cost Extrapolation Method for Maximal LTE Radio Base Station Exposure Estimation: Test and Validation", *Radiation Protection Dosimetry*, Oxford University Press, Nov. 2012.

[Wann12] Wannstrom,J., *LTE-Advanced*, 3GPP, 2012 (http://www.3gpp.org/IMG/pdf/lte_advanced_v2.pdf).

[ZZYB12] Zhao,K., Zhang, S., Ying,Z., Bolin,T. and He,S., "SAR Study of Different MIMO Antenna Designs for LTE Application in Smart Mobile Phones", in *Proc. of APSURSI 2012 - IEEE International Symposium on Antennas and Propagation Society*, Chicago, USA, IL, July 2012 (http://ieeexplore.ieee.org/stamp/stamp.jsp?tp=&arnumber=6348485).